



DESIGN AND IMPROVEMENT OF ANTI-CHILD LOCKING SYSTEM IN VEHICLE

اونيورسيتي تېكنيكل مليسيا ملاك
UNIVERSITI TEKNIKAL MALAYSIA MELAKA

**MUHAMMAD YUSOFF BIN ALI
B092110409**

**BACHELOR OF MECHANICAL ENGINEERING
TECHNOLOGY (AUTOMOTIVE) WITH HONOURS**

2025



Faculty of Mechanical Technology and Engineering

**DESIGN AND IMPROVEMENT OF ANTI-CHILD LOCKING SYSTEM
IN VEHICLE**

اونيورسيتي تيكنيكل مليسيا ملاك
UNIVERSITI TEKNIKAL MALAYSIA MELAKA

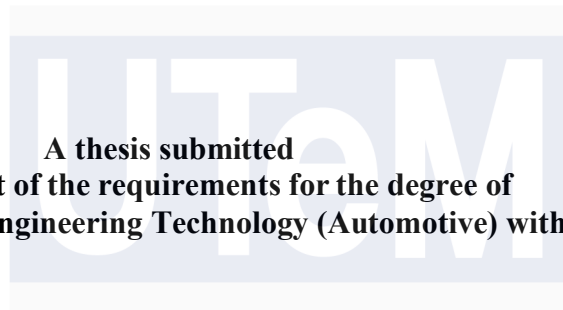
Muhammad Yusoff Bin Ali

Bachelor of Mechanical Engineering Technology (Automotive) with Honours

2025

**DESIGN AND IMPROVEMENT OF ANTI-CHILD LOCKING SYSTEM IN
VEHICLE**

MUHAMMAD YUSOFF BIN ALI



**A thesis submitted
in fulfillment of the requirements for the degree of
Bachelor of Mechanical Engineering Technology (Automotive) with Honours**

اونيورسيتي تيكنيكل مليسيا ملاك

UNIVERSITI TEKNIKAL MALAYSIA MELAKA

Faculty of Mechanical Technology and Engineering

UNIVERSITI TEKNIKAL MALAYSIA MELAKA

2025

BORANG PENGESAHAN STATUS LAPORAN PROJEK SARJANA MUDA

TAJUK: Design and Improvement of Anti-Child Locking System in Vehicle

SESI PENGAJIAN: 2024-2025 Semester 1

Saya **Muhammad Yusoff Bin Ali**

mengaku membenarkan tesis ini disimpan di Perpustakaan Universiti Teknikal Malaysia Melaka (UTeM) dengan syarat-syarat kegunaan seperti berikut:

1. Tesis adalah hak milik Universiti Teknikal Malaysia Melaka dan penulis.
2. Perpustakaan Universiti Teknikal Malaysia Melaka dibenarkan membuat salinan untuk tujuan pengajian sahaja dengan izin penulis.
3. Perpustakaan dibenarkan membuat salinan tesis ini sebagai bahan pertukaran antara institusi pengajian tinggi.
4. ****Sila tandakan (✓)**

☐

TERHAD

(Mengandungi maklumat yang berdarjah keselamatan atau kepentingan Malaysia sebagaimana yang termaktub dalam AKTA RAHSIA RASMI 1972)

☐

SULIT

(Mengandungi maklumat TERHAD yang telah ditentukan oleh organisasi/badan di mana penyelidikan dijalankan)

☒

TIDAK TERHAD

Disahkan oleh:

Alamat Tetap:

Cop Rasmi:

TS. DR. NUR RASHID BIN MAT NURI @ MD DIN
Pensyarah Kanan
Fakulti Teknologi dan Kejuruteraan Mekanikal
Universiti Teknikal Malaysia Melaka

Tarikh: 23/1/2025

Tarikh: 28 Januari 2025

**** Jika tesis ini SULIT atau TERHAD, sila lampirkan surat daripada pihak berkuasa/organisasi berkenaan dengan menyatakan sekali sebab dan tempoh laporan PSM ini perlu dikelaskan sebagai SULIT atau TERHAD.**

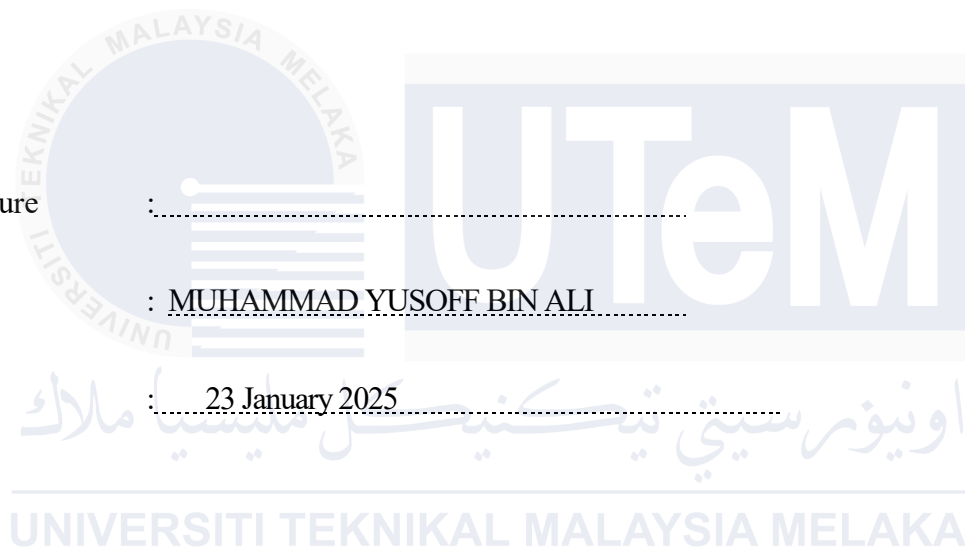
DECLARATION

I declare that this Choose an item. entitled “Design and Improvement of Anti-Child Locking System in Vehicle ” is the result of my own research except as cited in the references. The Choose an item. has not been accepted for any degree and is not concurrently submitted in candidature of any other degree.

Signature :

Name : MUHAMMAD YUSOFF BIN ALI

Date : 23 January 2025



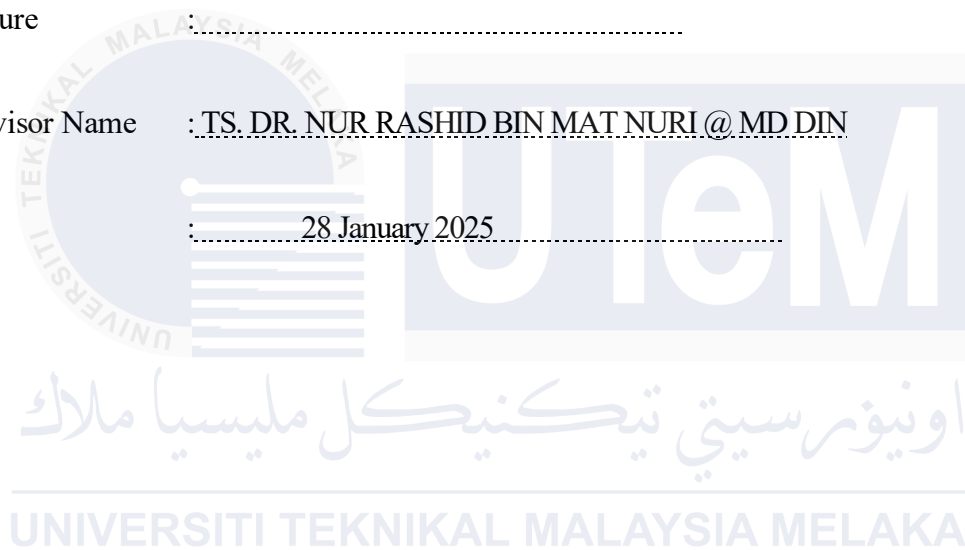
APPROVAL

I hereby declare that I have checked this thesis, and, in my opinion, this thesis is adequate in terms of scope and quality for the award of the Bachelor of Degree Engineering Technology (Automotive) with Honours.

Signature :

Supervisor Name : TS. DR. NUR RASHID BIN MAT NURI @ MD DIN

Date : 28 January 2025



DEDICATION

Hereby, I dedicate my deepest and heartfelt appreciation to my beloved father, mother, and fellow friends for their unwavering support, encouragement, and understanding. Their constant prayers, motivation, and belief in my abilities have been the cornerstone of my journey, enabling me to accomplish this significant milestone with honour and pride. I am forever grateful for their presence, guidance, and sacrifices that have inspired me to strive for excellence.

I would also like to extend my sincere gratitude to my project supervisor, Ts. Dr. Nur Rashid Bin Mat Nuri @ Md Din, for his invaluable guidance, constructive feedback, and encouragement throughout the preparation of this report. His expertise, patience, and dedication have been instrumental in shaping the success of this project.

My appreciation extends to the faculty members, especially the lecturers and staff of the Faculty of Mechanical Technology and Engineering, for their continuous support, resources, and knowledge-sharing throughout my academic journey. I am truly blessed to have had the opportunity to learn from such exceptional educators and mentors.

Finally, I would like to acknowledge my peers and colleagues, Affi Syahfizar & Ammar Rozaimin who have been a constant source of inspiration and collaboration. Their camaraderie, shared ideas, and teamwork have not only enriched this project but also made the entire learning process an enjoyable and memorable experience. To everyone who has directly or indirectly contributed to this achievement, I extend my heartfelt thanks and gratitude. This accomplishment is as much yours as it is mine.

ABSTRACT

People nowadays often prioritize their work and careers to support their lives, sometimes neglecting their immediate surroundings. This behavior can contribute to an increasing number of children who become trapped in vehicles, sometimes with fatal outcomes due to heatstroke after being left in vehicle. Thus, to encounter this problem the Anti-Child Locking System in Vehicles was designed and developed to address the critical issue of child entrapment in vehicles, which can result in life-threatening conditions such as heatstroke and suffocation. This innovative system objectives were to integrates with additional sustainable, solar-powered technology with advanced sensors and communication modules to ensure timely detection and response to hazardous conditions inside the vehicle. At its core, the system is built on an Arduino UNO microcontroller, supported by a polycrystalline solar panel and a sealed lead-acid battery to provide continuous operation even when the vehicle's ignition is off. The system incorporates a Passive Infrared (PIR) motion sensor to detect human presence, an NTC thermistor for real-time temperature monitoring, and an MQ-135 gas sensor to measure CO₂ concentration. Upon detecting motion or exceeding predefined thresholds for temperature at 45°C or CO₂ levels at 800 ppm, as the final objective of the project, the system triggers a GSM module to send text alerts and make missed phone calls, while simultaneously activating an LED alarm light to alert nearby individuals. The system's performance was rigorously tested under real-world scenarios for days, demonstrating its reliability in monitoring environmental conditions, transmitting data via IoT platforms like ThingSpeak, and issuing real-time alerts through Arduino IDE. Comparative data analysis revealed its responsiveness in detecting and mitigating risks, with the solar-powered design ensuring sustained functionality without depleting the vehicle's primary battery. This project offers a commercially viable, portable, and easy-to-install solution for enhancing child safety in vehicles. By leveraging renewable energy and smart technology, the Anti-Child Locking System provides a practical and effective safeguard, paving the way for broader adoption in both individual and industrial contexts to reduce preventable child injuries and fatalities.

ABSTRAK

Manusia pada masa kini, ramai yang lebih mengutamakan kerja dan kerjaya mereka untuk menyara kehidupan, kadangkala mengabaikan persekitaran sekeliling mereka. Tingkah laku ini boleh menyumbang kepada peningkatan bilangan kanak-kanak yang terperangkap dalam kenderaan, kadangkala dengan akibat yang fatal akibat strok haba selepas ditinggalkan dalam kenderaan. Oleh itu, untuk menangani masalah ini, Sistem Anti-Kunci Kanak-Kanak dalam Kenderaan telah direka dan dibangunkan untuk menangani isu kritikal penjeratan kanak-kanak dalam kenderaan, yang boleh mengakibatkan keadaan yang mengancam nyawa seperti strok haba dan sesak nafas. Objektif inovatif sistem ini adalah untuk mengintegrasikan teknologi solar yang mampan dengan sensor canggih dan modul komunikasi untuk memastikan pengesanan dan tindak balas yang tepat pada masanya terhadap keadaan berbahaya di dalam kenderaan. Pada terasnya, sistem ini dibina menggunakan mikropengawal Arduino UNO, disokong oleh panel solar polikristalin dan bateri timbal yang tertutup untuk menyediakan operasi berterusan walaupun ketika pencucuhan kenderaan dimatikan. Sistem ini menggabungkan sensor gerakan Infrared Pasif (PIR) untuk mengesan kehadiran manusia, termistor NTC untuk pemantauan suhu masa nyata, dan sensor gas MQ-135 untuk mengukur kepekatan CO₂. Setelah mengesan gerakan atau melebihi ambang suhu yang ditetapkan pada 45°C atau tahap CO₂ pada 800 ppm, sebagai objektif akhir projek ini, sistem ini mengaktifkan modul GSM untuk menghantar pemberitahuan teks dan membuat panggilan telefon yang terlepas, sambil mengaktifkan lampu isyarat LED untuk memberi amaran kepada individu berhampiran. Prestasi sistem ini telah diuji dengan teliti dalam senario dunia nyata selama beberapa hari, membuktikan kebolehpercayaannya dalam memantau keadaan persekitaran, menghantar data melalui platform IoT seperti ThingSpeak, dan mengeluarkan pemberitahuan masa nyata melalui Arduino IDE. Analisis data perbandingan menunjukkan tindak balasnya dalam mengesan dan mengurangkan risiko, dengan reka bentuk solar yang memastikan fungsi berterusan tanpa menghabiskan bateri utama kenderaan. Projek ini menawarkan penyelesaian komersial yang berdaya maju, mudah alih, dan mudah dipasang untuk meningkatkan keselamatan kanak-kanak dalam kenderaan. Dengan memanfaatkan tenaga boleh diperbaharui dan teknologi pintar, Sistem Anti-Kunci Kanak-Kanak menyediakan perlindungan yang praktikal dan berkesan, membuka jalan untuk penerimaan yang lebih luas dalam konteks individu dan industri bagi mengurangkan kecederaan dan kematian kanak-kanak yang boleh dielakkan.

ACKNOWLEDGEMENTS

First and foremost, In the name of Allah, The Most Gracious, the Most Merciful, to whom I would like to extend my deepest gratitude and praise for everything I received since the beginning of my journey. I would like to express my sincere appreciation especially to Universiti Teknikal Malaysia Melaka (UTeM) on providing all necessary platform, guidance, essential resources for me to complete this project. The facilities and opportunity were widely opened only in UTeM has enabling me to pursue and find my research objectives.

I owe a debt of gratitude to Ts. Dr. Nur Rashid Bin Mat Nuri @ Md Din, who has helped me through every stage and phase of this endeavor with his priceless counsel, tolerance, and support. Your knowledge and experience have been invaluable to the accomplishment of this project.

I express my gratitude to my instructors and the UTeM administrative team for their help and encouragement. We sincerely appreciate your commitment to creating a learning and innovative atmosphere. My sincere gratitude also goes out to my family and friends for their steadfast understanding and support. Your faith in my abilities has given me courage and strength.

Lastly, I would like to thank everyone who helped to complete this project, especially those who worked directly or indirectly in the Faculty of Mechanical Technology and Engineering. Your assistance and backing have been priceless, and I sincerely appreciate all that you have done.

TABLE OF CONTENTS

ABSTRACT	i
<i>ABSTRAK</i>	ii
ACKNOWLEDGEMENTS	iv
TABLE OF CONTENTS	v
LIST OF TABLES	viii
LIST OF FIGURES	ix
LIST OF SYMBOLS AND ABBREVIATIONS	xii
LIST OF APPENDICES	xiv
CHAPTER 1 INTRODUCTION	1
1.1 Background	1
1.2 Problem Statement	2
1.3 Project Objective	2
1.4 Scope of Project	3
CHAPTER 2 LITERATURE REVIEW	4
2.1 Introduction	4
2.2 Statistics of Child Death's Incident in Vehicle	5
2.3 Conventional Child Safety System	6
2.3.1 Child Safety Seats using belts or Lower Anchors and Tethers for Children (LATCH)	7
2.3.2 Implementation Of Child Safety Lock in Automobiles	8
2.3.3 Implementation of Window Locks in Automobiles	9
2.4 Overview of Existing Project Related to Child Safety Alert System	11
2.4.1 Project 1	12
2.4.2 Project 2	12
2.4.3 Project 3	13
2.4.4 Project 4	13
2.4.5 Project 5	14
2.4.6 Comparison of Existing Projects System	14
2.5 Microcontroller	16
2.5.1 Arduino 17	23
2.5.2 Espressif Module / ESP	27
2.5.3 Comparisons of Microcontrollers	28
2.6 Sensing Elements	29
2.6.1 Infrared Sensor	33
2.6.2 Temperature Sensor	36
2.6.3 Gas Detector Sensor	38
2.7 Major Element of Solar Power System	39
2.7.1 Solar Panels	44
2.7.2 Battery Bank	49
2.8 Global System for Mobile Communication (GSM)	49

2.8.1	Wi-Fi Module	49
2.8.2	GSM Module (SIM-900 A)	50
2.9	Summary	51
CHAPTER 3	METHODOLOGY	53
3.1	Introduction	53
3.2	Research Flowchart	54
3.3	Block Diagram of Anti-Child Lock System in Vehicle	55
3.4	Flowchart of Anti-Child Lock System in Vehicle	56
3.5	Hardware Development	57
3.5.1	Component Selection and Procurements	57
3.5.2	Circuit Design	69
3.5.3	Prototype Development	71
3.6	Threshold Selection	71
3.6.1	Temperature Threshold	72
3.6.2	Carbon Dioxide Concentration Level Threshold	72
3.7	Software Development	73
3.7.1	Software Arduino IDE	73
3.7.2	Individual Component Testing	75
3.8	Tools Equalizer	83
3.8.1	Multimeter	84
3.8.2	Soldering Iron	85
3.8.3	Handheld Thermocouple	86
3.9	Integration & Testing	87
3.9.1	Combining Component's Specific Codes	87
3.9.2	Debugging & Configurations	88
3.9.3	Calibration of Sensors	89
3.9.4	Real-Time Data Testing	93
3.10	Power And Energy Requirements for Anti-Child Locking System	95
3.11	Summary	99
CHAPTER 4	RESULT AND DISCUSSION	100
4.1	Introduction	100
4.2	Display of Result	100
4.2.1	Arduino IDE Serial Monitoring	101
4.2.2	Dashboard ThingSpeak	101
4.3	Data Collection and Comparison	102
4.3.1	Ambient Temperature Data (°C) Day-1 VS Day-2	103
4.3.2	CO ₂ Gas Concentration Level Data (PPM) Day-1 VS Day-2	104
4.3.3	Ambient Temperature VS Outdoor Temperature (°C) Day-1 & Day-2	105
4.3.4	Comparison of Ambient Temperature Data (°C) & CO ₂ Gas Concentration Level Data (PPM) Over Time (Minutes) Day-1 & Day-2	107
4.4	Response Time Comparison Between Arduino IDE and ThingSpeak	109
4.5	System Performance Under Different Conditions	111
4.5.1	Result of Summary Table	111
4.6	System Insights and Implications	115
4.7	Summary	119
CHAPTER 5	CONCLUSION AND RECOMMENDATION	120

5.1	Conclusion	120
5.2	Recommendations	121
REFERENCES		123
APPENDICES		128
Appendices A: Gantt Chart Project 1		128
Appendices B: Gantt Chart Project 2		129
Appendices C: Table of Analysis Data for 2 Days		130
Appendices D: Table of Time Response Data between Arduino IDE and ThingSpeak		140
Appendices E: 3D Print Casing for Sensor Design Drafting		141
Appendices F: Similarity Index Turnitin Report		142
Appendices G: AI Index Turnitin Report		143



LIST OF TABLES

TABLE	TITLE	PAGE
Table 2.1	Comparison Between the Components Used in Related Existing Project	15
Table 2.2	The Technical Specification of Arduino UNO	19
Table 2.3	The Technical Specification of Arduino NANO	20
Table 2.4	The Technical Specification of Arduino MEGA	22
Table 2.5	The Technical Specification of ESP 8266	25
Table 2.6	The Technical Specification of ESP 32	26
Table 2.7	Comparison of each Microcontrollers	28
Table 2.8	The Technical Specification of Passive Infrared Sensor (PIR)	32
Table 2.9	The Technical Specification of NTC Thermistor Sensor Module	34
Table 2.10	MQ-135 Air Quality Sensor Specifications	37
Table 2.11	Comparison Between Monocrystalline & Polycrystalline Solar Panel	43
Table 2.12	Comparison Between Lead-Acid, Lithium-ion & Nickel-Metal Hydride Batteries	45
<hr/>		
Table 3.1	Polycrystalline Solar Panel Specifications	58
Table 3.2	Rechargeable Battery Sealed Lead Acid Specifications	61
Table 3.3	Summary of Expected Responses for each Command	82
Table 3.4	Components and Power Consumptions	95
Table 4.1	System Performance Under Different Conditions	112

LIST OF FIGURES

FIGURE	TITLE	PAGE
Figure 2.1	Number of Cases of Heatstroke (PVH)	5
Figure 2.2	LATCH Concept System	7
Figure 2.3	Child Safety Lock in Automobiles	8
Figure 2.4	Window Lock in Automobiles	10
Figure 2.5	Window Lock in Automobiles Limitations	11
Figure 2.6	Structure of Arduino UNO R3	18
Figure 2.7	Structure of Arduino NANO	10
Figure 2.8	Structure of Arduino MEGA	22
Figure 2.9	Structure of ESP 8266	24
Figure 2.10	Structure of ESP 32	26
Figure 2.11	Infrared Sensor	29
Figure 2.12	Active Infrared Sensor Concept	31
Figure 2.13	Passive Infrared Sensor	32
Figure 2.14	PIR Sensor Working Principle	33
Figure 2.15	NTC Thermistor Sensor Module	34
Figure 2.16	MQ-135 Sensor	36
Figure 2.17	Monocrystalline Solar Panel	41
Figure 2.18	Polycrystalline Solar Panel	42
Figure 2.19	Lead-Acid Batteries	46
Figure 2.20	Lithium-ion Batteries	47
Figure 2.21	Nickel-Metal Hydride Batteries	48
Figure 2.22	ESP 8266 With Wi-Fi Module	50
Figure 2.23	GSM Module (SIM-900 A)	51

Figure 3.1	The Flowchart of The Overall Research	54
Figure 3.2	Block Diagram of Anti-Child Lock System in Vehicle	55
Figure 3.3	Flowchart of Anti-Child Lock System in Vehicle	56
Figure 3.4	Polycrystalline Silicon Solar Panel 8W	58
Figure 3.5	12V 10A Pulse Width Modulation Solar Charge Controller	59
Figure 3.6	Rechargeable Battery 6 V 4.5 AH Sealed Lead Acid	60
Figure 3.7	Arduino UNO R3	62
Figure 3.8	Passive Infrared (PIR) Sensor	63
Figure 3.9	MQ-135 Sensor	64
Figure 3.10	NTC Thermistor Sensor	66
Figure 3.11	GSM SIM-900A	67
Figure 3.12	LED Alarm Light Indicator	68
Figure 3.13	Wiring Diagram for Overall System	70
Figure 3.14	Arduino IDE Software	74
Figure 3.15	PIR Sensor Testing Code	76
Figure 3.16	Result of Testing PIR Sensor Functionality	76
Figure 3.17	NTC Thermistor Sensor Testing Code	77
Figure 3.18	Result of Testing NTC Thermistor Sensor Functionality	78
Figure 3.19	MQ-135 Testing Code	79
Figure 3.20	Result of Testing MQ-135 Sensor Functionality	79
Figure 3.21	GSM module Signal Testing Code	81
Figure 3.22	AT Command Signal Testing Code	83
Figure 3.23	Multimeter	84
Figure 3.24	Soldering Iron	85
Figure 3.25	Handheld Thermocouple	86
Figure 3.26	Pin Assignment Table or Code Snippet	88
Figure 3.27	Sensor Threshold Configuration	88
Figure 3.28	PIR Sensor Calibration Setup	90
Figure 3.29	Calibrating Onboard Potentiometer	90

Figure 3.30	Messages shown in Arduino IDE Serial Monitor	91
Figure 3.31	Mathematical Coding for MQ-135 Sensor	92
Figure 3.32	Offset value in mapping	92
Figure 3.33	Resistance Calculated Based on Formula	92
Figure 3.34	Steinhart-Hart Equation	93
Figure 3.35	Calibration Offset is applied in the coding	93
Figure 3.36	Real-Time Data Testing in Serial Monitor	94
Figure 4.1	Arduino IDE Serial Monitor Interface	101
Figure 4.2	Display of ThingSpeak Dashboard	102
Figure 4.3	Ambient Temperature Data (°C) Day-1 vs Day-2	103
Figure 4.4	CO ₂ Gas Concentration Level Data (°C) Day-1 vs Day-2	104
Figure 4.5	Ambient Temperature VS Outdoor Temperature (°C) Day-1	105
Figure 4.6	Ambient Temperature VS Outdoor Temperature (°C) Day-2	106
Figure 4.7	Comparison of Ambient Temperature Data (°C) & CO ₂ Gas Concentration Level Data (PPM) Over Time (Minutes) Day-1	107
Figure 4.8	Comparison of Ambient Temperature Data (°C) & CO ₂ Gas Concentration Level Data (PPM) Over Time (Minutes) Day-2	108
Figure 4.9	Response Time Comparison Between Arduino IDE and Thingspeak	109
Figure 4.10	The message sent to the registered phone number	113
Figure 4.11	The messages sent to the registered phone number	114
Figure 4.12	(a) Anti-Child Locking System call logs (b) The GSM missed calls to the registered phone	114
Figure 4.13	(a) The LED Alarm Light Indicator is turned ON (b) Closer view of LED Alarm Light Indicator activation	115
Figure 4.14	Comparison of Insight and Implications of Day-1	116
Figure 4.15	Comparison of Insight and Implications of Day-2	117

LIST OF SYMBOLS AND ABBREVIATIONS

NTC	-	Negative Temperature Coefficient
IR	-	Infrared
NiMH	-	Nickel-Metal Hydride
Li-ion	-	Lithium-ion
LED	-	Light-Emitting Diode
PIR	-	Passive Infrared
GSM	-	Global System for Mobile Communications
CO ₂	-	Carbon Dioxide
AC	-	Alternate Current
DC	-	Direct Current
RAM	-	Random Access Memory
EEPROM	-	Electrically Erasable Programmable Read-Only Memory
ROM	-	Read-only Memory
OTP	-	One Time Programmable
USB	-	Universal Serial Bus
PVH	-	Pediatric Vehicular Heatstroke
NHTSA	-	National Highway Traffic Safety Administration
LATCH	-	Lower Anchors and Tethers for Children
CPU	-	Central Processing Unit
I/O	-	Input/Output
ICSP	-	Interagency Council on Standards Policy
SRAM	-	Static Random-Access Memory
PWM	-	Pulse Width Modulation
GPIO	-	General-Purpose Input/Output
Wi-Fi	-	Wireless-Fidelity
SD	-	Secure Digital
TCP/IP	-	Transmission Control Protocol/ Internet Protocol
IoT	-	Internet of Things
RTD	-	Resistance Temperature Detectors
VCC	-	Voltage at Common Collector
GND	-	Ground
NH ₃	-	Ammonia
NO _x	-	Nitrogen Oxides
AO	-	Analog Output
DO	-	Digital Output
PV	-	Photovoltaic
Li-ion	-	Lithium-ion
NiMH	-	Nickel-Metal Hydride
ETSI	-	European Telecommunications Standards Institute
SoC	-	System on Chip
GPRS	-	General Packet Radio Service
MPPT	-	Maximum Power Point Tracking
SIM	-	Subscriber Identity Module
PCB	-	Printed Circuit Board

PPM	-	Particle Per Million
°C	-	Degree Celsius
Wh	-	Watt Hour
E	-	Energy
P	-	Power
V	-	Voltage
I	-	Current



اونيورسيتي تېكنيكل مليسيا ملاك

UNIVERSITI TEKNIKAL MALAYSIA MELAKA

LIST OF APPENDICES

APPENDIX	TITLE	PAGE
APPENDIX A	List of distribution network parameters.	26
APPENDIX B	Typical daily load profile data	27
APPENDIX C	Typical daily load profile data	27



CHAPTER 1

INTRODUCTION

1.1 Background

In today's fast-paced world, people often prioritize their work and careers to support their lives, sometimes neglecting their immediate surroundings. This behavior can contribute to an increasing number of accidents or incidents, a trend that has persisted over time despite various efforts to address it. One particularly tragic example is the number of children who become trapped in vehicles, sometimes with fatal outcomes. The Malaysian Institute of Road Safety Research reported that more than a dozen cases of children aged 0–19 died from heatstroke after being left in automobiles during 2018–2022 (Mohamed et al., 2021)

This issue has prompted various communities and vehicle, or any safety development companies to search for solutions, yet the problem remains unsolved to this day. Recognizing the urgent need to address this safety hazard, the development of an Anti-Child Locking System in vehicles has been proposed as an enhancement to current car safety measures. This system aims to minimize the occurrence of incidents where children are left in vehicles for short or extended periods, thereby preventing potential harm or fatalities.

The proposed system utilizes various sensors and communication modules to detect hazardous conditions within the vehicle and promptly alert the vehicle owner and nearby pedestrians. By advancing car safety technology, the Anti-Child Lock System aims to offer a reliable and effective solution to a persistent problem, ultimately safeguarding children's lives.

1.2 Problem Statement

Children being trapped in a vehicle is one situation that still poses a high risk, with the children mainly experiencing severe injuries or death due to extremely high or low temperatures or hazardous gases. With increased awareness and prevention campaigns, they still do occur and usually involve forgotten or accidentally locked children inside cars. This, therefore, calls for the urgent need for an automated solution that is able to detect the presence of a human inside a vehicle and send immediate alerts to the owner of the vehicle or other parties. This project focuses on the development of a complete and sustainable Anti-Child Locking System, portable, easy to install, and commercially viable, to increase the safety of the vehicle and reduce such tragic incidents.

1.3 Project Objective

The main objective of this project is to propose a systematic and effective methodology of Anti-Child Locking System in Vehicle by detecting the presence of a child left in a car and issuing timely alerts to prevent harm. Specifically, the objectives are as follows:

- a) To design and develop a functional sustainable prototype that is able to detect human presence inside the vehicle cabin.
- b) To test the temperature, carbon dioxide and motion detection sensors in a real vehicle cabin environment.
- c) To implement alert mechanisms to notify the vehicle owners via GSM communication and warn surrounding individuals via LED alarm light indicator.

1.4 Scope of Project

The scope of the project is defined as follows:

- a) The system will include a PIR sensor to detect motion, an NTC thermistor sensor to monitor temperature, and an MQ-135 gas detector to measure carbon dioxide levels.
- b) The system will test under various conditions to validate its response time, detection accuracy, and alert mechanisms for over 2 days test period.
- c) The system will use a SIM 900-A GSM module to send alerts via text message and phone call, and an alarm strobe light to visually signal surrounding pedestrians.
- d) The system emphasizes ease of installation and operation, making it accessible to non-technical vehicle owners.
- e) The primary focus is to prevent fatalities or injuries caused by occupants, particularly children or infants, being trapped in vehicles under hazardous conditions.

CHAPTER 2

LITERATURE REVIEW

2.1 Introduction

A literature review is a body of text that aspires to review the critical points of current knowledge or methodological approaches on a particular topic. Literature reviews are secondary sources and, as such, do not report any new or original experimental work. Most often associated with academic-oriented literature, a literature review usually precedes a research proposal and results section. A well-structured literature review is characterized by a logical flow of ideas.

The present chapter has summarized the theories and system designs for an anti-child lock system in vehicles. In this regard, a brief overview of the conventional child lock system has been provided. This chapter further includes statistics from road accidents leading to child deaths. In addition, this chapter will discuss and compare existing projects from relevant articles, journals, and other works in order to keep the results of this project more improved and effective.

By analyzing these sources, generating design a more advanced and reliable anti-child locking system in vehicle to avoid such tragic incidents. With new technologies and improved design principles, vehicles can have better safety features for children.

2.2 Statistics of Child Death's Incident in Vehicle

A literature These days, Children getting stuck in cars is a major worry on a global scale. An average of 37 children each year pass away from heatstroke because of being left in hot cars; since 1998, there have been 968 cases of Pediatric Vehicular Heatstroke (PVH), according to NoHeatStroke.org as shown in Figure 2.1 and the National Highway Traffic Safety Administration (NHTSA). Given the seriousness of the issue, this figure emphasizes how urgently awareness and action must spread throughout the world. These terrible occurrences impact families and communities everywhere and they are not limited to just one area (Abubakar et al., 2023; Jan Null, 2023).

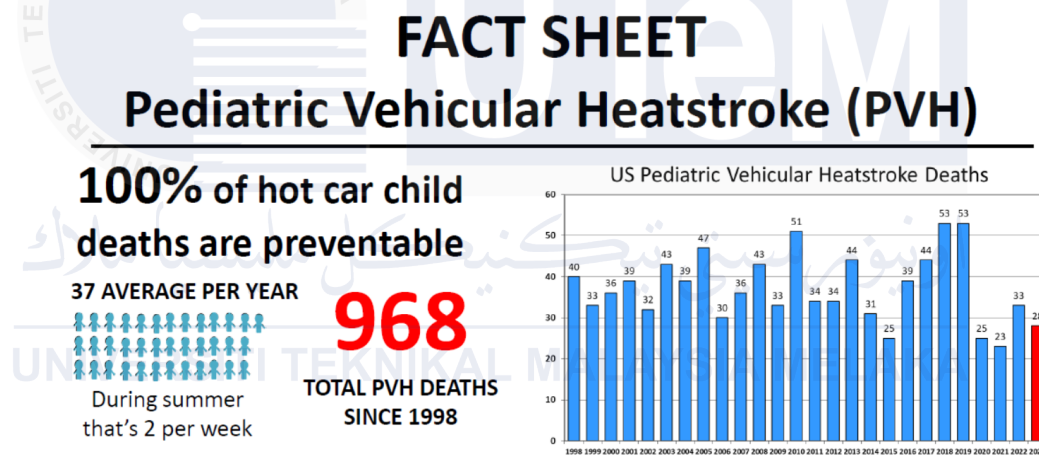


Figure 2.1: Number of Cases of Heatstroke (PVH) (Jan Null, 2023)

The situation in Malaysia is also quite alarming. According to a 2011 summary of road traffic injuries among children in Malaysia, the Malaysian Institute of Road Safety Research reported that more than a dozen cases of children aged 0–19 died from heatstroke after being left in automobiles during 2018–2022 (Mohamed et al., 2021). In a statement to the media, The Office of the Children's Commissioner of The Human Rights Commission of Malaysia (SUHAKAM) said it was sad to learn about the recent deaths of children from vehicular hyperthermia, where they were left to fend for themselves inside their cars (Farah Nini Dusuki, 2023).

Such a problem requires a multilevel solution. First and foremost, the solution would lie in technological development. For example, an alarm system can be installed in automobiles that will ring as a reminder to drivers if a child is left behind in the car. Parental awareness of the dangers of leaving children in vehicles can be raised by education programs that offer valuable advice and reminders. Another way is legislation, which may require these safety features in all cars, for example, and can be much more effective in preventing accidents (Mahdin et al., 2016).

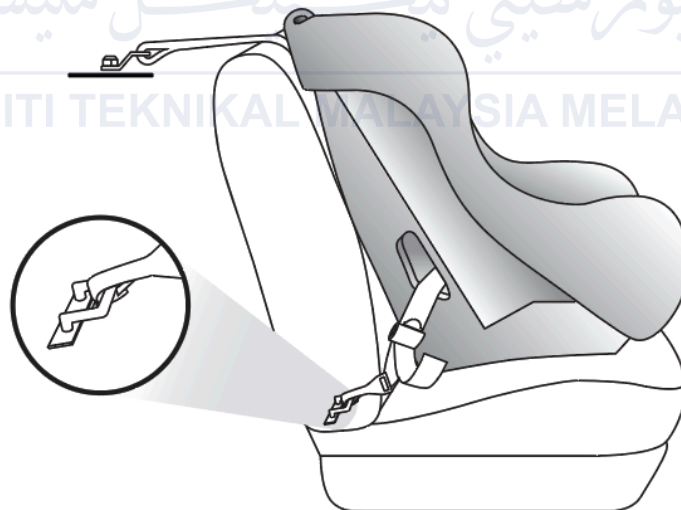
2.3 Conventional Child Safety System

Arguments around car safety in the modern day indicate that car manufacturers have clearly developed and upgraded sophisticated child safety systems to satisfy changing requirements and safety recommendations. Ensuring safety for the youngest passengers while traveling by car has become one of the key responsibilities in the world of modern automotive industrial manufacturing. Unfortunately, accidents when children are left in cars have become much too common, raising serious concerns around the world and demanding strong precautions.

This is especially true in the industrial manufacturing sector, where the safety and welfare of child passengers lie with the design and manufacture of vehicles. The rising numbers of youngsters being left in cars, which often ends in heat stroke and death, underlines the critical need for superior safety solutions. Such cases show how important it is to include detailed child safety features in the design of cars to reduce hazards and provide better protection for the passengers who are more vulnerable. Hence, conventional, or traditional child safety systems of cars are comprised of several integral components, each one of which is designed to address some aspect of passenger safety (Li & Ge, 2021).

2.3.1 Child Safety Seats using belts or Lower Anchors and Tethers for Children (LATCH)

This Lower Anchors and Tethers for Children, abridged as LATCH, is a standardized process used in fastening child safety seats in cars without the use of the seat belts. Figure 2.2 indicates the LATCH concept system and certain parts of the LATCH must be included in the car and the kid safety seat for the system to function correctly. These include lower anchor straps and a top tether on the kid safety seat, and lower anchors and top tether anchors in the car. The LATCH system aims to increase the overall safety of young occupants by simplifying the connection procedure and reducing the likelihood of incorrect installation. To this end, to optimize the protective benefits provided by a kid safety seat in a car, it must be understood, and the correct installation procedures of the LATCH system followed (Cicchino & Jermakian, 2015; York State Department of Health, 2002).



CAR SEAT PARTS ILLUSTRATED

Figure 2.2: LATCH Concept System

Source: <https://www.bedfordnissan.com/blogs/1502/bedford-nissan-dealer/bedford-nissan-tips-how-to-use-the-latch-system/>

2.3.2 Implementation Of Child Safety Lock in Automobiles

Child safety locks in cars are vital for small passengers. It is important that these locks prevent doors from opening accidentally when the car is in motion or being driven. It is, therefore, paramount to have all measures of safety put in place because modern road conditions pose many forms of distractions and threats. Among these precautions, car child safety locks rank as vital but often overlooked components. The objective of this tutorial is to explain the importance of these locks and their mechanisms of operation and how they assist in preventing accidents and injuries. Therefore, reduce the chances of falling and getting hurt. Even if the child pulls on the handle, the child safety lock as shown in Figure 2.3 prevents the door from being opened from the inside, but the door may be opened from the outside once the car has been brought to a stop (Abdulrahman Abdullah et al., 2020).



Figure 2.3: Child Safety Lock in Automobiles

Source: <https://gogirl.co.uk/news-and-advice/child-lock-what-how/>

However, several limitations and disadvantages of the kid safety locks should be recognized. First and foremost, their application is restricted by their location; they are

mostly available in the back doors, which makes them ineffective in some seats. In addition, there are some misuse possibilities if the locks are not used appropriately, for instance, if the owner forgets to turn the locks on, something which may compromise the mentioned safety benefits. This also means that child safety locks require frequent maintenance to ensure they are properly working, thus increasing the car maintenance burden (Garg & Agrawal, 2020).

2.3.3 Implementation of Window Locks in Automobiles

The Vehicle Window Locks are essential for safety in a car since they provide the driver with ultimate control of the operation of the windows, thus minimizing the chances of unwanted instances where children can manipulate the windows on their own. This device efficiently prevents young children from lowering or raising windows inadvertently. This may result in injuries or even trapping them. This is one of the precautionary measures. Window locks provide an additional level of safety for young passengers, especially by giving the driver control and creating a safer environment inside the car. Discussion in academic or research circles on window locks extends beyond their usage to their technological intricacies, such as the mechanisms for controlling how well they work, how well they work in actual safety situations, and the ongoing developments meant to make them more reliable and efficient as shown in figure 2.4 (Selvakumar, 2023).



Figure 2.4: Window Lock in Automobiles

Source: <https://www.wikihow.life/Childproof-Your-Car%27s-Interior>

Vehicle window locks are an important safety feature, especially when protecting young passengers from possible risks regarding power windows. These locks lower the possibility of accidents or entrapment by keeping kids from unintended opening of the window. Parents can ensure that their children can't access or close the back windows by employing the power-window lock feature, usually from a button located on the driver's side of the vehicle. Because of the huge force exerted by power windows and the risk of injury, this simple but effective system aids in the prevention of major accidents. Window locks and other safety features, like "pull up/push down" switches, help in creating a safer environment inside the car by reducing the chances of accidental window activation (Stela Muncut & Ioana Culda, 2022).

Still, there are several limitations and potential drawbacks to relying solely on window locks for safety. One of the limitations of window locks in vehicle safety system is

the fact that they cannot substitute continuous monitoring and training regarding the potential dangers of power windows (Yang & Yamamoto, 2021). Figure 2.5 shows even if window locks are turned off or are inadvertently switched off, there is still the potential for injury as shown in figure 2.5. Additionally, window locks only shut off the rear windows. There is no equivalent protection available for the passenger windows up front. This can be dangerous if adults are unaware of the potential dangers, or if children are sitting up front (Kruizinga et al., 2023).



Figure 2.5: Window Lock in Automobiles Limitations (Anwar Ahmad, 2018)

2.4 Overview of Existing Project Related to Child Safety Alert System

This section discusses and compares five contemporary projects focused on the design and implementation of kid safety alarm systems in automobiles. As time has passed, with growing concerns about kid entrapment and safety in cars, many researchers and developers have come up with a number of remedies. The characteristics of these systems, the technology used, and their efficacy in accomplishing the goal of kid safety have been considered.

2.4.1 Project 1

The Implementation of Child Safety Alert System in Automobiles project aims to tackle the serious issue of children being left in cars, which can lead to dangerous conditions like hyperthermia and heart strokes. Through research, it's been found that children are more vulnerable to these risks than adults, highlighting the need for a child safety alert system. Using sensors like PIR, temperature, carbon dioxide, flame, and smoke sensors that are connected to an Arduino and a GSM module is the method. The precision of these sensors has been calibrated. The outcomes include circuit simulations, sensor calibration information, and features that allow the automobile owner to receive alerts and detect things like temperature, carbon dioxide levels, flames, smoke, and human presence. During the implementation stage, Proteus software is used to simulate the sensors and GSM module connected to an Arduino UNO. The findings demonstrate the system's capacity to identify different criteria and issue alarms in response, with the goal of averting mishaps and deaths involving kids left in cars (Srinavya et al., 2021).

2.4.2 Project 2

The An Electronic System with Integrated Alerting and Cooling Mechanism to Save The Life of An Unattended Child in A Vehicle aim was to address an estimated forty children in the US pass away from hyperthermia each year as a result of unintentionally leaving their car unattended in a hot environment. Even the most vigilant parent may unintentionally leave a youngster in the car seat when their routine changes. In just 20 minutes, the temperature inside an automobile can rise from 80 °F to 109 °F, which can lead to a child's death from hyperthermia. As of right now, dependable electronic cooling and reminder systems that operate without the car's engine are nonexistent. This article describes a smart car seat that has an embedded electronic system that alerts users when a simulated child is left in the seat

after the car engine is turned off. It also sends a distress signal to emergency services after two minutes and automatically activates a cooling mechanism to keep the child's temperature comfortable and prevents hyperthermia. An Arduino-controlled thermoelectric cooling system that was integrated into the electronic system that kept the child's surroundings at a constant temperature provided the cooling (Vaish, 2021).

2.4.3 Project 3

The aim of This Project 3 which is Child Car Seat Alert System via Load and Temperature Sensing project was inspired by ongoing problems that lead to the terrible deaths of newborns whose parents were unaware that they were left unattended in cars. A safety feature system for child's car seats was created in response to this issue to reduce the possibility of unintentional child desertion. When a newborn is found in a child car seat with the engine off and the device senses temperature increase inside the vehicle, it notifies parents. The system consists of a load cell, temperature sensor, buzzer, and microprocessor. According to test results, the technology sends out a high-frequency signal to alert users to potential temperature and passenger hazards when the weight reaches 3500g and the temperature climbs above 35°C (Rustam et al., 2023).

2.4.4 Project 4

This Project 4 intends to create a system that notifies the car owner and emergency contacts if a child is left unattended by designing a smart alarm system to prevent child heatstroke in vehicles. It has been a severe concern for children to become trapped in hot cars, which can result in heatstroke and even death. An infrared motion sensor and image processing will be utilized to detect movement within the car. An accelerometer will provide

the vehicle's displacement at predetermined intervals, providing information on its status. The Raspberry Pi microcontroller is the sole component of the suggested system that connects with all system sensors and initiates all necessary operations to assist the passenger.(Saleh et al., 2022)

2.4.5 Project 5

This project 5, Vehicle Cabin Safety Alert System indicated how temperature increases and oxygen deprivation in car cabins contribute to mishaps and fatalities. It promotes the use of a sophisticated monitoring system to ensure the comfort and safety of passengers. The suggested system makes use of sensors for temperature, humidity, oxygen, and PIR, as well as an LPC1768 Microcontroller, to monitor the levels of temperature, humidity, and oxygen concentration and control the interior temperature of the car to improve passenger security, safety, and well-being, whether the car is running or not. In terms of the results, the system automatically lowers windows in response to temperature and oxygen levels, protecting the safety of the people, especially in severe weather (Shyma Sasidharan & Venkatesan Kanagarajan, 2015).

2.4.6 Comparison of Existing Projects System

After examining a number of projects targeted at improving child safety especially in the vehicle, it is clear that each one provides a different approach in components used such as sensing elements, microcontroller, and also different actuator to the pressing problem of preventing heatstroke and guaranteeing the safety of children left alone in cars. These initiatives work to put in place practical safeguards to keep children in car seats safe, from a combined warning and cooling mechanism system to load and temperature detecting

technologies. Every study highlights how innovation and technology are critical to reducing the hazards connected with child-related vehicle heatstroke accidents, whether through smart alarm systems or cabin safety alert mechanisms.

Table 2.1: Comparison between the components used in the related existing project

Components Existing Project	Raspberry Pi	Arduino UNO	LPC 1768	GPS	Temp. Sensor	PIR Sensor	CO ² Sensor	Pressure Sensor	Power Window	Alarm	GSM Module
Project 1: Implementation of Child Safety Alert System in Automobiles											
Project 2: An Electronic System with Integrated Alerting & Cooling Mechanisms to Save The Life of Unattended Child in A Vehicle											
Project 3: Child Car Seat Alert System via Load & Temperature Sensing											
Project 4: Designing a Smart Alarm System to Prevent Child Heatstroke in Vehicles											
Project 5: Vehicle Cabin Safety Alert System											

2.5 Microcontroller

A microcontroller is a small integrated circuit computer that is used to control some electronic system functions. It is a small computer on one integrated circuit consisting of memory, input/output interfaces, and a central processing unit. Microcontrollers can be used in almost every embedded control system, including industrial control systems, medical equipment, automotive systems, and home appliances. They also are used in consumer electronics, such as digital cameras, audio players, and game systems. A microcontroller basically consists of a processing core, memory for volatile and non-volatile data, input/output peripherals, and different communication interfaces. The core is the CPU that guides other components in the microcontroller and executes instructions. Memory is used to store both program code and data, while input/output peripherals interface with the outside world. Microcontrollers are programmable, which means they can implement specific tasks (Ben Lutkevich, 2023; Bondavenko V.E, 2019).

The programming language for microcontrollers can be done in various languages, depending on the brand and type of microcontroller. The most common programming languages are assembly languages, C, and C++. A microcontroller is a self-contained device and can work independently in an embedded system (Yuan et al., 2021). Some microcontrollers may use four-bit expressions and run at fixed clock rates. Since most devices they control are battery-driven, microcontrollers usually need to be low-power. They are used in many products, from consumer electronics, car engines, computer peripherals, and test and measurement equipment (Martinez-Acosta et al., 2021).

2.5.1 Arduino

In recent times, Arduino has become a favorite open-source electronics platform because of its ease of use with hardware and software among educators, professionals, and enthusiasts. A programmable circuit board, referred to as a microcontroller, forms the base of the Arduino hardware. It may be equipped with various parts, which are normally supplied with a USB connection for power supply and programming, a reset button, and digital and analogue I/O pins that interact with sensors and actuators (Ernesto Serrato Maldonado et al., 2020).

There are numerous Arduino boards, but some are more special than others. The Arduino Mega is a popular choice for complicated projects because of its high number of I/Os and better memory. The Arduino Nano is highly regarded because of its small size, making it possible to fit in tight locations. With its inbuilt USB, the Arduino Leonardo can mimic a keyboard and mouse from a PC. But because of its ease of use and flexibility, the most famous board is the Arduino Uno, an entry-level board.

Arduino has been versatile and can be used for a wide range of applications. Some of its other uses include robotic systems, wearable electronics, home automation systems, and environmental monitoring equipment other than interactive artworks. One of the major advantages associated with Arduino is the huge and active community that offers a lot of tools and resources for debugging and helps in learning at all levels. Books, courses, online forums, and official tutorials aid in making Arduino a very resourceful and accessible tool for all kinds of users (De Oliveira et al., 2021).

2.5.1.1 Arduino UNO R3

Arduino Uno R3 is a microcontroller board built around the ATmega328P (datasheet). The device is equipped with 14 digital input/output pins, 6 analogue inputs, a 16 MHz ceramic resonator (CSTCE16M0V53-R0), a USB port, a power jack, an ICSP header, and a reset button as shown in figure 2.6. Additionally, it comprises a 16 MHz ceramic resonator. Everything required to support the microcontroller is included; all you need to do is power it with a battery or an AC-to-DC adapter or connect it to a computer via a USB cable to get started. Table 2.2 shows the technical specification of Arduino UNO (Marinho da Silva et al., 2024; Via Andrea Appiani, 2024).

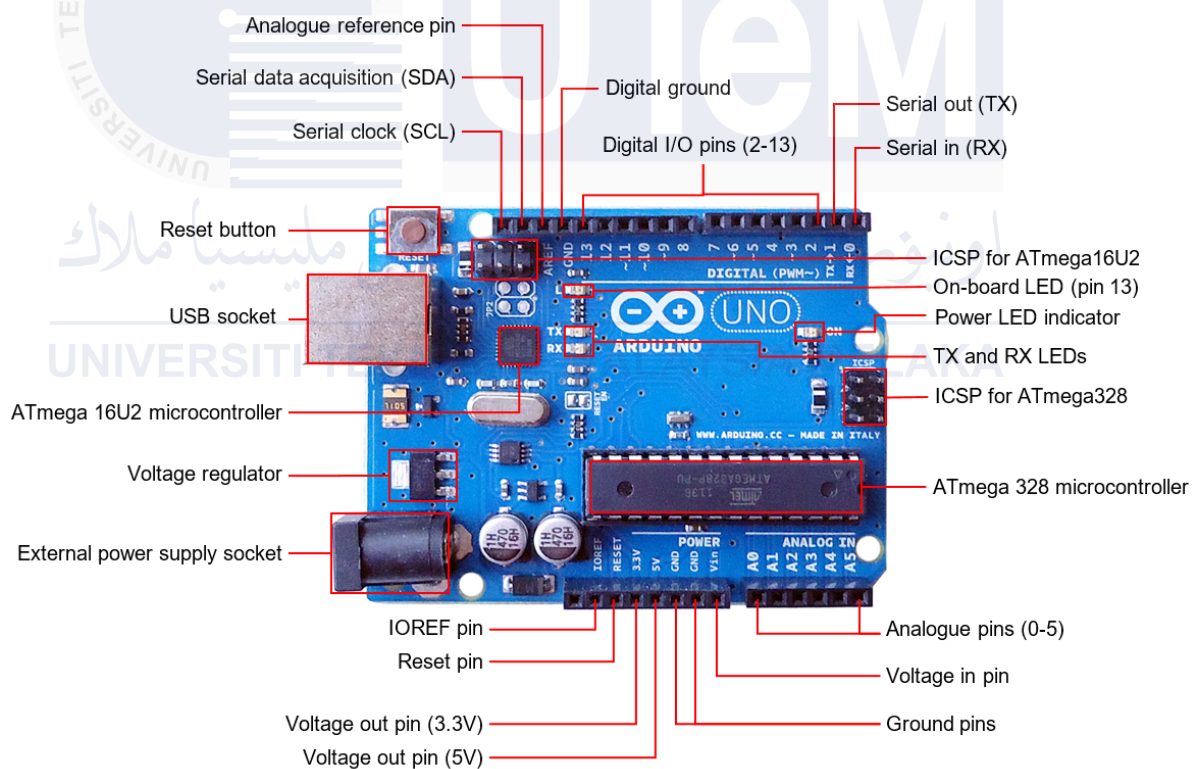


Figure 2.6: Structure of Arduino UNO R3

Source: <https://bdavison.napier.ac.uk/iot/Notes/microprocessors/arduino/>

Table 2.2: The Technical Specification of Arduino UNO

Microcontroller	ATmega328P
Operating Voltage	5V
Recommended Input Voltage	7-12 V
Input Voltage Limits	6-20 V
Digital I/O Pins	14 (Which 6 provide PWM Output)
PWM Digital I/O Pins	6
Analog Input Pins	6
DC Current per I/O Pin	20 mA
DC Current for 3.3V Pin	50 mA
Flash Memory	32 KB (Which 0.5 used by bootloader)
SRAM	2 KB
EEPROM	1 KB
Clock Speed	16 MHz

2.5.1.2 Arduino NANO

The well-known microcontroller board Arduino Nano has been the subject of many studies that investigate its possible uses. Inspired by the famous Arduino platform, the Arduino Nano as shown in figure 2.7 is an incredibly small and flexible microcontroller board, easily integrated into breadboards and small spaces. Depending on the version, it uses either an ATmega328 or ATmega168 microcontroller and operates at a clock speed of 16 MHz. The Nano is a tiny device, approximately 18 x 45 mm in size, yet full of functionality: it includes eight analog input pins and 14 digital input/output pins, among which six can be used as PWM outputs. This board operates on 5V and can be powered either by a regulated 7–12V power supply via the Vin pin or by a Mini-B USB connection as shown in table 2.3. The power and flexibility that the Arduino board combines with its small size make it perfect for a good many applications. It's very detailed documentation and very large supportive community enhance its attractiveness as a tool for projects of advanced complexity and for

prototyping and education (Sudhan et al., 2015; Villarreal-Rios et al., 2019).

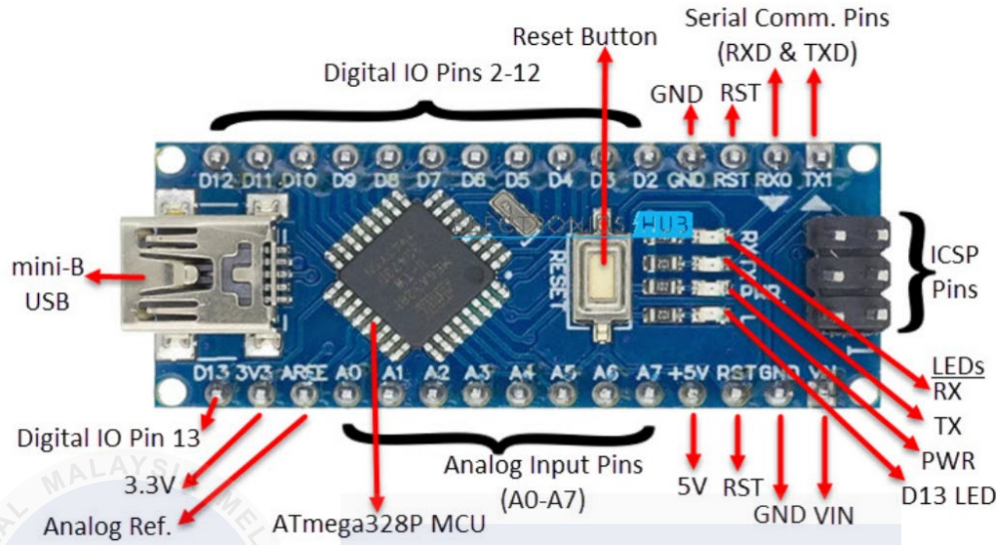


Figure 2.7: Structure of Arduino NANO

Source: <https://www.nextpcb.com/blog/arduino-nano-pinout>

Table 2.3: The Technical Specification of Arduino NANO

Microcontroller	ATmega328
Operating Voltage	5V
Recommended Input Voltage	7-12 V
Input Voltage Limits	6-20 V
Digital I/O Pins	22 (Which 6 provide PWM Output)
PWM Digital I/O Pins	6
Analog Input Pins	8
DC Current per I/O Pin	20 mA (I/O Pins)
DC Current for 3.3V Pin	50 mA
Flash Memory	32 KB (Which 2 used by bootloader)
SRAM	2 KB
EEPROM	1 KB
Clock Speed	16 MHz

2.5.1.3 Arduino MEGA R3

In The Arduino Mega is an advanced board of a microcontroller designed for sophisticated projects that use a large memory with advanced input/output features. The heart of this board is the ATmega2560 microprocessor running at 5V, although the board can accept an input voltage between 6 and 20 V, but it is typically supplied between 7 to 12 V. Having huge connectivity choices for a wide variety of sensors and actuators, it offers 16 analogue input pins and 54 digital I/O pins, out of which 15 are capable of Pulse Width Modulation (PWM) outputs. The 3.3V pin can provide a maximum of 50 mA, while any I/O pin can supply a maximum of 40 mA of DC current. Many studies have demonstrated the versatility and applicability of the Arduino Mega 2560 microcontroller (Kurnia & Li Sie, 2019).

One of the best features of the Arduino Mega is its busy community, from which one can get the maximum number of learning and troubleshooting resources. Such resources include official tutorials, internet forums, books, and courses that help both the beginner and the advanced developer utilize the board effectively. In conclusion, the Arduino Mega is a powerful and versatile microcontroller board due to its broad I/O capabilities and considerable memory resources, making it ideal for challenging and sophisticated applications (Pérez et al., 2019).

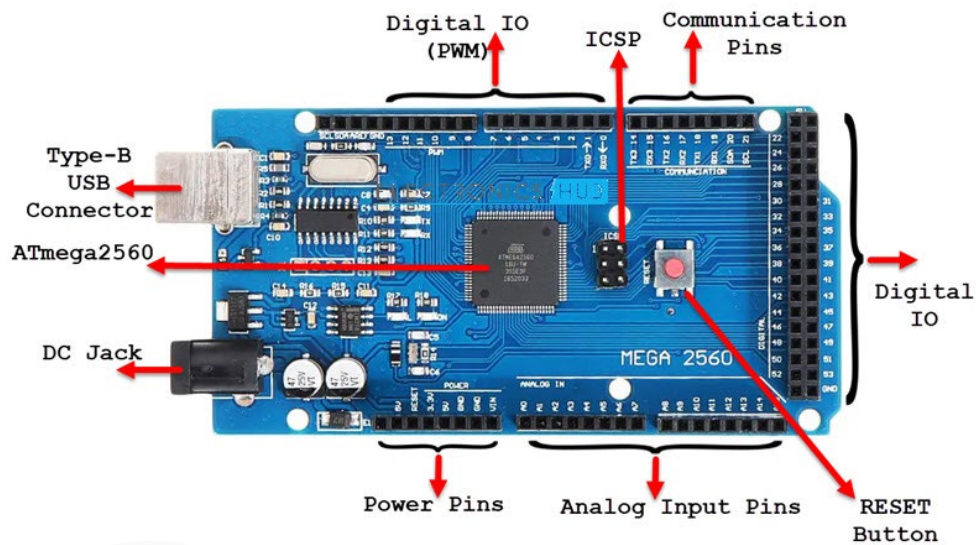


Figure 2.8: Structure of Arduino MEGA

Source: <https://www.electronicshub.org/arduino-mega-pinout/>

Table 2.4 The Technical Specification of Arduino MEGA

Microcontroller	ATmega2560
Operating Voltage	5V
Recommended Input Voltage	7-12 V
Input Voltage Limits	6-20 V
Digital I/O Pins	54 (Which 15 provide PWM Output)
PWM Digital I/O Pins	54
Analog Input Pins	16
DC Current per I/O Pin	20 mA (I/O Pins)
DC Current for 3.3V Pin	50 mA
Flash Memory	256 KB (Which 8 used by bootloader)
SRAM	8 KB
EEPROM	4 KB
Clock Speed	16 MHz

2.5.2 Espressif Module / ESP

This section will cover about the ESP series, which are a family of modules that are quite famous for their onboard Wi-Fi and Bluetooth combined with powerful microcontroller capabilities, a Chinese semiconductor maker producing high-quality advanced microcontroller modules, especially for use in embedded systems and IoT applications. Based on the groundwork set by the ESP8266, Espressif brought the ESP32 into the world, a more advanced microcontroller chip that added Bluetooth capability in addition to Wi-Fi (Kot et al., 2019).

The ESP32 became popular due to its dual-core processor, more GPIO ports, and compatibility for several communication protocols, hence becoming the go-to in more advanced IoT applications that require wireless connectivity and high processing power (Picking et al., 2017). The ESP series chips are designed with processing power and reliable connectivity in compact, low-cost packaging. It is considered an important milestone when the ESP8266, which was introduced in 2014, became a low-cost way of adding Wi-Fi connectivity to a wide variety of projects. Since then, several variants of the ESP8266 have been developed, enhancing the functionality, performance, and ease of integration of the board.

Other than chip manufacture, Espressif offers a broad range of tools and support, including but not limited to documentation, integrated development environments, software development kits, and an active developer and enthusiast community. This ecosystem has been instrumental not just in driving innovations but also in using Espressif modules, which are commonplace in wearables, Internet of Things appliances, home gadgets, and industrial automation.

2.5.2.1 ESP 8266 / NodeMCU

In Espressif Systems manufactures a low-cost Wi-Fi microcontroller called ESP8266 as shown in figure 2.9, which includes a full TCP/IP stack and microcontroller functionality. Its versatility, low cost of purchase, and ease of use make it significantly gaining huge popularity among the IoT community. Its low price allows developers and enthusiasts working on budget-conscious projects to reach out to it. The ESP8266 is integrated with extra functionality like USB-to-serial converters and more GPIOs on development boards like the NodeMCU and WeMos D1 Mini, making development and prototyping easy (*ESP 8266 DATASHEET*, 2015).

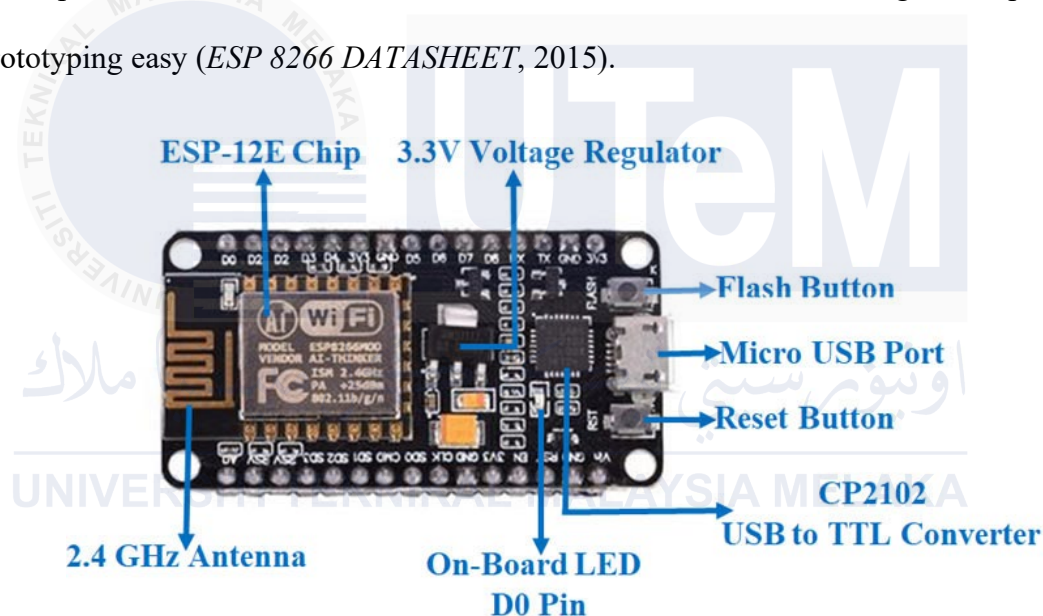


Figure 2.9: Structure of ESP 8266

Source: [NodeMCU ESP8266 Pinout, Specifications, Features & Datasheet](#)
([components101.com](#))

The ESP8266 can be programmed in a variety of settings such as Arduino IDE, MicroPython a lean implementation of Python 3 for microcontrollers, and NodeMCU a Lua-based firmware. Several power-saving modes are supported, making it perfect for applications that run on batteries. There is a vast and vibrant community surrounding the ESP-8266 that provides an immense number of libraries, tutorials, and projects enhancing

its functionality and reducing the time taken to build a project. In summary, the ESP-8266 has emerged as a central element for many IoT applications in that it provides a flexible, powerful, and low-cost way of adding Wi-Fi connectivity to a wide variety of projects, including those running on batteries (Slamin et al., 2019). Table 2.5 shows the technical specification of ESP 8266.

Table 2.5: The Technical Specification of ESP 8266

Microcontroller	Tensilica 32-bit RISC CPU Xtensa LX106
Operating Voltage	3.3V
Recommended Input Voltage	5 V
Input Voltage Limits	2.5 – 3.6 V
Digital I/O Pins	16
PWM Digital I/O Pins	Up to 11 GPIO Pins
Analog Input Pins	1
DC Current per I/O Pin	12 mA
DC Current for 3.3V Pin	50 mA
Flash Memory	4 MB
SRAM	160 KB
EEPROM	Not Available
Clock Speed	80 MHz

2.5.2.2 ESP 32

The ESP32 microcontroller, developed by Espressif Systems, is a highly valued element within the Internet of Things ecosystem, thanks to its versatile functionality and exceptional connectivity. From inside, it is powered by a dual-core Tensilica Xtensa LX6 processor, which offers better processing power and multitasking capabilities essential for processing a variety of jobs related to the Internet of Things effectively. One of the unique selling points of the ESP32 is its support for Wi-Fi and Bluetooth protocols, such as Classic

Bluetooth and Bluetooth Low Energy. Its dual-mode nature provides a way of connecting with a wide range of devices and networks in a seamless manner, making it easier to realize complex IoT applications across various fields (Picking et al., 2017). Figure 2.10 shows the structure of the ESP 32.

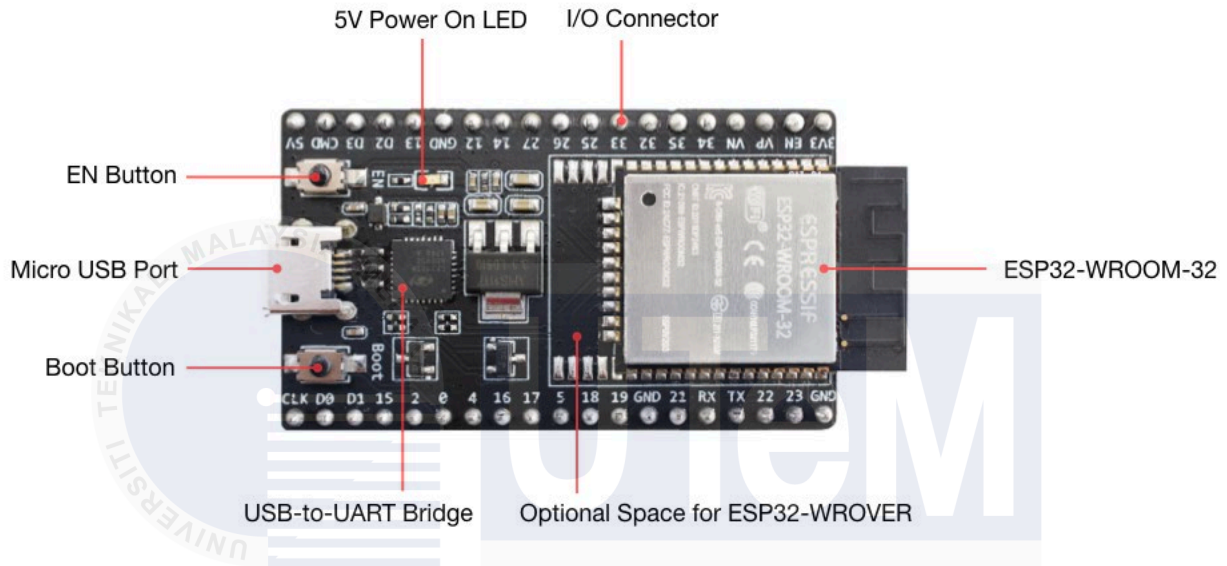


Figure 2.10: Structure of ESP 32

Source: <https://isphome.co.za/shop/all-products/esp32-devkit-v1-wroom-32/>

Another strong points about the design philosophy of the ESP32 is energy efficiency. This is reflected in its low-power modes and functions. Especially, deep sleep mode can be used to drastically cut power consumption when the ESP32 is not in use. This makes it useful for battery powered IoT devices that require extended battery life (Dietz et al., 2022). Table 2.6 indicated the technical specification of ESP 8266.

Table 2.6: The Technical Specification of ESP 32

Microcontroller	Dual-Core, Tensilica 32-bit RISC CPU Xtensa LX106
Operating Voltage	3.3V
Recommended Input Voltage	5 V
Input Voltage Limits	2.3 – 3.6 V
Digital I/O Pins	36
PWM Digital I/O Pins	Up to 16 GPIO Pins

Analog Input Pins	18
DC Current per I/O Pin	12 mA
DC Current for 3.3V Pin	50 mA
Flash Memory	4 MB
SRAM	520 KB
EEPROM	Not Available
Clock Speed	80 MHz (Can be boosted up to 240 MHz)

The ESP32 can be programmed using various development frameworks and languages. The most used programming language is C++, and it can be programmed using the Arduino IDE or Platform IO. In addition, the ESP-IDF (Espressif IoT Development Framework) provides a comprehensive set of libraries and tools specifically for ESP32 development. Performance capabilities and versatility make the ESP32 a valuable component in different IoT applications, including environmental sensing, wearable technology, home automation, and industrial monitoring and control. Its energy efficiency, extensive development support, and seamless integration of bleeding-edge features make it a top option for developers looking to develop creative Internet of Things solutions (Hercog et al., 2023).

2.5.3 Comparisons of Microcontrollers

This section will compare several well-known microcontrollers from Arduino: the Arduino Uno, Arduino Nano, Arduino Mega; and from Espressif Modul: ESP8266 NodeMCU and ESP32 NodeMCU. This section reveals unique features and functionalities worth considering when choosing the best platform for various embedded systems and Internet of Things applications. Table 2.7 shows the comparison between mentioned

microcontrollers.

Table 2.7: Comparison of each Microcontrollers

Microcontroller	Microcontroller	Operating Voltage (V)	Input Voltage (V)	Input Voltage Limits (V)	Digital I/O Pins	PWM Digital I/O Pins	Analog Input Pins	DC Current per I/O Pins (mA)	DC Current for 3.3V Pin (mA)	Flash Memory (KB)	SRAM (KB)	EEPROM (KB)	Clock Speed (MHz)
Arduino UNO R3	ATmega328P	5	7-12	6-20	14	6	6	20	50	32	2	1	16
Arduino NANO	ATmega328	5	7-12	6-20	22	6	8	20	50	32	2	1	16
Arduino MEGA R3	ATmega2560	5	7-12	6-20	54	54	16	20	50	256	8	4	16
ESP 8266 NodeMCU	Tensilica & Xtensa	3.3	5	2.5-3.6	16	8	1	12	50	4	160	N/A	80
ESP 32 NodeMCU	Tensilica & Xtensa	3.3	5	2.3-3.6	36	16	18	12	50	4	520	N/A	80

2.6 Sensing Elements

A range of devices are designed in sensing technology for the measurement and detection of distinct physical events. Within this category, temperature sensors, gas detectors, and motion sensors play vital roles across many applications. A good example of sensing technology would be the infrared sensors, most used for motion detection, which are classified into two groups which are passive and active. Most applications, whether from an industrial or consumer perspective, require a reliable functioning temperature, and such temperatures are monitored through sensors like thermocouples, NTC thermistor modules.

Gas detector sensors, for their part, are also required in identifying different gases, such as an MQ-135, to monitor air quality. Each of these sensors uses special concepts and technological advancements that help them work best with distinct tasks. Responding to a vast range of physical qualities and environmental situations.

2.6.1 Infrared Sensor

A gadget as shown in figure 2.11 that analyses and picks up infrared radiation in its surroundings electrically is called an infrared, or IR, sensor. The astronomer William Herschel made the accidental discovery of infrared radiation in 1800 while he was measuring the temperatures of various colors of light that were divided by prisms (Perera, 2021). Infrared radiation is located just past the red portion of the visible spectrum. He noticed there was infrared radiation present because the temperature was highest just past the red light. Because this radiation has a longer wavelength than visible light, it is invisible to the human eye. Everything that generates heat, or everything that is warmer than around five degrees Kelvin, emits infrared radiation (Danny Jost, 2019; Popa et al., 2019).

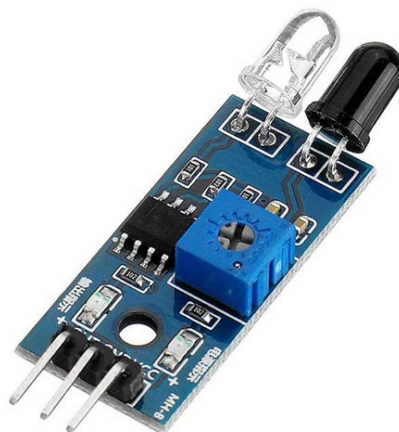


Figure 2.11: Infrared Sensor

Source: <https://www.circuits-diy.com/hw201-infrared-ir-sensor-module/>

Infrared sensors are integral parts of contemporary motion detection systems, serving a vital function in energy management, automation, and security applications. Based on an object's temperature, these sensors pick up infrared radiation, a type of electromagnetic radiation that is released by all objects. Infrared sensors are able to identify the existence and movement of objects, especially living ones, inside a specified region since they are able to sense this radiation (Yeom, 2021).

2.6.1.1 Active Infrared Sensor

Active IR sensors are composed of two major parts: a light-emitting diode and a receiver to emit and detect infrared radiation. The LED produces infrared light, which, when reflecting from surrounding objects, is received by the receiver as shown in figure 2.12. This allows the sensor to recognize movement, or a person, and infer their distance thanks to the technology often applied in radar systems. This makes the technology applicable for proximity sensing or obstacle detection in robotics applications.

Active infrared sensors are applicable both indoors and outdoors and have a wider range of detection. They can be subject to environmental factors like fog, dust, or other particles that deflect the emitted radiation. However, they are more complex and expensive than passive infrared sensors (Asyrani et al., 2013; Chi et al., 2020).

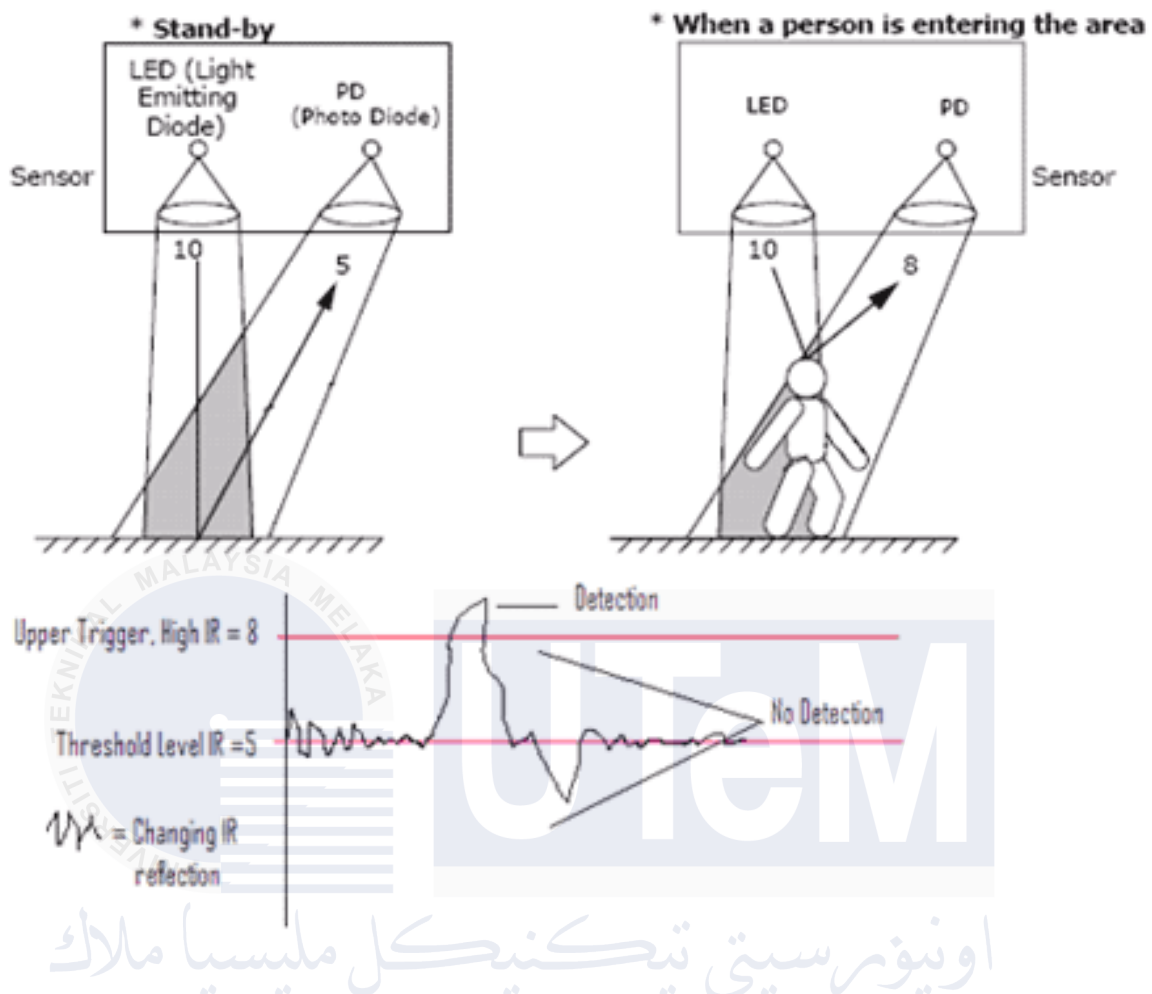


Figure 2.12: Active Infrared Sensor Concept

Source: https://www.researchgate.net/figure/Active-Infrared-Sensor_fig2_287003681/actions#reference

2.6.1.2 Passive Infrared Sensor

The abbreviation for passive infrared is PIR as shown in Figure 2.13. The word "passive" refers to the fact that the sensor observes infrared radiation emanating from the human body in the surrounding area without actively participating in the process. In other words, it does not emit the referred IR signals itself. PIR sensors, being extensively used in motion-detecting applications, include those in home security systems and are extremely common in use cases related to physical security (Cecelia, 2022).



Figure 2.13: Passive Infrared Sensor

Source: <https://www.sciencedirect.com/topics/computer-science/passive-infrared-sensor>

PIR sensors do not emit any radiation to detect infrared radiation emitted by surrounding objects. Table 2.8 shows the technical specification of Passive Infrared Sensor (PIR) (Kastek et al., 2013).

Table 2.8 The Technical Specification of Passive Infrared Sensor (PIR)

Model	HC-SR501
Range of Working Voltage	4-12V (+5 Recommended)
Output Voltage	3.3 V
Working Voltage	3.3-5 V
Current Drain	< 60 uA
Detection Angle	< 140°
Number of Output Pins	3 (Vcc, Output & Gnd)
Blockade Time	2.5s (Default)
Working Temperature	-20 – +80 °C

When an infrared-emitting moving item enters the sensor's field of vision, PIR working principle will detect a difference in infrared levels between the two pyroelectric elements, which sends an electrical signal to an embedded computer. The latter, upon detecting an anomaly, such as a heated object like an intruder blasts the alert. PIR sensors have the advantages of ease of use, affordability, and energy efficiency. Their performance will be affected by changes in temperature around them or by obstacles in their line of view and can only detect within the detecting area (Asyrani et al., 2013; Cecelia, 2022).

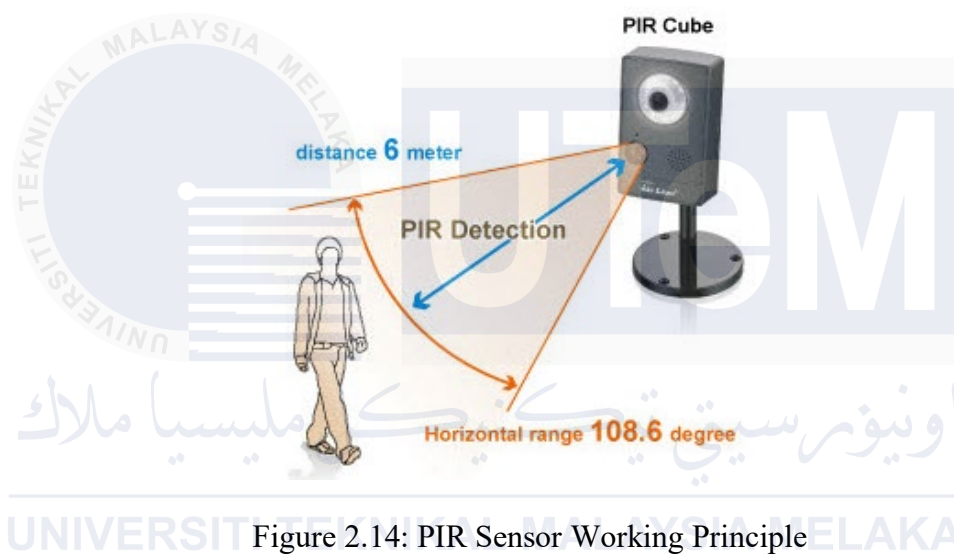


Figure 2.14: PIR Sensor Working Principle

Source: <https://www.elprocus.com/passive-infrared-pir-sensor-with-applications/>

2.6.2 Temperature Sensor

The temperature sensors are essential to many different sectors and applications because they offer precise and dependable temperature readings. With the help of these sensors, which translate temperature variations into electrical impulses, thermal conditions can be precisely monitored and controlled. In this project, findings about the NTC Thermistor Sensor Module are the most popular temperature sensors, each with special features and benefits for measuring temperature.

2.6.2.1 NTC Thermistor Sensor Module

The NTC thermistor sensor module, as illustrate in Figure 2.15 measures the ambient temperature by making use of the change in resistance with temperature. Thermistor semiconductors have a characteristic of reducing in resistance with an increase in temperature. In general, a sensor module consists of the NTC thermistor, an output terminal, and a signal conditioning circuit. The fluctuation in resistance of an NTC thermistor can be interpreted as a temperature reading because of a change in temperature as shown in the Table 2.9 technical specifications of NTC Thermistor Sensor Module (Aleksic et al., 2019; Hardian et al., 2021).

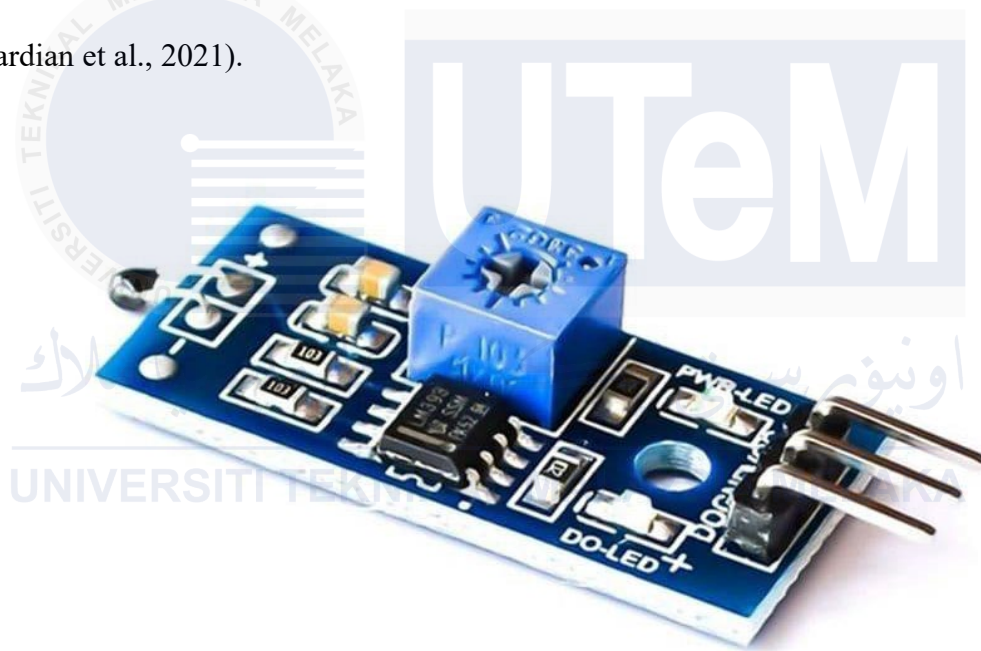


Figure 2.15: NTC Thermistor Sensor Module

Source: <https://www.sainapse.com.my/sensor/temperature/ntc-thermistor-temperature-digital-sensor-module>

Table 2.9 The Technical Specification of NTC Thermistor Sensor Module

Model	MF52-103
Recommended Input Voltage	3.3 – 5 V
Output Current	15 mA
Output Type	Digital (High & Low)

Resistance at 25°C	10 k Ω \pm 1%
Beta Value	3950K \pm 1%
Operating Temperature Range	-40°C to +125°C
Accuracy	\pm 0.5°C
Response Time	< 10s
PCB Size	32 mm x 14 mm

Several advantages of using NTC thermistor sensor modules include high sensitivity to temperature changes for precise and accurate temperature readings. NTC thermistors are largely available for a wide range of applications due to their cost-effective nature and ease of use. Furthermore, they are fast response devices and detect the temperature change with speed, making them ideally suited for cases where real-time monitoring is required (Hardian et al., 2021).

However, there are some drawbacks to NTC thermistor sensor modules. One of the limitations of NTC thermistors is that they have a non-linear response to temperature changes, making calibration and adjustment necessary to ensure accurate temperature readings along the full operating range. Furthermore, there is generally a self-heating effect in NTC thermistors, whereby heat is generated when an electrical current passes through the thermistor, thus causing errors in temperature readings. The accuracy and stability of the NTC thermistor can deteriorate over time due to factors such as aging, environmental conditions, and mechanical stress (Williams et al., 2021).

2.6.3 Gas Detector Sensor

A gas detector sensor is a device that produces an output signal in response to the presence of a certain gas in the air. These sensors play an important role in many sectors and applications for safety, environmental monitoring, and process control depending on the kind of gas being detected, several concepts underlie the operation of gas detector sensors.

Most common applications of gas detector sensors are in gas detection systems, environmental monitoring stations, stationary gas detection systems applied to industrial sites, or portable gas detectors. They are crucial to avoid accidents, ensuring safety, protecting the environment, and in compliance with laws related to exposure limits for gases.

2.6.3.1 MQ-135 Sensor

The MQ-135 sensor as shown in Figure 2.16 is widely used in air quality monitoring applications because it can detect a wide range of gases, including ammonia (NH_3), nitrogen oxides (NO_x), alcohol, benzene, smoke, and carbon dioxide (CO_2). This sensor can be used under several detection and monitoring configurations, owing to its analogue and digital outputs. Flexibility in adjusting its sensitivity under diverse environmental circumstances is achieved with a potentiometer on the module (Lumbangaol et al., 2022).

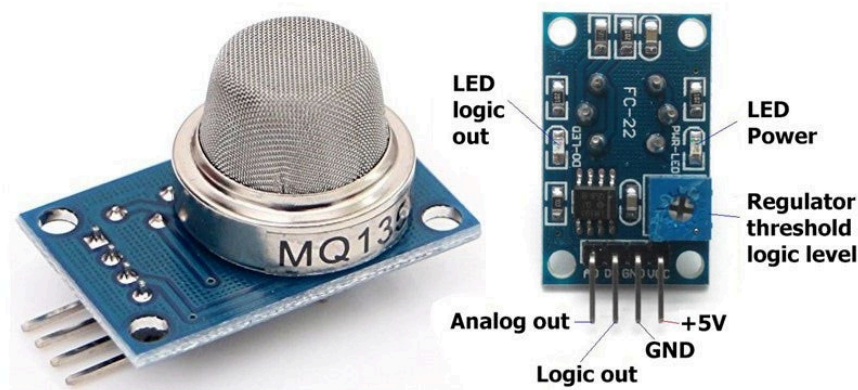


Figure 2.16: MQ-135 Sensor

Source: <https://vishaworld.com/products/mq135-air-quality-control-gas-sensor-module>

The basis of the operation of the MQ-135 sensor is a chemical reaction between the components inside the sensor and the target gases. As a response to this reaction, the output voltage changes by altering the internal resistance of the sensor. To realize reliable readings, the sensor needs to be calibrated. In pure air exposure, a baseline value must be created. Real-time data is subsequently contrasted with this baseline to ascertain the concentration of identified gases. Table 2.10 shows the MQ-135 air quality sensor specifications.(Chiu et al., 2021).

Table 2.10: MQ-135 air quality sensor specifications

Detection Scope	Wide
Sensitivity & Response	High & Fast
Recommended Operating Voltage	+5 V
Targeted Gases	NH ₃ , alcohol, NO _x , Benzene, CO ₂ , smoke, etc
Range of Analog Output Voltage	0 – 5 V
Range of Digital Output Voltage	0 – 5 V
Duration of Pre-Heating	20 s
Heating Voltage	5V±0.1
Load Resistance	Adjustable
Heater Resistance	33ohms±5%
Heating Consumption	<800mW
Operating Temperature	-10°C to 45°C
Storage Temperature	-20°C to 70°C
Related Humidity	<95%Rh
Oxygen Concentration	21%
Sensing Resistance	30kiloohms to 200kiloohms
Concentration Slope Rate	≤0.65
Pre-Heat Time	over 24 hrs

The use of the MQ-135 sensor is diverse and includes smart home automation, industrial safety systems, air quality monitoring, vehicle safety system, and healthcare settings. An Arduino or other microcontroller can be used in the incorporation of the MQ-135. A simple Arduino code example reads the digital value from the DO pin and the analogue value from the AO pin of the sensor, followed by the outputting to the serial monitor (Reza, 2022).

2.7 Major Element of Solar Power System

Solar power is a renewable energy source that generates electricity and heat from the sun. This source of clean, abundant, and sustainable energy provides a healthy substitute for fossil fuels and makes a significant contribution to reducing greenhouse gas emissions. Solar energy is another source of alternative energy that is affordable and environmentally friendly. It is also a source of energy that can be harnessed throughout the year and replace conventional energy, whose raw materials are ever becoming less and less and have disastrous long-term effects on the environment, such as noise, air pollution, and waste (Sofijan, 2019).

In solar power systems, concentrated solar radiation is converted into electrical energy through photovoltaic (PV) panels. At the same time, it also produces thermal energy. With advancing technology and reduced costs, solar electricity is increasingly obtainable and economically viable for commercial, industrial, and residential purposes. As the world continues to shift to sustainable sources of energy, solar power is key for the sustainability of the environment and maintaining energy independence (Seri et al., 2021; Sofijan, 2019).

A solar power system consists mainly of solar panels, a charge controller, a battery bank, an inverter, electrical appliances (load), mounting systems, and wiring and electrical

parts. The main component of the system is solar panels, which absorb solar light and convert it into direct current (DC) electricity. The DC electricity generated by these solar panels is stored in the battery bank for the time when the solar panels are not generating electricity, like at night or during a cloudy day. The charge controller regulates voltage and current from the solar panels to prevent overcharging and thus deliver efficient power to the battery bank. Since most domestic and commercial equipment use alternating current, an inverter changes DC electricity, stored from the sun, into AC. Other necessary parts of the system are wiring and electrical components, like cables, connectors, switches, and circuit breakers, needed to connect all the components of the solar power system safely and efficiently (Prof. Neha V. Sulakhe et al., 2022).

2.7.1 Solar Panels

A solar panel is a device that utilizes photovoltaic cells to transform sunlight into electricity. Photovoltaic cells contain components that, upon being exposed to light, create excited electrons. When those electrons flow through a circuit, they produce direct current (DC) electricity. This electricity could be stored in a battery for later use, or it could be directly used to power various gadgets (Prof. Neha V. Sulakhe et al., 2022).

A solar panel is a component that is integral to every solar power system, for it offers a sustainable and clean alternative to traditional energy sources. They are therefore very important in tapping renewable energy sources because they cut down greenhouse gas emission and reliance on fossil fuels. Solar panels are usually installed in large collections called arrays or systems. A photovoltaic system usually contains one or more solar panels, an inverter that changes DC electricity into AC electricity, and sometimes other parts such as controllers, meters, and trackers (Nicola et al., 2021).

Such systems are often seen on the rooftop of residential, commercial, and industrial

buildings, as well as in solar farms that feed electricity into the grid. Other than reducing greenhouse gas emissions and the cost of electricity, solar panels use clean, renewable energy. They have, however, some disadvantages: they are highly expensive initially, rely on the availability and intensity of sunlight, and require frequent cleaning (Drozd & Scherbak, 2021; Teixeira & Pinto, 2020).

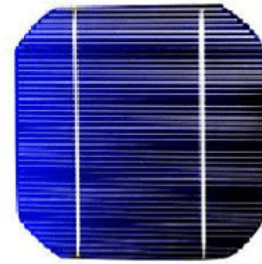
Despite these challenges, solar panels have been used for a wide array of applications in the commercial, industrial, and residential sectors. It is also used in space missions as a reliable source of power in remote locations, frequently with batteries. Solar panel use is increasingly becoming very common as the prices continue to drop and the technology advances, making a great contribution to the sustainability of the world's energy supply (Gong et al., 2019).

2.7.1.1 Monocrystalline Solar Panels

Monocrystalline solar panels as shown in Figure 2.17 are made of single, continuous crystal silicon. In addition to excellent efficiency and a long lifespan, some of their other distinguishing features are cut corners and a uniform black color (Cotfas & Cotfas, 2019). During the fabrication process, a single silicon crystal is grown so that more electrons can be free for energy conversion. These panels work best in applications that require the highest power output but have very little space (Fluieraru et al., 2019).



Solar panel



Solar cell

Figure 2.17: Monocrystalline Solar Panel

Source: <https://learn4electrical.altervista.org/difference-between-monocrystalline-and-polycrystalline-solar-panels/>

Regarding the efficiency, monocrystalline solar panels are the most efficient kind of silicon-based solar panels available, with typical efficiency rates ranging from 15% to 23% (AL-SULTAN & ALTINOLUK, 2022; Tamara Jude & Angela Bunt, 2024). They are able to produce more electricity from the same amount of sunlight because they have better efficiency than polycrystalline or thin-film panels. Based on the above, monocrystalline solar panels are the best option to optimize performance and efficiency, mainly when there is not much space. Their high efficiency, robustness, aesthetic appeal, and adaptability to different applications often make them a must use panel for many residential, commercial, and industrial solar projects.

2.7.1.2 Polycrystalline Solar Panels

Several silicon crystals are fused together to form polycrystalline solar panels as shown in Figure 2.18. They are less effective than monocrystalline panels and have a distinct bluish color. Since silicon is melted and run into a mold, the process of making the wafers is less complex and costly. This is usually used for giant solar farms and industrial uses because they find application when cost is a principal factor, and space is not as much of a concern (Shekoofa et al., 2020).

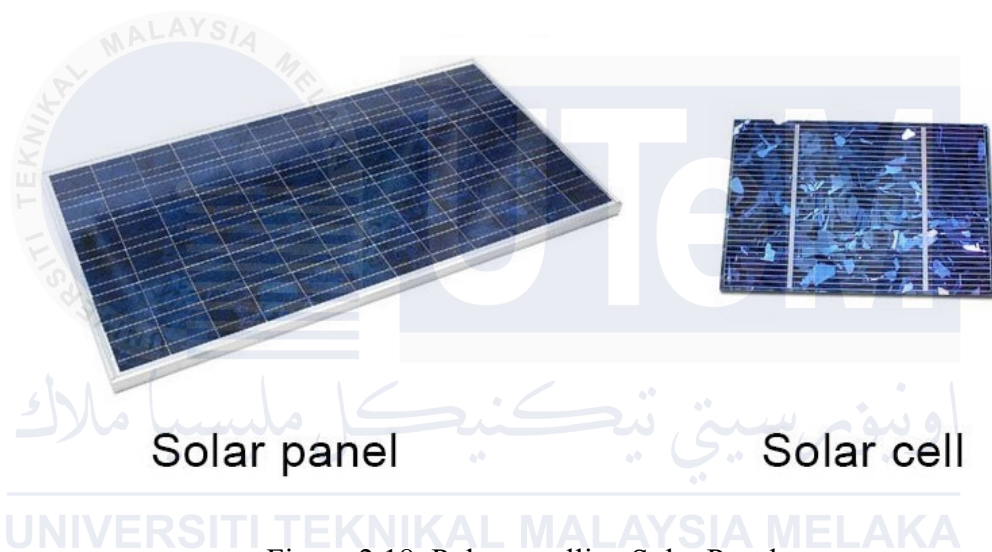


Figure 2.18: Polycrystalline Solar Panel

Source: <https://learn4electrical.altervista.org/difference-between-monocrystalline-and-polycrystalline-solar-panels/>

The efficiency rates of polycrystalline solar panels are often lower, ranging from 13% to 16%. Lower energy conversion efficiency in polycrystalline cells is caused by the many crystal barriers that obstruct electron passage (Almadhhachi et al., 2022; Tamara Jude & Angela Bunt, 2024). Nonetheless, polycrystalline panel efficiency keeps improving due to unending technological advancement. Polycrystalline solar panels represent the more affordable way to generate solar energy. Although polycrystalline panels are less effective than monocrystalline, they nevertheless fit perfectly for large-scale installations and budget projects due to their lower cost and less complex process of manufacturing. Their ability to

be strong, last long, and be versatile in many applications secures them a continued and broad future in the solar energy sector.

2.7.1.3 Comparison of Solar Panels

The decision between monocrystalline and polycrystalline solar panels is important when looking at solar energy choices. varied types have varied features, costs, and efficiency, which affect which applications and installations they are appropriate for. It is essential to comprehend the distinctions between these two well-known solar panel technologies in order to make wise choices about solar power systems. In Table 2.11 determined the comparison between Monocrystalline & Polycrystalline solar panels(Tamara Jude & Angela Bunt, 2024).

Table 2.11: Comparison between Monocrystalline & Polycrystalline Solar Panel

Factors	Monocrystalline	Polycrystalline
Silicone Structure	Single Continuous Crystal Structure	Multiple Crystals Melted Together
Panel Appearance	Uniform Black Color with Cut Corners	Distinctive Blue Hue with A Square Shape
Average Cost	More Expensive	Less Expensive
Efficiency	15% to 23%	13% to 16%
Space Efficiency	Less Space for Same Power Output	More Space for Same Power Output
Durability	Longer Lifespan & Higher Durability	Shorter Lifespan & Lower Durability
Temperature Coefficient	Lower Temperature Coefficient, More Efficient in Heat	Higher Temperature Coefficient, Less Efficient in Heat
Aesthetic Appeal	Sleeker, More Appearance	Less Uniform, More Speckled Appearance
Manufacturing Process	More Energy Intensive	Less Energy Intensive

2.7.2 Battery Bank

A battery bank, storing electrical energy produced by solar or wind turbines, is a requisite in most renewable energy systems. In case the energy-generating source is sporadic or unavailable, the extra energy stored in the battery banks assures a steady and dependable power supply. This feature makes them indispensable for backup power solutions, off-grid systems, and the increasing of the effectiveness of renewable energy setups (Lopez-Garcia et al., 2019).

To obtain the required voltage and capacity, a battery bank is made up of several batteries hooked either in series or parallel. These configurations, sometimes called battery strings, are an essential element of standalone solar energy systems. When demand for electric devices goes beyond solar energy supply, batteries store the energy generated by solar panels and disperse it. The battery should hold enough energy to power electronics for a few days through all the cloudy and nighttime conditions. When a solar battery is fully charged and discharged, it goes through a cycle, where the depth of discharge of a solar battery is the amount of discharge that occurs.

There are various varieties of rechargeable batteries, all with their pros and cons, utilized to store the excess energy produced by solar panels. Even though lead-acid batteries are renowned for their dependability and affordability, their lifespan is comparatively short, and their energy density is lower (Ullah et al., 2021). Because of its high energy density, extended longevity, and low maintenance needs, lithium-ion batteries are perfect for both portable devices and home solar installations.

Nickel-metal hydride batteries have an energy density lower than lithium-ion batteries but higher than lead-acid batteries and hence offer a compromise between price and performance. They are utilized in smaller applications like portable electronics and hybrid

cars, and they are more environmentally friendly than lead-acid batteries (Lopez-Garcia et al., 2019). Table 2.12 shown the comparison between Lead-Acid, Lithium-ion & Nickel-Metal Hydride Batteries.(Haram et al., 2021)

Table 2.12: Comparison between Lead-Acid, Lithium-ion & Nickel-Metal Hydride Batteries

Specifications	Lead-Acid	Lithium-ion	Nickel-Metal Hydride
Specific Energy Density (Wh/kg)	30-50, Low	90-120, High	60-120, Moderate
Internal Resistance	Very Low	Very low	Low
Life cycle (80% Depth of Discharge)	200-300	1000-2000	300-500
Charge time	8-16 Hours	1-2 Hours	2-4 Hours
Overcharge tolerance	High	Low	Low
Self-discharge/month (Room Temperature)	5%	<5%	30%
Cell Voltage (nominal)	2V	3.2-3.3V	1.2V
Charge Temperature	-20 to 50°C	0 to 45°C	0 to 45°C
Discharge Temperature	-20 to 50°C	-20 to 60°C	-20 to 65°C
Maintenance Requirements	3-6 Months	Maintenance-Free	Full Discharge Every 90 Days
Cost	Low	High	Moderate
Safety Requirements	Thermally Stable	Protection Circuit Mandatory	Thermally Stable, Fuse Protection
Environmental Impact	Moderate	Low	Low
Charging Efficiency	Moderate	High	Moderate
Self-Discharge Rate	High	Low	Moderate

2.7.2.1 Lead-Acid Batteries

Lead-acid batteries as shown in Figure 2.19 are one of the oldest and most widely applied rechargeable batteries for the storage of energy. They consist of sponge lead plates and lead dioxide dissolved in sulfuric acid as the electrolyte. In most applications, they have seen very wide use due to their reliability, affordability, and ease of recycling. Compared to other types of batteries, lead-acid batteries are heavier and physically larger for the same capacity. Moreover, they have a much shorter lifespan from 3 to 5 years and a lower energy density. They must also be kept in top condition by periodic additions of electrolyte and proper charging. With these drawbacks, they are commonly applied to large-scale, off-grid systems and backup power supplies where space is not a key issue and cost is a major concern.



Figure 2.19: Lead-Acid Batteries

Source: <https://www.lazada.com.my/products/wei-sheng-6v-45ah-rechargeable-sealed-lead-acid-battery-rb645-i2385495245.html>

2.7.2.2 Lithium-ion (Li-ion) Batteries

Energy storage is increasingly being focused on Lithium-ion batteries, which boast a long life, high-energy density, and low maintenance requirements. Figure 2.20 shown the Lithium-ion batteries. These batteries are powered by lithium-ions, which move through the anode and cathode during discharge and charging cycles. They are more compact and lightweight compared to lead-acid batteries, which makes them perfect in applications where weight and space are of importance, such as portable devices, electric vehicles, and home solar systems. Therefore, lithium-ion batteries have been characterized by great efficiency, long life, and short charging times. In general, they may be a little more expensive upfront but pay themselves back through increased efficiency and longer life. Thus, lowering overall expenses over time. Lithium-ion batteries retain their charge longer because their self-discharge rate is very low.



Figure 2.20: Lithium-ion Batteries

Source: <https://npplithium.com/li-ion-vs-ni-mh-battery-which-one-is-better/>

2.7.2.3 Nickel-Metal Hydride (NiMH) Batteries

Nickel-Metal Hydride Batteries as shown in Figure 2.21 make a good balance between performance and cost. Their composition includes alkaline electrolyte, hydrogen-absorbing negative electrode, and nickel hydroxide positive electrode. The energy density offered by NiMH batteries is greater than that of lead-acid batteries, although less than that of lithium-ion batteries. Not containing harmful heavy metals like cadmium makes lead-acid batteries more environmentally responsible. NiMH cells are also less maintenance than lead-acid batteries and have a shorter lifespan of five to ten years. A large application in large-scale energy storage systems is not so usual for them, but they are in wide use in small applications like consumer electronics and portable devices and, recently, hybrid cars.

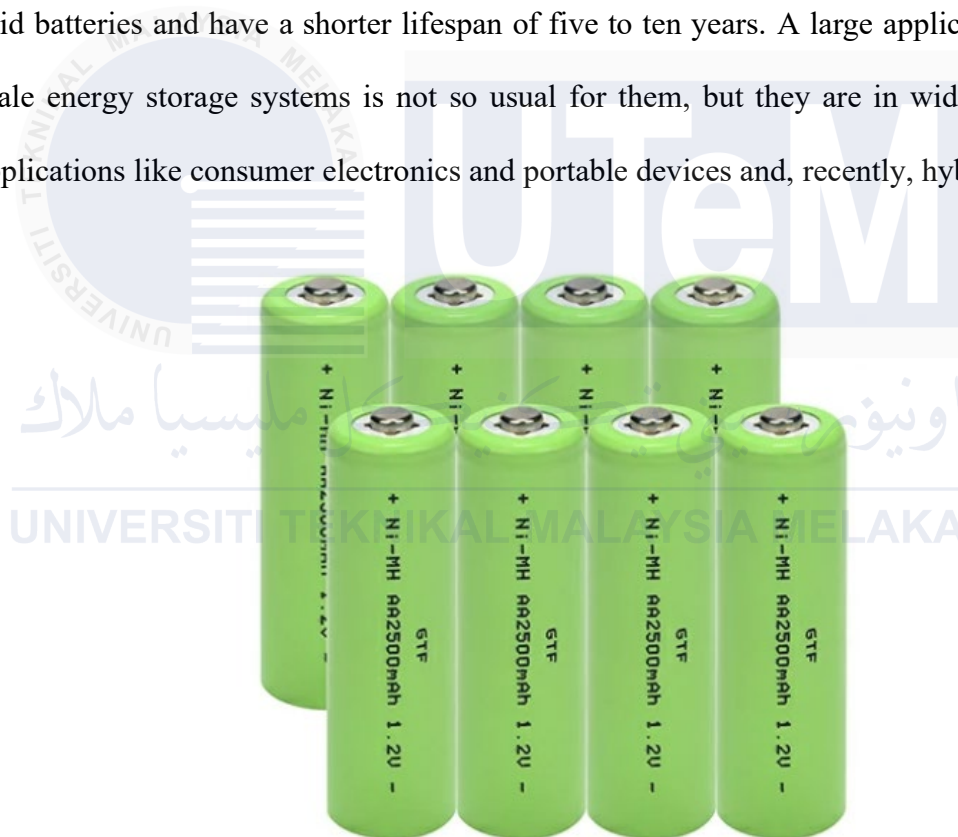


Figure 2.21: Nickel-Metal Hydride Batteries

Source: <https://npplithium.com/li-ion-vs-ni-mh-battery-which-one-is-better/>

2.8 Global System for Mobile Communication (GSM)

The Global System for Mobile Communication was designed for the second generation 2G of digital cellular networks, due to its superiority in voice and data services over the former analogue cellular networks. GSM is the most used mobile communication standard in the world, created by ETSI, providing dependable and stable communication technology (Ibrahim et al., 2021).

A Wi-Fi module and a SIM card module with an Arduino can activate GSM capabilities. These parts enable cellular and internet communication for the Arduino, opening up a whole range of possibilities such as IoT devices, communication systems, and remote monitoring, just to mention a few.

2.8.1 Wi-Fi Module

For internet-based communication, an Arduino could communicate with WiFi networks using a WiFi module, such as the ESP 8266 or ESP32. These modules are responsible for a few internet communication protocols because they have an integrated microcontroller and a TCP/IP stack. The integration of Wi-Fi modules in Arduino projects is able to send data to web servers, receive data from online sources, and easily integrate with a number of internet-based applications and Application Program Interfaces, APIs (Aithal et al., 2024).

Among the well-known WiFi modules such as the ESP8266 NodeMCU as shown in Figure 2.22 is a microcontroller and a System-on-Chip (SoC) that can execute a full TCP/IP protocol stack. Because of its low price in market industry, ease of use, and strong community support, it is highly suggested. With the ESP8266, developers can quickly create

internet-of-things applications that need internet connectivity, control devices remotely, and transfer sensor data to the cloud.

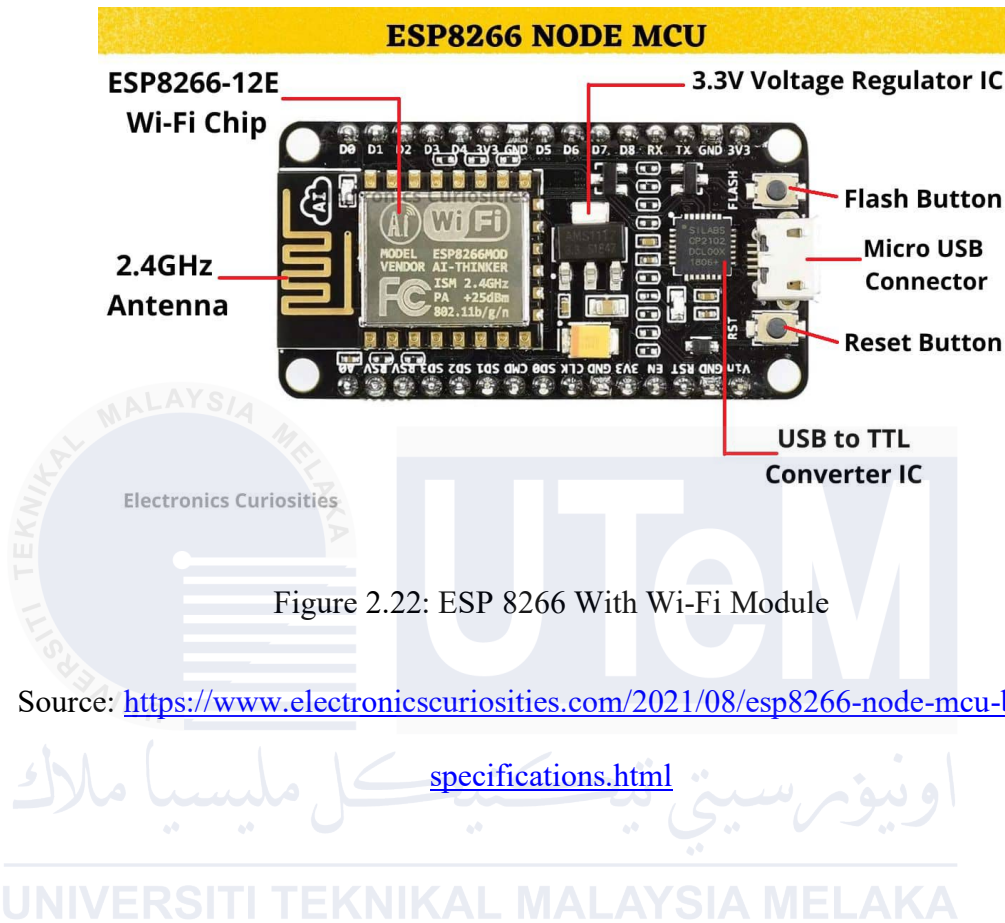


Figure 2.22: ESP 8266 With Wi-Fi Module

Source: <https://www.electronicscuriosities.com/2021/08/esp8266-node-mcu-board-specifications.html>

2.8.2 GSM Module (SIM-900 A)

The entire aspect of GSM discussed herein, therefore, requires a GSM module in order to be fully harnessed. In this device, it was based on a Dual Band GSM/GPRS-based SIM900A modem from the SIMCOM company. The GSM/GPRS modem allows programmers to open GPRS connections to the internet using the integrated TCP/IP stack, which enables a host of data transfer activities. The rugged small size of the SIM900A wireless module also makes it suitable for most applications (Pawar et al., 2008). This SMT-type full GSM/GPRS module has an inbuilt AMR926EJ-S core and a powerful single-chip CPU. It provides project developers with a compact and cost-effective solution to implement GSM/GPRS in their products (Qasim et al., 2023).



Figure 2.23: SIM-900A

Source: <https://www.utmel.com/components/sim900a-gsm-module-how-to-use-sim900a?id=2114>

2.9 Summary

The Anti-Child Locking System combines several elements to improve child safety and alerting mechanisms in vehicles. Starting with the fundamentals, the system is made up of a strong set of carefully chosen hardware and software components that enable it to perform as planned. A polycrystalline solar panel, an PWM charge controller, and a battery bank are the main parts of the solar power system. With this solar design, the system is guaranteed a sustainable power source, reducing dependency on traditional power sources by using renewable energy. In parallel, the Arduino UNO microcontroller serves as the central processing unit, orchestrating the system's operations with efficiency and minimal power consumption. The selection of Arduino UNO is based on its simplicity and low power consumption, making it an ideal choice for this application. Sensor integration is a crucial aspect of the system, with the PIR sensor serving as the main sensing elements for detecting

motion within the vehicle simultaneously working along with a gas detector sensor and a temperature sensor. Additionally, the system incorporates a suite of actuators, including the GSM module for alerting the vehicle owner and the LED alarm light indicator for visual signaling that both will successfully execute both objectives of this project. Through strategic planning and combinations of these components, the Anti-Child Locking System detects and mitigates potential hazards proactively, thereby keeping children safe inside the vehicle.



CHAPTER 3

METHODOLOGY

3.1 Introduction

Methodology is a systemically structured study of procedures employed in a subject, and it is not only applied procedures but also constitutes the analysis of the rules, guidelines, and postulates involved in a particular study field. This set of coherently philosophical theories, conceptions, and ideas provides a logical basis for undertaking research through the scientific method. Methodology in project development is a step-by-step process where each step contributes to the project's completion. It ensures that activities are performed following procedures for risk reduction and the achievement of objectives.

Such a systematic method improves the validity and reliability of findings, productivity, and identification and rectification of problems at an early stage, it also ensures consistency and reproducibility. The process of a project will typically consist of stages that must be followed with care in the production of quality outcomes. In this chapter will be included with planning, designing, implementation, software development, and evaluation. In every field of study, following a systematic methodology is paramount since it enhances the chances of the completion of a project effectively with fewer problems and more in line with the set initial objectives.

3.2 Research Flowchart

A research flowchart as shown in Figure 3.1 represents the visual aid to provide a systematic roadmap or planning that enables to execute a project of listing tasks that must be done one after the other.

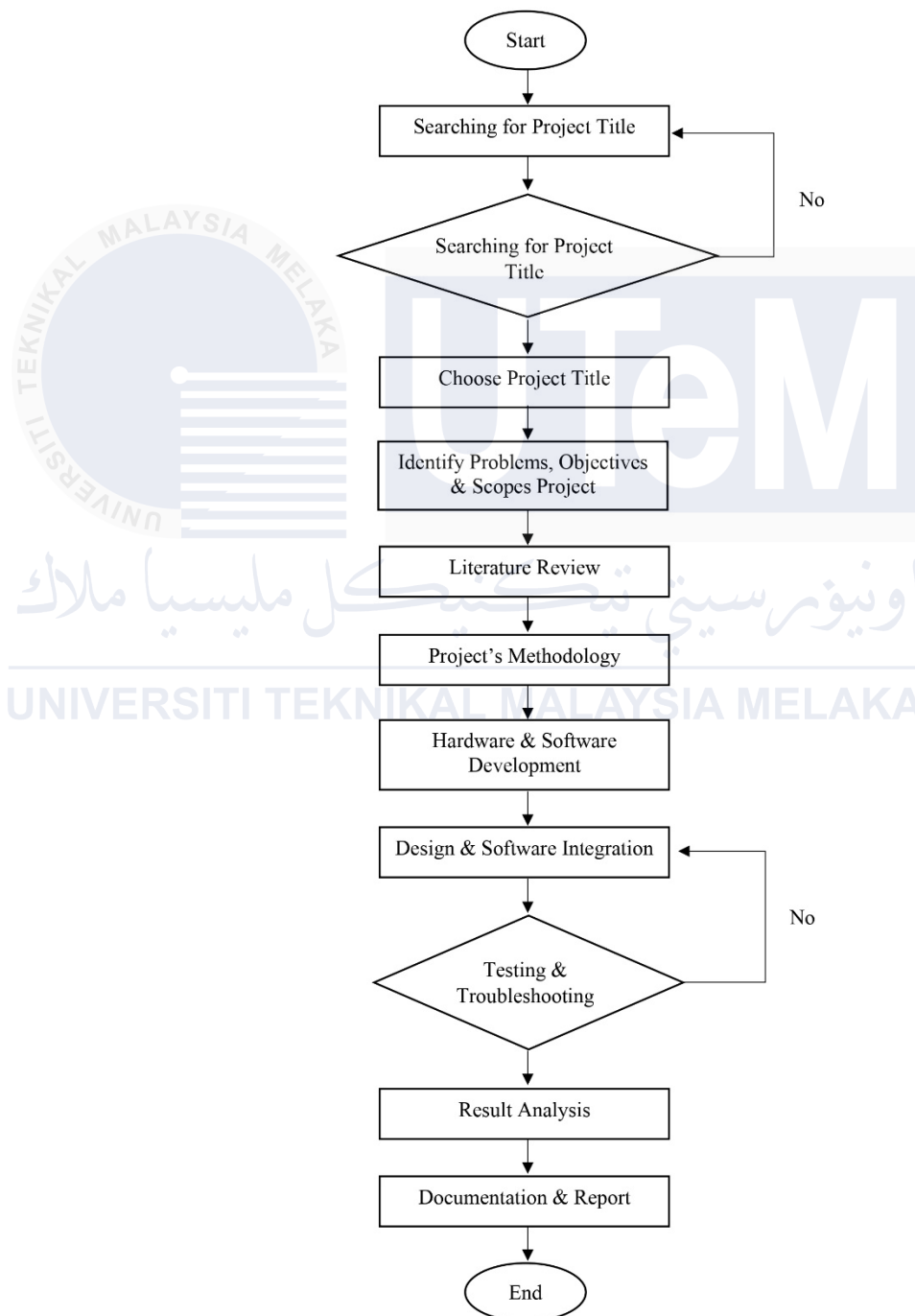


Figure 3.1: The Flowchart of the Overall Research

3.3 Block Diagram of Anti-Child Lock System in Vehicle

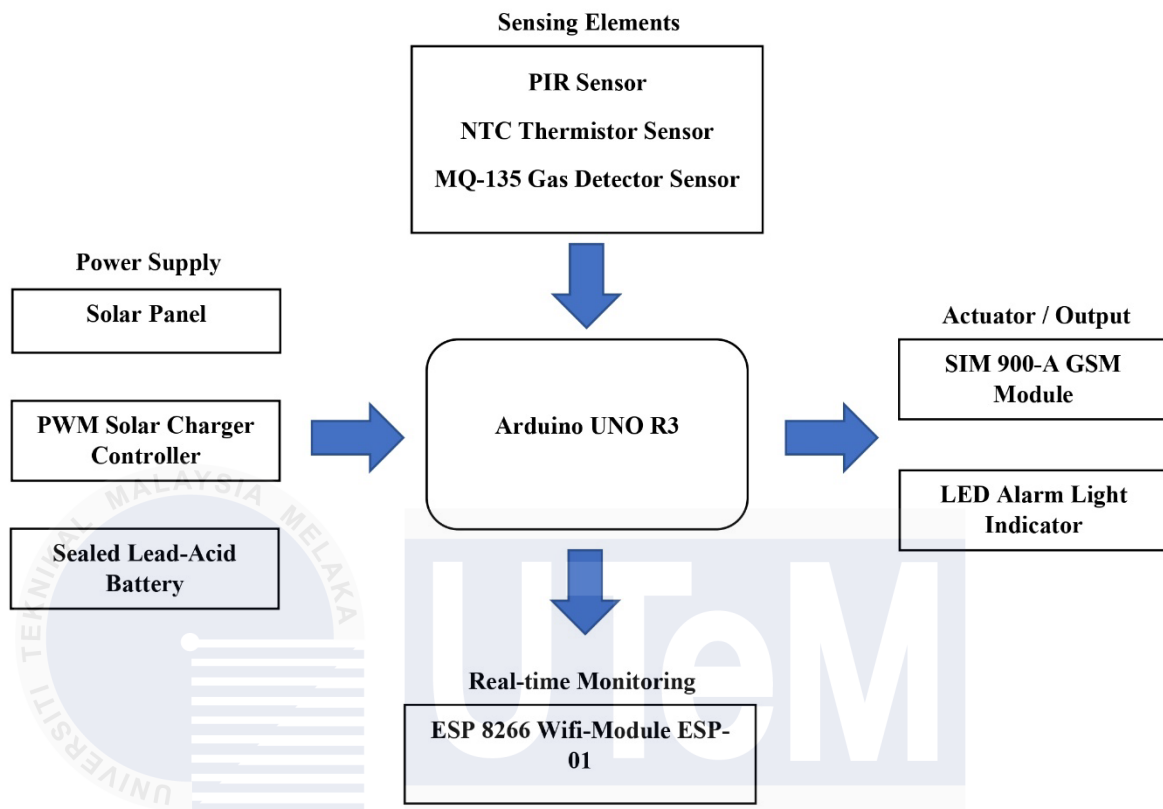


Figure 3.2: Block Diagram of Anti-Child Lock System in Vehicle

Figure 3.2: Block diagram of Anti-Child Lock System in a vehicle. In this system, the main controller is an Arduino UNO R3 microcontroller, acting as a focal point, where integration of all the other components is controlled. Sealed lead-acid batteries are used along with a solar panel to provide sustainable input; a PWM solar charge controller regulates the power for stability. Its basic sensing elements would be a sensor- like, MQ-135 gas detector sensor, an NTC thermistor sensor, or a PIR sensor-three of which interfaced via Arduino to check on an environment. And processing inlet data obtained with Arduino sends the signals triggering the actuations of the components of its outlet: such as a communication module composed of a GSM module 900-A sim and light indicator LED Alarm. Other functionalities include real-time data monitoring enabled by the ESP8266 WiFi module-ESP-01, which transmits data to IoT platforms such as ThingSpeak. This also integrates the

operation for efficient monitoring of critical parameters with much ease, adding on the overall functionality and safety of the system.

3.4 Flowchart of Anti-Child Lock System in Vehicle

As illustrated in Figure 3.3, this flowchart will entirely describe how Anti-Child Lock System working principle in vehicle especially after ignition switched off.

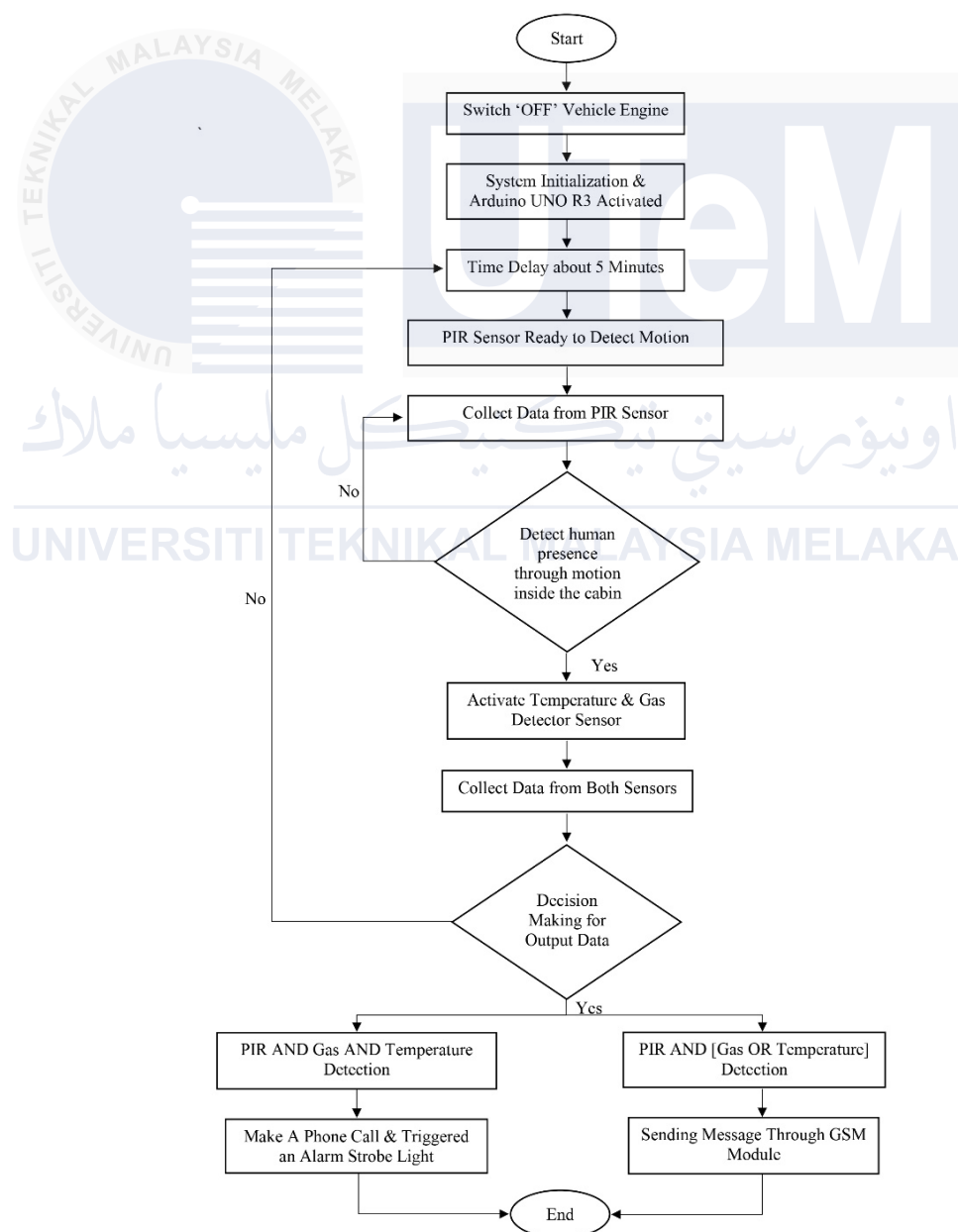


Figure 3.3: Flowchart of Anti-Child Lock System in Vehicle

3.5 Hardware Development

This section focuses on hardware development, which involves constructing and preparing the physical components needed for the system. It includes selecting and assembling sensors, communication modules, and microcontrollers based on system requirements. Each component is tested individually before being integrated, with troubleshooting and adjustments ensuring smooth operation as the foundation for the complete system.

3.5.1 Component Selection and Procurements

In order for a proposed Anti-Child Lock system in vehicle to function effectively, its components need to be installed and programmed. By way of prevention of the child lock on-off, this device aims at enhancing safety and ensuring that all the detected passengers, especially the young ones, can safely get noticed that they were trapped unattended in the car whenever it can be. Precise control and conversion of electrical energy, coupled with a sustainable and reliable power supply, are required for the realization of this. The components required to develop an Anti-Child Lock system include power sources such as solar panels, different types of sensor elements, and actuators capable of meeting all the required objective specifications.

3.5.1.1 Polycrystalline Silicon Solar Panel

Polycrystalline or multi-crystalline silicon solar panels, made of many silicon crystals, are highly effective converters of sunlight into electric power. These solar panels use solar energy to charge the device's battery and are the primary power source for the Anti-Child Locking system. This ensures that even when the car's engine is turned off, the system will remain functional through the use of a reliable and independent power source. Table 3.1

illustrated Polycrystalline solar panel specifications.

Table 3.1: Polycrystalline solar panel specifications.

Working Voltage	6 V
Maximum Power	85 W
Working Current	0 – 700 mA
Open-Circuit Voltage	5.5 V
Short-Circuit Current	1 A
Material	ABS/PC

However, Polycrystalline Solar Panels are reasonably priced, thus perfectly meeting the financial limits of the project, with their durability considered in this system that is meant for outdoor use, especially in mobile applications. The polycrystalline silicon solar panel is illustrated in Figure 3.4.



Figure 3.4: Polycrystalline Silicon Solar Panel 8W

Source: <https://newqualityware.com/product/cclamp-solar-panel-6v-8w/>

3.5.1.2 12V 10A Pulse Width Modulation Solar Charge Controller

The 12V 10A PWM Solar Charge Controller as shown in Figure 3.5 below plays a crucial role in powering the Anti-Child Locking System in your vehicle by managing the energy harvested from the solar panels. This system, which enhances vehicle safety, requires reliable and sustainable power for continuous operation, particularly when the vehicle's engine is off or the electrical system is not actively charging. The PWM Solar Charge Controller is used in regulating the power flow from the solar panel to the system battery through Pulse Width Modulation technology. It ensures the battery is charged efficiently but prevents overcharging or deep discharge, which might cause damage to the battery.

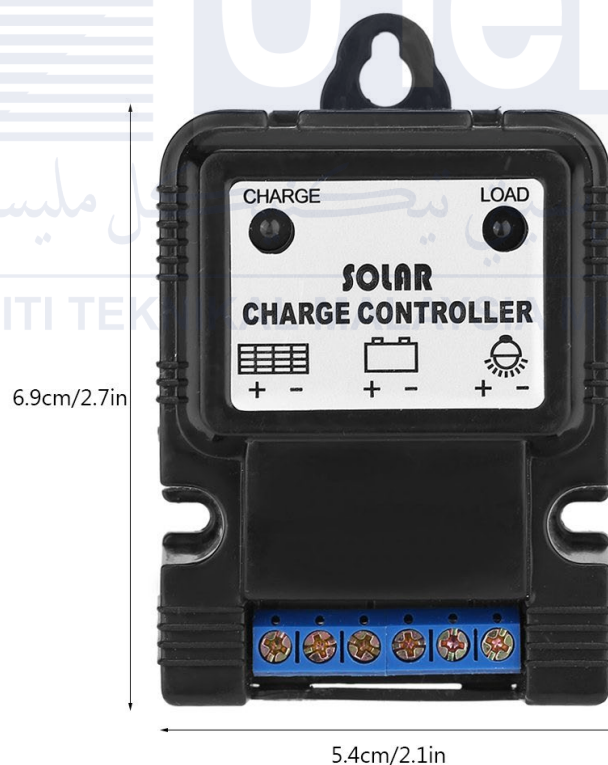


Figure 3.5: 12V 10A Pulse Width Modulation Solar Charge Controller

Source: <https://www.amazon.com/Controller-Intelligent-Regulator-Adjustable-Indicator/dp/B07RNNXXWV>

3.5.1.3 Lead Acid Rechargeable Battery

Lead-acid rechargeable batteries as shown in Figure 3.6 are so inexpensive and reliable in contrast to Lithium-ion and others, that they are used in many applications. One such solution for energy storage in this project is the sealed lead-acid battery used for the Anti-Child Locking system. This ensures the smooth operation of the system, especially during low or no-light conditions, especially at night. In selecting this type of battery, dependability, longevity, operating temperature, and cost-effectiveness are the factors to be considered in order to keep the system running smoothly for the whole day.



Figure 3.6: Rechargeable Battery 6 V 4.5 AH Sealed Lead Acid

Source: <https://howesmodels.co.uk/product/6-volt-4-5ah-rechargeable-lead-acid-battery/0607-lead-acid-6v-7ah-sla-wp7-6-emb-0606-sealed-for-exit-sign-emergency-light-bat67-7000mah>

Because sealed lead-acid batteries operate dependably, they are adaptable to be used in Anti-Child Locking system demanding applications. They ensure continuous operation by means of constant power output over long periods of time. are suitable for use in a wide range of climatic conditions, like the interior of automobiles, where temperatures may vary dramatically, for they can operate well in a wide temperature range. Table 3.2 indicated the Rechargeable Battery Sealed Lead Acid specifications.

Table 3.2: Rechargeable Battery Sealed Lead Acid Specifications.

Model No.	XN620202409
Battery Glossary	6 V -4.5 AH / 20 HR
Cycle Used	7.2 V - 7.5 V (25°C)
Initial Current	No Limit
Standby Use	6.30 V - 6.75 V (25°C)
Terminal Pin	4.8 mm

3.5.1.4 Arduino Uno R3

The Arduino Uno R3 processes the collected data from these sensors and applies the system's predefined logic to determine the necessary actions. When motion is detected by the PIR sensor, the Arduino activates the NTC thermistor and MQ-135 gas sensor to assess the environmental conditions within the vehicle cabin. Based on the sensor readings, the system evaluates two key conditions: if the PIR sensor detects motion along with high temperature and elevated gas levels, it triggers an alarm strobe light and initiates a phone call via the GSM module. Alternatively, if the PIR sensor detects motion along with either high temperature or elevated gas levels, the system sends a text message notification. These decision-making processes are facilitated by logic gates integrated into Arduino's programming, ensuring accurate and timely responses to potential dangers. Additionally, the Arduino logs the sensor data onto the ThingSpeak IoT platform, allowing for remote monitoring and analysis of the vehicle's cabin conditions. This seamless coordination of hardware and software components highlights the critical role of the Arduino Uno R3 as the central controller in the Anti-Child Locking system.

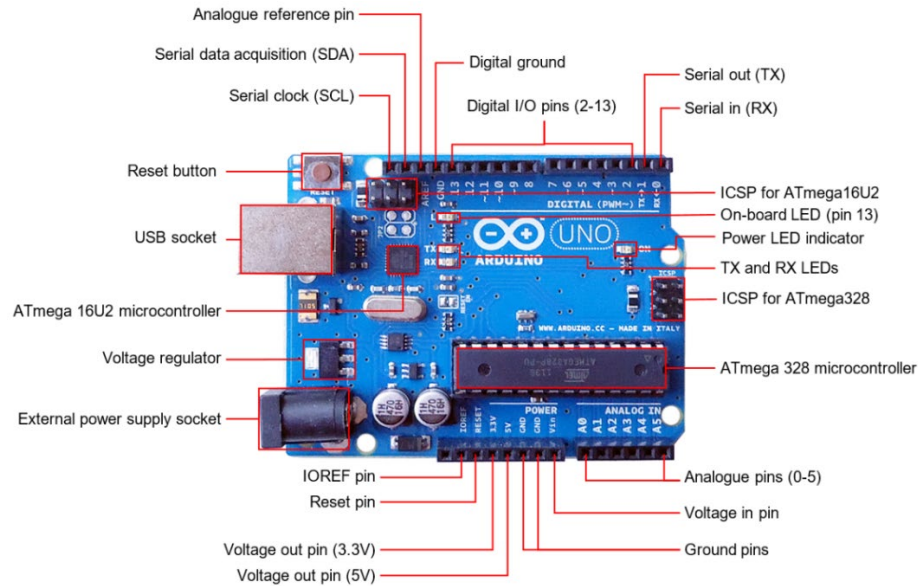


Figure 3.7 Arduino UNO R3

Source: <https://bdavison.napier.ac.uk/iot/Notes/microprocessors/arduino/>

Power supply management on the Arduino Uno R3 as shown in Figure 3.7 above is facilitated by a DC-DC converter & DC- Barrel Jack, ensuring a steady 5V supply necessary for the operation of the Arduino and all connected components. When the vehicle is switched OFF and Anti-Child Locking System is turned ON, A 5-minute delay is introduced and can be changed based on customer desired to avoid false triggers before the system becomes fully active. Once operational, the Arduino continuously monitors detection data from the PIR motion sensor, NTC thermistor, and MQ-135 gas detector to identify potential hazards inside the vehicle.

The Arduino Uno R3 is an ideal choice for this project due to its reliability, versatility, and compatibility with a wide range of sensors and modules. Its integration with the Arduino IDE and support from an extensive user community make programming and troubleshooting straightforward. Furthermore, its cost-effectiveness does not compromise performance, making it suitable for safety-critical applications like the Anti-Child Locking System. By efficiently managing the system's inputs and outputs, the Arduino Uno R3 ensures enhanced vehicle safety and helps prevent situations where children may be

unintentionally left in locked vehicles.

3.5.1.5 Passive Infra-red (PIR) Sensor (HC-SR501)

Among the most critical components of the Anti-Child Locking System in the vehicle is the Passive Infrared (PIR) sensor as shown in Figure 3.8, which detects motion within the car. The PIR sensor works by detecting changes in infrared radiation across its field of view. When a warm object, such as a human being, enters the sensor's detection area, the infrared radiation levels change. This change triggers the PIR sensor to send a signal to the microcontroller, indicating the presence of motion. Once the PIR sensor detects movement, it communicates this immediately to the microcontroller, which then activates the GSM module to send text message alerts or calls to the owner's selected contacts, informing them of the observed motion.



Figure 3.8: Passive Infrared (PIR) Sensor

Source: <https://www.sciencedirect.com/topics/computer-science/passive-infrared-sensor>

The PIR sensor is particularly suitable for this project due to its ability to specifically detect human presence, based on the unique infrared radiation emitted by the human body,

which is significantly warmer than other objects in the environment. This is a key advantage in the Anti-Child Locking System, as it ensures that only human movement is detected, minimizing false alarms caused by other motion sources, such as pets or environmental changes. This capability is crucial in ensuring the safety of young children, as the system needs to focus on detecting any unauthorized movements or risks related to human presence.

The passive detection technique of the PIR sensor ensures high reliability, operating effectively under various environmental conditions. Additionally, due to its low power consumption, the PIR sensor is ideal for continuous monitoring, making it a perfect fit for this system without draining the vehicle's energy resources.

3.5.1.6 Carbon Dioxide Concentration Level Sensor (MQ-135 Sensor)

The MQ-135 sensor, as shown in Figure 3.9, will be used to detect a variety of hazardous gases at dangerous levels inside the vehicle's cabin. In the context of the Anti-Child Locking System in the vehicle, the MQ-135 sensor will specifically monitor the concentration of carbon dioxide (CO₂). The sensor is programmed with a predefined threshold level considered safe for CO₂ concentrations within the vehicle. If the CO₂ level exceeds this threshold, the sensor will send a signal to the Arduino UNO R3, which will trigger a phone call via the GSM module to alert the vehicle owner.

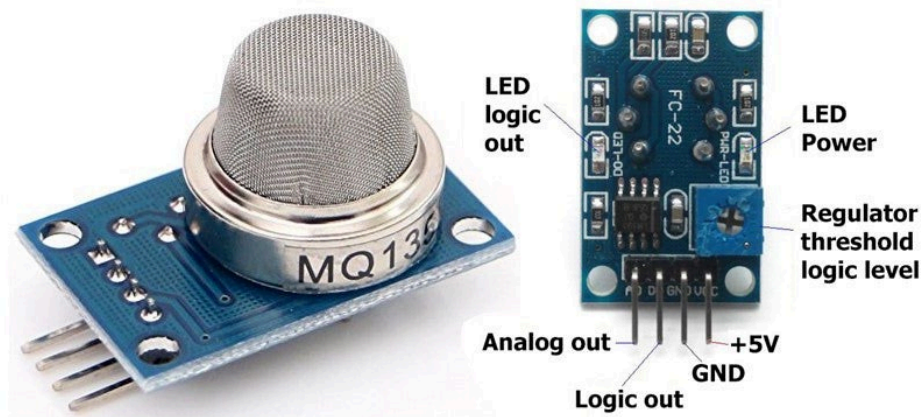


Figure 3.9: MQ-135 Sensor

Source: <https://vishaworld.com/products/mq135-air-quality-control-gas-sensor-module>

The solar-powered Anti-Child Locking system takes advantage of the low power consumption of the MQ-135 sensor, ensuring that it can operate continuously without depleting the system's energy resources. This makes the system both effective and reliable in enhancing vehicle safety. The integration of the MQ-135 sensor provides protection for passengers, particularly young children, by detecting potentially dangerous levels of CO₂ and triggering an immediate alert, contributing to overall safety and well-being inside the vehicle.

3.5.1.7 NTC Thermistor Sensor Module

In the Anti-Child Locking System, temperature sensing plays a critical role in addressing heatstroke, a leading cause of child deaths in vehicles due to dangerously high temperatures inside the car. Figure 3.10 shows the NTC Thermistor Sensor, which is specifically used for continuous real-time temperature monitoring to detect any rise in temperature. The Negative Temperature Coefficient (NTC) property of the sensor means that its electrical resistance decreases as the temperature increases. When the temperature readings exceed predefined safety thresholds, the sensor sends data to the microcontroller, which then activates the gas detector sensor and triggers an alert through the GSM module, notifying the vehicle owner that the temperature inside the vehicle has reached an unsafe level.

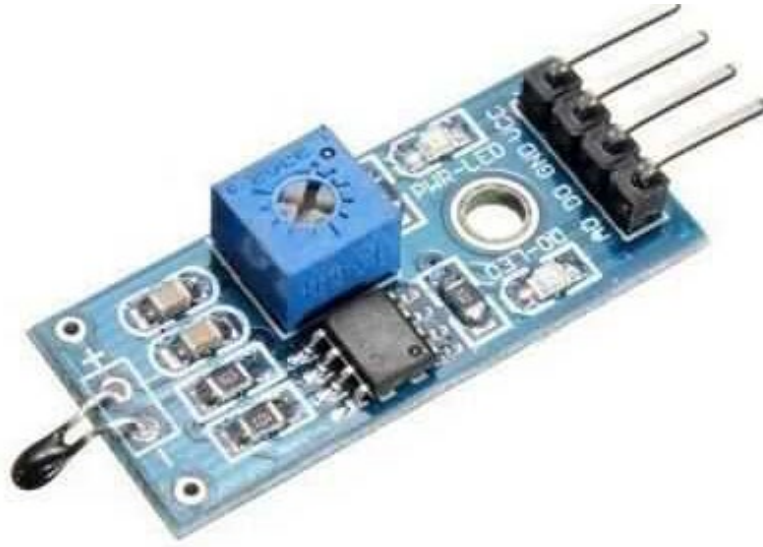


Figure 3.10: NTC Thermistor Sensor

Source: <https://www.motorobit.com/ntc-thermistor-sensor-board-digital-and-analog-output>

The NTC thermistor sensor is crucial to the effectiveness and reliability of the Anti-Child Locking System, serving as an essential tool for reducing heat-related accidents in vehicles. By continuously monitoring the temperature, it ensures that any potentially dangerous conditions are detected and communicated promptly, helping to protect vulnerable passengers, especially children, from heatstroke and other temperature-related risks.

3.5.1.8 GSM Module (SIM-900 A)

The GSM Module, specifically the SIM-900A module, serves as a key component in executing the system's actuator functions. It provides critical communication capabilities by enabling the system to send text messages (SMS) and make missed phone calls using the GSM network. This element is vital in fulfilling the project's objective of alerting the vehicle owner and emergency contacts about potential dangers inside the vehicle. Figure 3.11 shows the SIM-900A GSM module.



Figure 3.11: GSM SIM-900A

Source: <https://www.utmel.com/components/sim900a-gsm-module-how-to-use-sim900a?id=2114>

When the PIR sensor detects motion inside the vehicle, the NTC Thermistor & MQ-135 Sensor identifies a temperature and carbon dioxide gas level rise beyond the predefined threshold, the Arduino UNO microcontroller processes the sensor inputs. The decision-making process then takes place, where the system evaluates whether a missed call or SMS should be triggered based on the data. If the PIR sensor detects motion, the system will assess the sensor readings to determine if both motion and a temperature increase are present.

If both conditions (high temperature and high carbon dioxide level) are detected, the microcontroller commands the GSM module to make a missed call to the pre-programmed phone numbers. If only motion is detected, the system may still choose to make a missed call as a primary alert. Additionally, if either the temperature or gas level exceeds the threshold without any motion detected, a predefined SMS is sent, such as: “Hello, this is ANTI-CHILD LOCKING SYSTEM! Currently, there’s someone in Vehicle! (TEMP/CO2 HIGH)”. This approach ensures that the system responds intelligently to potential dangers,

providing the necessary alerts either through a missed call or SMS based on the severity of the situation.

3.5.1.9 LED Alarm Light Indicator

The LED alarm light indicator, as illustrated in Figure 3.12, is a bright visible alerting device that will be noticed by people passing around and the general public. This is essential in the case of car parks and public places where the quick mobilization of action can be based on such an emergency. In this project, a modified bicycle taillight was used by attaching it directly to the Arduino with customized wiring. This bright red colour-emitting light from the taillight design has provided a strong visual signal in a dangerous situation.



Figure 3.12: LED Alarm Light Indicator

Source: <https://shopee.com.my/Bicycle-Taillight-Headlight-Mountain-Bike-Light-Bike-Accessories-Night-Cycling-Equipment-Warning-Flashing-Light-USB-Charging-i.341053500.17476140314>

With a high luminous intensity, it boasts low power consumption - just right for the energy-saving concept of the system. Moreover, the original lens and housing are made from

durable polycarbonate engineering plastic noted for its heat and impact resistance, assuring reliability and durability that will make the modified light fit for the Anti-Child Locking System even in the harshest of conditions inside a parked vehicle with temperature highs.

The alarm light does not turn on under normal conditions, it only turns on in the case of critical data being provided to the microcontroller from all sensors, including the PIR motion sensor, NTC thermistor, and gas detector. In such a case, the red flashing light of the alarm serves the very purpose of the project in case of an emergency to make sure that the passengers inside the vehicle are aware of an impending danger and draw the attention of people around the critical condition of the vehicle.

3.5.2 Circuit Design

This section outlines the complete process of circuit design, starting from the development of a schematic diagram to the simulation of the system's behavior, followed by the physical assembly of the hardware components. Each of these steps is crucial in ensuring that the final system functions reliably and efficiently, meeting the objectives of the project. The circuit design process involves careful planning and testing, allowing for the identification of potential issues before assembly, and ensuring that all components work together seamlessly.

The Figure 3.13 below presents the wiring diagram for the overall system, providing a clear visualization of how all the components are interconnected in the final assembly. This diagram serves as an essential guide for the physical construction and troubleshooting of the system.

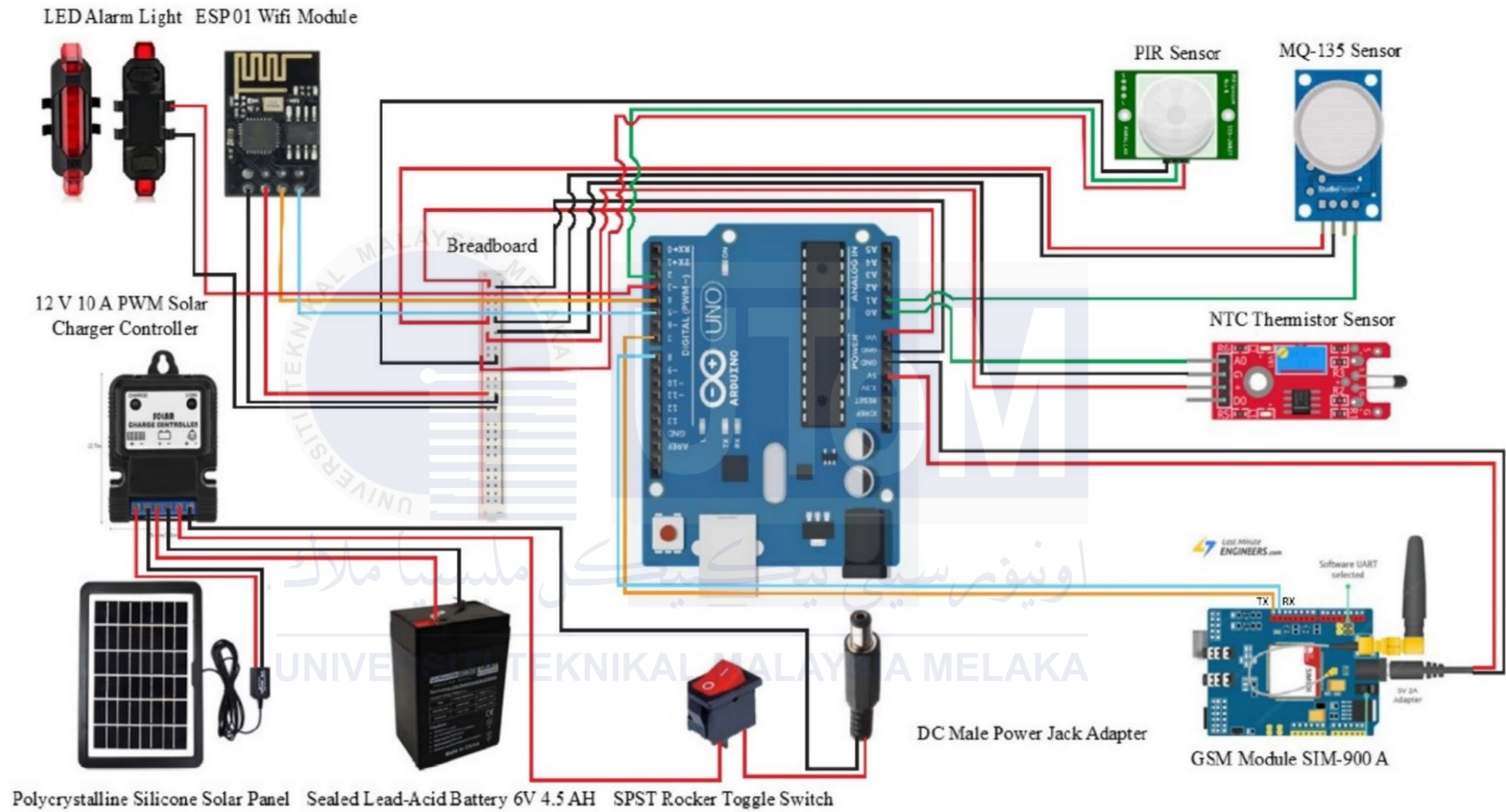


Figure 3.13: Wiring Diagram for Overall System

3.5.3 Prototype Development

The product development now focused on the transformation of the initial circuit design into a working prototype. Further, this was an actual construction of a physical model of the system, which integrated all designed components. It started by designing a small, solid, and easy-to-install 3D-printed housing, specially for three sensors. It was supposed to be durable, easy to assemble, and protect the interior components. These characteristics were achieved by using Fused Deposition Modeling with PLA filament, one of the most used materials due to its strength, low cost, and ecological properties. This technology provided a strong structure while maintaining acceptable detail and accuracy for the prototype.

The 3D-printed housing that is specifically made to fit three sensors is included in the draft that is displayed in Appendix E. This housing facilitates simple installation and smooth system integration while guaranteeing correct alignment and safe positioning of the sensors.

3.6 Threshold Selection

This section covers the selection and justification of thresholds of the Anti-Child Locking System in a vehicle with regard to temperature and CO₂ concentration levels. These are crucial thresholds that guarantee the effectiveness of the system in detecting and averting dangerous conditions within vehicle cabins. The temperature threshold of °C and the CO₂ concentration limit of ppm were identified based on extensive scientific research and real-world observations. It involved analyzing human physiological limits, environmental conditions, and existing safety standards to define threshold values that guarantee timely intervention. These thresholds will form the basis on which the system's safety mechanisms

will always ensure the appropriate response to prevent life-threatening situations.

3.6.1 Temperature Threshold

In these conditions, even with relatively moderate ambient temperatures, the temperature inside a vehicle cabin can rapidly rise. Studies have shown that in a vehicle exposed to direct sunlight at an ambient temperature of 36.5°C, the interior temperature could reach as high as 49.5°C within three hours, thus becoming lethal to any occupants inside (CC Goh et al., 2016). At such high temperatures, thermoregulation mechanisms become overwhelmed, and the risk of heatstroke increases dramatically. Studies have also pointed out that prolonged exposure to air temperatures above 45°C raises the core body temperature beyond levels considered survivable, above 43°C, especially in children and the elderly (Vanos et al., 2023)

Concomitantly, they become more vulnerable, and their body temperature rises 3-5 times faster compared to the one of a grown-up, hence leading to heat-related illnesses, such as multi-organ failure. Further, research from the KidsAndCars.Org indicated that 80% of the increase in temperature inside a vehicle happens within the first 10 minutes of exposure, thereby reaffirming the importance of early warnings for a child. Having a threshold at 45°C makes sure critical measures can be taken before these conditions can turn fatal.

3.6.2 Carbon Dioxide Concentration Level Threshold

Carbon dioxide (CO₂) levels are a key indicator of air quality within confined spaces like vehicle cabins. A threshold of 800 ppm is widely recognized as the point where adverse health effects begin to emerge, including reduced cognitive performance and drowsiness. In enclosed vehicles, CO₂ levels can rise rapidly, especially when the air circulation is limited.

Research demonstrates that CO₂ concentrations can exceed 1200 ppm within just 10 minutes when two occupants are present, contributing to slow reaction times and impaired decision-making (CC Goh et al., 2016).

Cognitive impairments at levels above 800 ppm are well-documented, with studies linking elevated CO₂ levels to fatigue and poor cognitive outcomes, particularly in stressful or high-stakes environments such as driving (Barch et al., 2019). This threshold serves as an early-warning mechanism to signal inadequate ventilation before the air quality deteriorates to a dangerous extent.

3.7 Software Development

This section focuses on the creation and refinement of the software logic to control the system's operation. The process begins with designing algorithms for sensor data acquisition, data processing, and decision-making. The Arduino IDE was used to write and compile the code, ensuring compatibility with the hardware. Key features include real-time monitoring, threshold-based alerts, and data transmission to IoT platforms like ThingSpeak via the ESP8266 ESP 01 WiFi module. The GSM module was integrated to send notifications and debugging tools within the IDE were used to identify and resolve any software issues.

3.7.1 Software Arduino IDE

The Arduino IDE as shown in Figure 3.14, an open-source tool from Arduino.cc, was utilized to write, compile, and upload code to the Arduino Uno microcontroller used in this project. This platform supports various Arduino modules and provides access to extensive libraries that streamline the integration of sensors and modules, such as the MQ-

135 gas sensor, NTC thermistor, PIR sensor, GSM module, and ESP01 WiFi module.

The core program, referred to as a sketch, was developed within the IDE to facilitate the system's functionality, including data acquisition, analysis, and communication with external platforms like ThingSpeak or Blynk. The IDE generates a Hex file that is uploaded to the Arduino Uno, enabling the microcontroller to execute the required operations.



Figure 3.14: Arduino IDE Software

Source: <https://apps.microsoft.com/detail/9nblggh4rsd8?hl=en-us&gl=US>

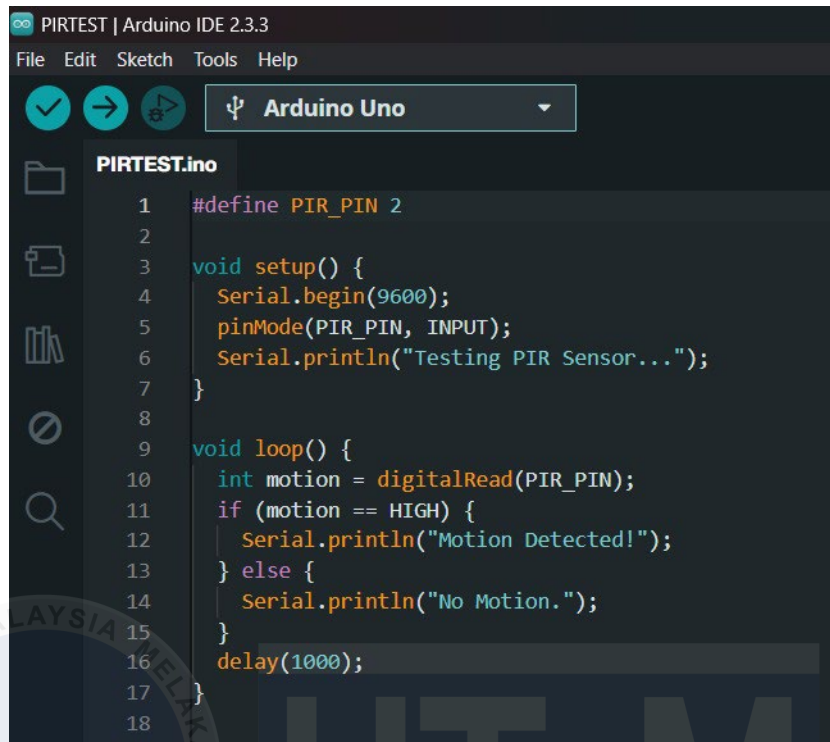
The Arduino IDE environment consists of two essential components: the Editor and the Compiler. The Editor was used to develop the code, while the Compiler ensured proper compilation and uploading to the microcontroller. With support for both C and C++ languages, the Arduino IDE provided flexibility and efficiency in managing the software development needs of this project.

3.7.2 Individual Component Testing

The individual component testing is an important development phase wherein each component is checked for functionality and reliability in isolation before setting up the full system. This testing ensures that sensors and modules-for example, the MQ-135 gas sensor, NTC thermistor, PIR motion sensor, GSM module, and ESP01 WiFi module-operate correctly for their intended purposes. Additionally, it involves electrical testing of the components for their interfaces and interaction under controlled conditions with test inputs. In such a systematic test of each and every element, it ensures smooth communication among components, locates potential problems such as wiring errors or bugs in coding, and performs troubleshooting with calibration. This step is considered crucial for any connectivity or performance issues to be identified as early as possible, while the entire system functions as intended when all components are assembled.

3.7.2.1 Motion Detection Testing (PIR Sensor)

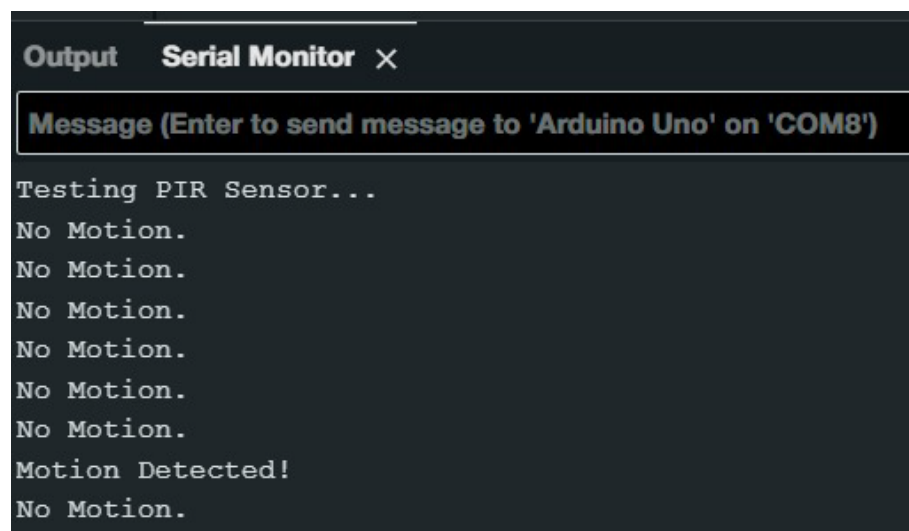
For the motion detection testing, the PIR sensor was connected to the Arduino microcontroller by wiring the sensor's power, ground, and signal pins to their respective terminals. A test code was uploaded to the Arduino to enable the monitoring of motion signals. The test code was designed to detect any movement in the sensor's range and output a corresponding message to the Serial Monitor. The test code used for this procedure is shown in Figure 3.15.



```
1 #define PIR_PIN 2
2
3 void setup() {
4   Serial.begin(9600);
5   pinMode(PIR_PIN, INPUT);
6   Serial.println("Testing PIR Sensor...");
7 }
8
9 void loop() {
10  int motion = digitalRead(PIR_PIN);
11  if (motion == HIGH) {
12    Serial.println("Motion Detected!");
13  } else {
14    Serial.println("No Motion.");
15  }
16  delay(1000);
17 }
18
```

Figure 3.15: PIR Sensor Testing Code

To verify the sensor's functionality, motion was simulated by waving a hand in front of the PIR sensor and resulted as shown in Figure 3.16. The Serial Monitor displayed the message "Motion Detected!" whenever motion was detected, confirming the sensor's accuracy and responsiveness. This testing ensured the proper operation of the PIR sensor and its compatibility with the Arduino system.



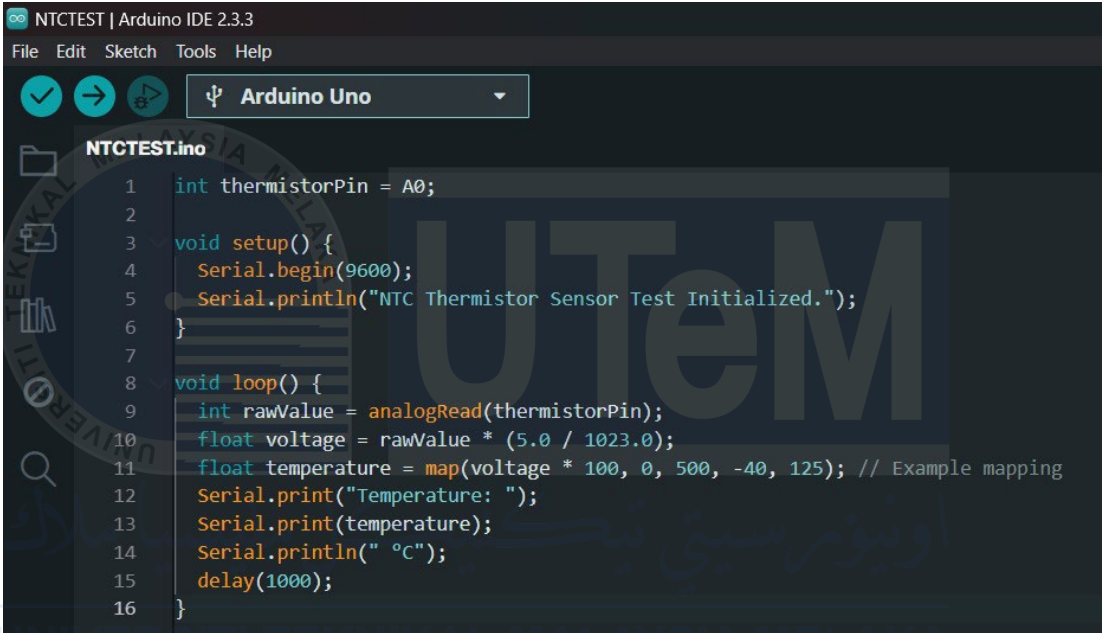
```
Output  Serial Monitor X
Message (Enter to send message to 'Arduino Uno' on 'COM8')

Testing PIR Sensor...
No Motion.
No Motion.
No Motion.
No Motion.
No Motion.
No Motion.
Motion Detected!
No Motion.
```

Figure 3.16: Result of Testing PIR Sensor Functionality

3.7.2.2 Temperature Sensing Testing (NTC Thermistor Sensor)

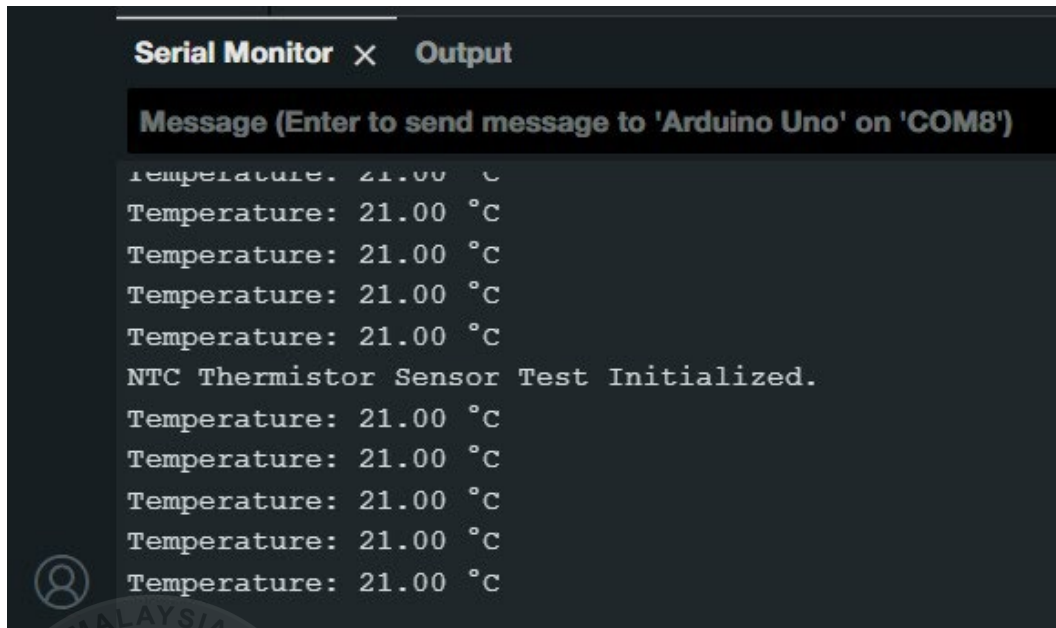
For the individual testing of the NTC thermistor sensor, the sensor was connected to the Arduino microcontroller by wiring its terminals to the appropriate pins for power, ground, and signal input. A test code was uploaded to the Arduino to convert the sensor's resistance changes into temperature readings, which were displayed on the Serial Monitor. The code used for this test is shown in Figure 3.17.



```
NTCTEST | Arduino IDE 2.3.3
File Edit Sketch Tools Help
Arduino Uno
NTCTEST.ino
1 int thermistorPin = A0;
2
3 void setup() {
4   Serial.begin(9600);
5   Serial.println("NTC Thermistor Sensor Test Initialized.");
6 }
7
8 void loop() {
9   int rawValue = analogRead(thermistorPin);
10  float voltage = rawValue * (5.0 / 1023.0);
11  float temperature = map(voltage * 100, 0, 500, -40, 125); // Example mapping
12  Serial.print("Temperature: ");
13  Serial.print(temperature);
14  Serial.println(" °C");
15  delay(1000);
16 }
```

Figure 3.17: NTC Thermistor Sensor Testing Code

The test focused on verifying the stability of the sensor's readings under consistent ambient conditions. The observed data shown in Figure 3.18 demonstrated that the NTC thermistor provided stable temperature measurements, confirming its reliability for integration into the overall system. This stabilization test ensured the sensor's functionality without the need for external temperature variations.

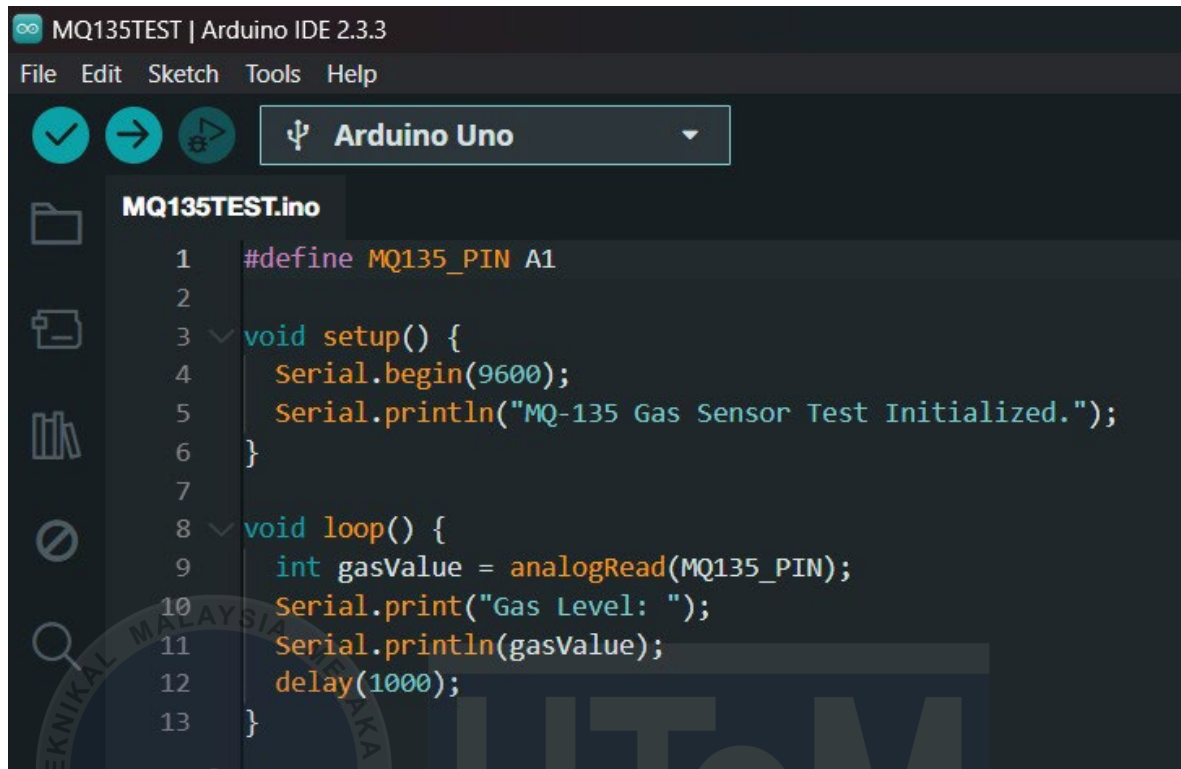
A screenshot of a Serial Monitor window titled "Serial Monitor x Output". The window has a dark background with white text. At the top, it says "Message (Enter to send message to 'Arduino Uno' on 'COM8')". Below this, the text shows a series of temperature readings: "Temperature: 21.00 °C" repeated several times, followed by "NTC Thermistor Sensor Test Initialized.", and then "Temperature: 21.00 °C" repeated again. A small circular icon with a person silhouette is visible in the bottom left corner of the window.

```
Serial Monitor x Output
Message (Enter to send message to 'Arduino Uno' on 'COM8')
Temperature: 21.00 °C
Temperature: 21.00 °C
Temperature: 21.00 °C
Temperature: 21.00 °C
Temperature: 21.00 °C
NTC Thermistor Sensor Test Initialized.
Temperature: 21.00 °C
Temperature: 21.00 °C
Temperature: 21.00 °C
Temperature: 21.00 °C
Temperature: 21.00 °C
```

Figure 3.18: Result of Testing NTC Thermistor Sensor Functionality

3.7.2.3 Carbon Dioxide Concentration Level Testing (MQ-135 Sensor)

To assure the accuracy and reliability of the MQ-135 gas sensor for carbon dioxide concentration levels, individual testing of the sensor was performed. The sensor was connected with the Arduino microcontroller; its pins were wired in connection to power, ground, and signal output. A simple test code as shown in Figure 3.19 was uploaded to the Arduino so that the output values of the sensor could be monitored in parts per million via the Serial Monitor.



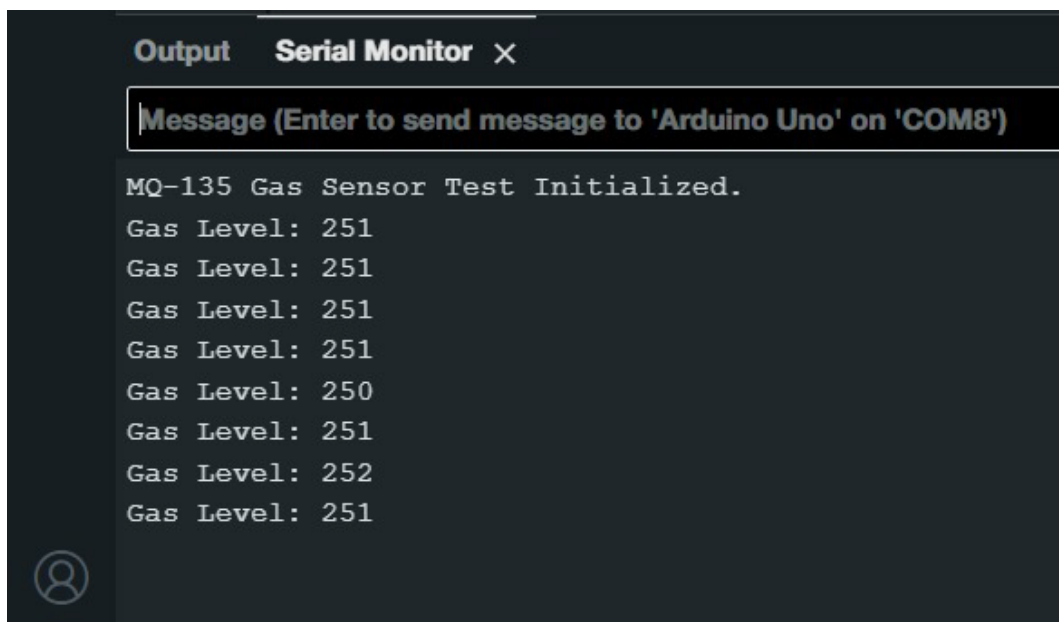
```
MQ135TEST | Arduino IDE 2.3.3
File Edit Sketch Tools Help

Arduino Uno

MQ135TEST.ino
1  #define MQ135_PIN A1
2
3  void setup() {
4      Serial.begin(9600);
5      Serial.println("MQ-135 Gas Sensor Test Initialized.");
6  }
7
8  void loop() {
9      int gasValue = analogRead(MQ135_PIN);
10     Serial.print("Gas Level: ");
11     Serial.println(gasValue);
12     delay(1000);
13 }
```

Figure 3.19: MQ-235 Testing Code

Testing was done for the stabilization of sensor readings under controlled environmental conditions. The sensor was allowed to preheat for a certain duration to measure accurately, as specified in the MQ-135 sensor specifications. Readings were recorded and analyzed once the readings stabilized as shown in Figure 3.20.



```
Output Serial Monitor X
Message (Enter to send message to 'Arduino Uno' on 'COM8')

MQ-135 Gas Sensor Test Initialized.
Gas Level: 251
Gas Level: 251
Gas Level: 251
Gas Level: 251
Gas Level: 250
Gas Level: 251
Gas Level: 252
Gas Level: 251
```

Figure 3.20: Result of Testing MQ-135 Sensor Functionality

This test proved that the MQ-135 sensor would provide reliable CO₂ concentration values under ambient conditions repeatedly. The results confirmed that the sensor was functional for integration into the system.

3.7.2.4 GSM Module Signal Testing

For the individual testing of the GSM module, the module was connected to the Arduino microcontroller via the appropriate RX and TX pins for communication. A test code was uploaded to the Arduino to send a series of AT commands to the GSM module and monitor its responses through the Serial Monitor.

To check if the GSM module is fully functional, several AT commands are sent, and their responses are analyzed. First, the AT command is used to initialize the module. If the response is "OK," it means the module is working. The AT+CPIN? command checks the SIM card status. If the response is +CPIN: READY, the SIM card is ready; if it's +CPIN: SIM PIN, the SIM card needs a PIN.

Next, the AT+CREG? command checks if the module is connected to the network. A response of +CREG: 0,1 means the module is registered on the network, while +CREG: 0,5 means no service. The AT+CSQ command checks the signal strength. A value between 10 and 30 indicates a good signal. The code used for this test is shown in Figure 3.21.



```
GSM_TEST_SIGNAL | Arduino 1.8.19
File Edit Sketch Tools Help

GSM_TEST_SIGNAL

#include <SoftwareSerial.h>

SoftwareSerial gsmSerial(7, 8); // RX, TX (Pin 7 and Pin 8 on Arduino)

void setup() {
  Serial.begin(9600);           // Initialize Serial Monitor
  gsmSerial.begin(9600);        // Initialize GSM Module with baud rate 9600
  delay(1000);                  // Wait for the GSM module to initialize

  Serial.println("Initializing GSM Module...");

  // Send basic AT test command
  sendATCommand("AT");

  // Check SIM card status
  sendATCommand("AT+CPIN?");

  // Check GSM network registration
  sendATCommand("AT+CREG?");

  // Check signal quality
  sendATCommand("AT+CSQ");
}

void loop() {
  // No loop functionality; runs setup commands only
}

void sendATCommand(String command) {
  Serial.println("Sending: " + command);
  gsmSerial.println(command);
  delay(1000); // Wait for the GSM module's response

  // Print GSM module's response
  while (gsmSerial.available()) {
    Serial.write(gsmSerial.read());
  }
  Serial.println("\n");
}
```

Figure 3.21: GSM module Signal Testing Code

Finally, a 1-second delay is added between commands to give the GSM module time to respond. If the module answers correctly to all commands, it confirms that the GSM module, SIM card, network connection, and signal strength are all functioning properly.

Table 3.3 indicated the summarizes the expected responses for each command.

Table 3.3: Summary of Expected Responses for each Command

Test	AT Command	Expected Response	Interpretation
GSM Module Initialization	AT	OK	If the response is "OK", the module is responding.
Sim Card Status	AT+CPIN?	+CPIN: READY or +CPIN: SIM PIN	READY means the SIM card is ready, SIM PIN means PIN is required.
Network Registration Status	AT+CREG?	+CREG: 0,1 (registered) or +CREG: 0,5 (no service)	0,1 means registered on the network, 0,5 means no service.
Signal Quality	AT+CSQ	+CSQ: <rssi>,<ber> (e.g., +CSQ: 19,0)	RSSI value between 10-30 indicates a good signal strength.
Response Delay	-	1 second delay between commands	Delay ensures that the GSM module has time to respond.

3.7.2.5 Wi-Fi Module Signal Testing (ESP-01)

The AT command was transmitted to the ESP-01 Wi-Fi module using a pre-defined setup. The module was connected to the Arduino microcontroller via the SoftwareSerial library, which enabled communication on custom RX and TX pins (Arduino pins 5 and 4). A baud rate of 9600 was configured for both the Serial Monitor and the ESP-01 module to establish synchronous communication. The signal test for AT command was conducted through the code in Figure 3.22 .

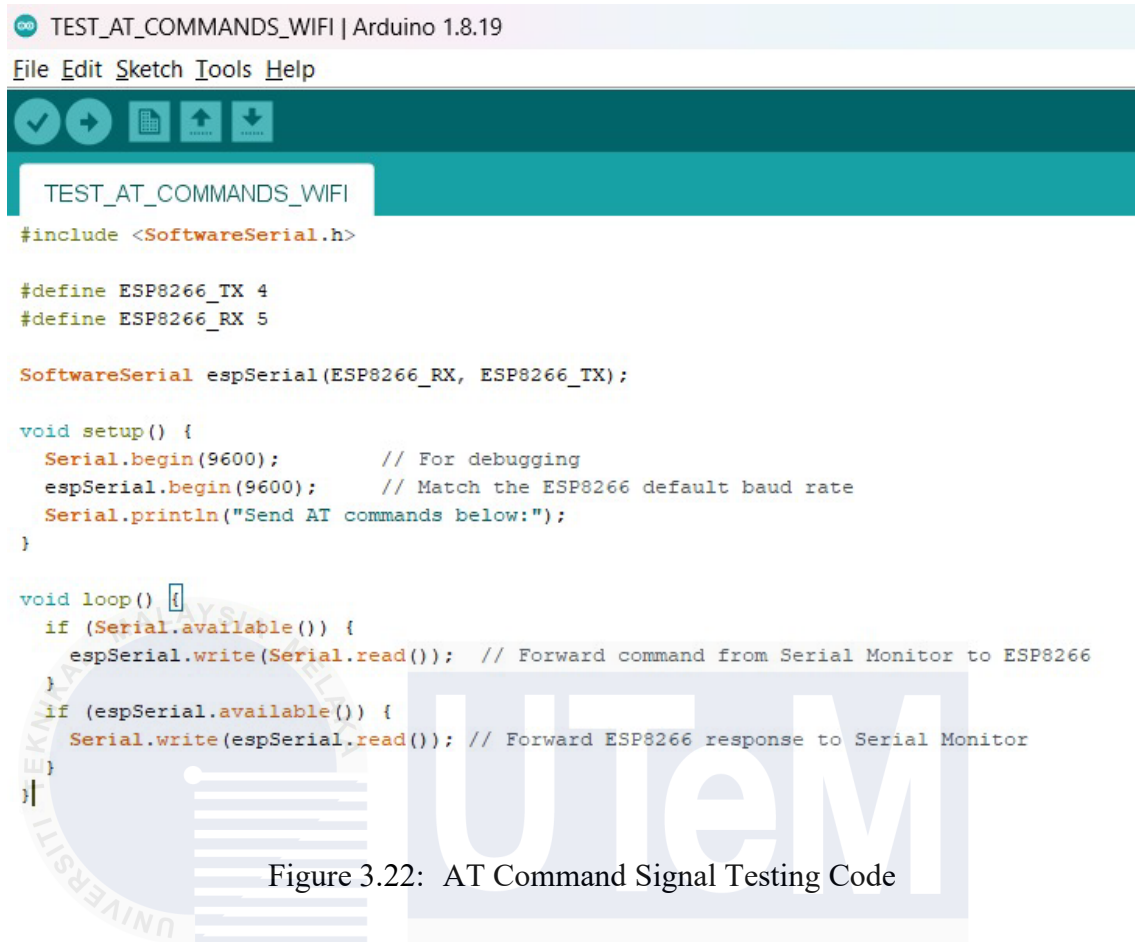


Figure 3.22: AT Command Signal Testing Code

The test code was structured to forward inputs from the Serial Monitor directly to the ESP-01 module. Upon sending the AT command, the module's response was captured and displayed on the Serial Monitor for analysis. A 1-second delay was maintained to ensure sufficient time for the module to process the command and respond.

3.8 Tools Equalizer

In this section, the tools used in the development of this project will be described. The tools are necessary to improve the effectiveness of the project development and troubleshooting.

3.8.1 Multimeter

In any electrical development or project, multimeter as shown in Figure 3.23 will be used as a measuring equipment to measure basic quantities of electrical such as voltage, current and resistance. Besides that, it's also can be used to check continuity of the wires and connections in the circuit. With the use of multimeter can guarantee in ensuring that all of the connections are intact and properly connected. When problems occur, like sensors not working or an alarm not going off, the multimeter is used to identify the issue by measuring the voltage, current, and continuity at various places in the circuit.



Figure 3.23: Multimeter

Source: <https://shopee.com.my/Digital-Multimeter-Kit-Ohmmeter-Tester-Volt-Voltmeter-Ammeter-Electronics-i.375945279.20486440348>

3.8.2 Soldering Iron

A soldering iron is another vital tool required in electronic development or projects to join electronic wiring and components, as illustrated in Figure 3.24. Soldering allows for the development of component assemblies of the Anti-Child Lock System, its repair, and strong and reliable electrical connections. In this system, the Arduino microcontroller must be firmly attached to the MQ-135 gas sensor, PIR sensor, and NTC thermistor sensor. The soldering iron ensures these parts are firmly connected, which guarantees reliable data transfer. System stability is therefore guaranteed by firmly attaching the Arduino Uno R3 to other components. Accurate soldering avoids intermittent connections that might cause system failure.

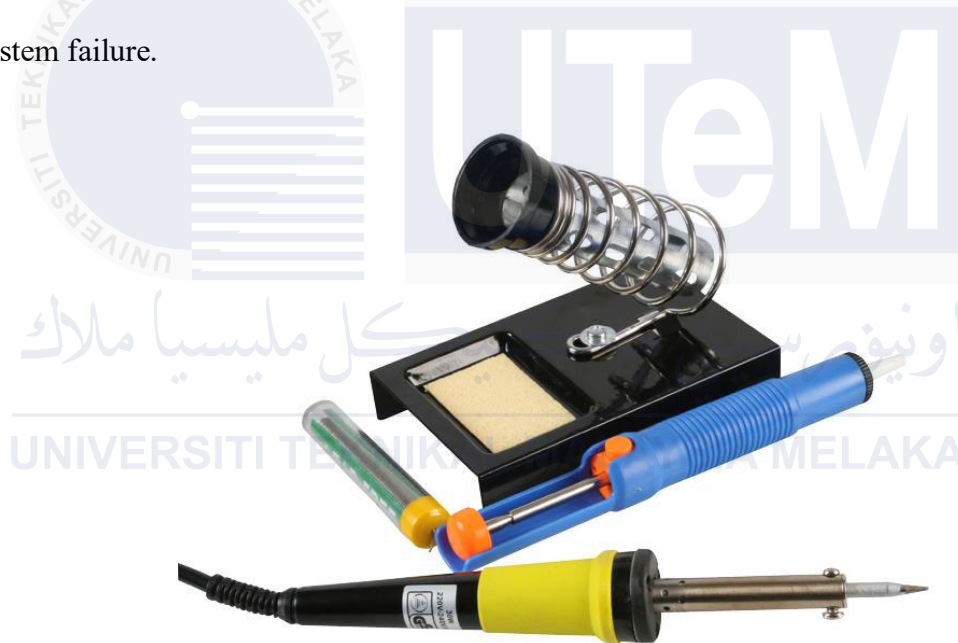


Figure 3.24: Soldering Iron

Source: <https://my.element14.com/duratool/d01855/soldering-iron-kit-pump-stand/dp/2542920>

3.8.3 Handheld Thermocouple

A The calibration of the NTC thermistor sensor was done using a handheld thermocouple for higher accuracy. The thermocouple as shown in Figure 3.25 acts as a reference device that will provide the real values of temperature, which are then compared with the raw output of the thermistor. During calibration, temperatures from the thermocouple and the thermistor were measured simultaneously over a wide range of environmental conditions.



Figure 3.25: Handheld Thermocouple

Source: https://sellmmar.best/product_tag/81823108_.html

The obtained data was used to create a mapping function or correction factor in the coding of the system. This would ensure that the temperature readout of the thermistors corresponded to the calibrated thermocouple readings to the closest degree possible and made the sensor data much more reliable. Later, the calibrated readings had to be integrated into the code of the system for accurate temperature outputs on real-time applications. This calibration step was vital to eradicate any discrepancy resulting from sensor tolerances or

environmental factors and to make very accurate temperature monitoring possible as the project required.

3.9 Integration & Testing

After successful testing with each component individually, this system was integrated into a single program to manage its overall functionality. This integrated system focuses on the development of smooth communication among sensors, the GSM module, and the ESP01 WiFi module for data transmission to ThingSpeak. Standard libraries were used to perform the connectivity in a proper manner.

This involved adjusting the code, debugging, and testing so that everything would work in harmony. Every module was set up to exchange data correctly, including monitoring in real time, alerting, and visualization. This stage validated the performance of the system in conditions simulated to be real-world conditions and ensured that the final implementation met the project's objectives.

3.9.1 Combining Component's Specific Codes

These codes were combined into a single sketch on the Arduino IDE. In doing so, much caution had to be taken to ensure that no part of the code canceled the other out or brought about redundancies in the code. The integration required the combination of readings from the sensors with communication by the GSM and Wi-Fi modules, along with the necessary outputs, like notifications and cloud uploads.

3.9.2 Debugging & Configurations

The integrated code went through extensive debugging to iron out bugs. Overlapping libraries and pin assignments were fixed by the isolation of the section that was problematic, refinement in the implementation. Timing conflicts, especially of the GSM module with the rest of the sensors, have been resolved using non-blocking techniques and delays optimized for smooth operation. Figure 3.26 indicates the pin assignment table and code snippet where all of the sensors, WiFi module, and GSM are defined.

```
// Define PINs for sensors and outputs
#define PIR_PIN 2           // PIR sensor pin
#define NTC_PIN A0         // Temperature sensor pin (NTC Thermistor)
#define MQ135_PIN A1       // Gas sensor pin (MQ-135)
#define ALARM_PIN 3        // Alarm strobe light pin
#define GSM_TX 7           // GSM module Tx
#define GSM_RX 8           // GSM module Rx
String phoneNumber = "+60187824526"; // Your phone number
```

Figure 3.26: Pin Assignment Table or Code Snippet

Configuration played an important role in ensuring stability. Each module was assigned to specific pins with a test for operational independence of each. Proper initialization routines were established for sensors and communication modules, including the GSM and ESP-01 Wi-Fi module. The configuration process also included defining thresholds for the NTC thermistor and MQ-135 sensors to ensure that the system responded appropriately to critical conditions such as high temperatures or elevated CO₂ levels as shown in Figure 3.27.

```
// Sensor thresholds
#define TEMP_THRESHOLD 45 // Temperature threshold in Celsius
#define GAS_THRESHOLD 800 // Gas sensor threshold in PPM
```

Figure 3.27: Sensor Threshold Configuration

Careful adjustments to the code ensured the system operated efficiently, with delays synchronized to maintain responsiveness while preventing unnecessary energy consumption.

3.9.3 Calibration of Sensors

Calibration of sensors is a process of fine-tuning sensors to ensure that their readings are accurate and reliable. It is the adjustment of the sensor output to match known standards or reference values for consistency and precision in measurements.

In the Anti-Child Locking System, calibration will make sure that the PIR sensor accurately detects motion, the NTC thermistor provides correct temperature readings, and the MQ-135 sensor measures the level of gas with accuracy. This step is very important in making the system respond to appropriate real situations, thus triggering alerts when necessary and enhancing safety and reliability in general.

3.9.3.1 PIR Sensor Calibration

The PIR sensor calibration as shown in Figure 3.28 process involved not only stabilization but also adjustments to its sensitivity and delay time to ensure optimal performance. After connecting the sensor to the Arduino microcontroller with power, ground, and signal pins properly configured, the sensor was left undisturbed for 30 to 60 seconds to allow stabilization. This initial step ensured the sensor could establish a baseline for detecting infrared radiation in the environment.

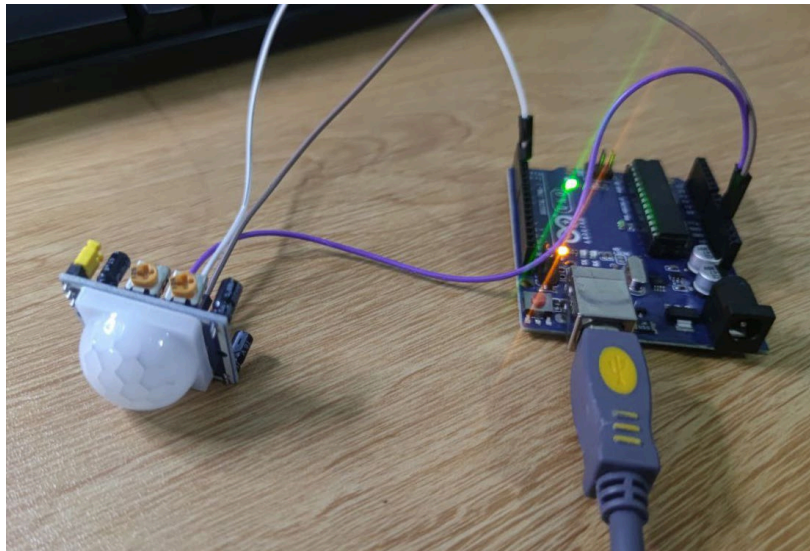


Figure 3.28: PIR Sensor Calibration Setup

The sensitivity and delay time of the sensor were then adjusted using two onboard potentiometers. The sensitivity adjustment was for fine-tuning the detection range to ensure that the sensor would just perfectly detect motion within a certain distance. The delay time adjustment set the period during which the output of the sensor would stay on after it had detected motion a-balance between responsiveness and system requirements. Figure 3.29 shows two onboard Potentiometer is calibrated.

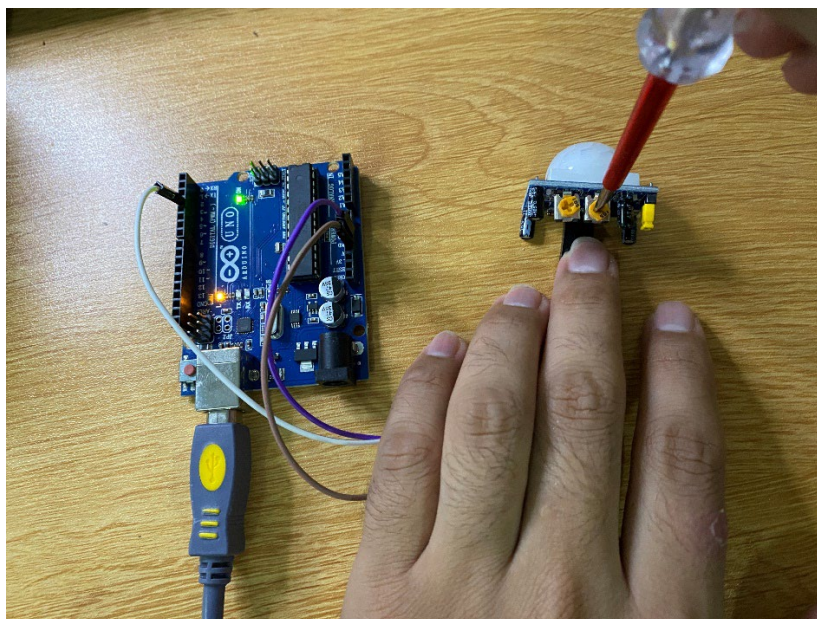


Figure 3.29: Calibrating Onboard Potentiometer

This was further verified by ensuring that messages “Motion Detected!” in the Arduino IDE Serial Monitor as shown in Figure 3.30 due to intentional motions within the sensor’s detecting range. These adjustments allowed the PIR Sensor to be able to accurately detect motion without ‘False Positives’ so that it would be suitable to integrate into the Anti-Child Locking System in Vehicle.

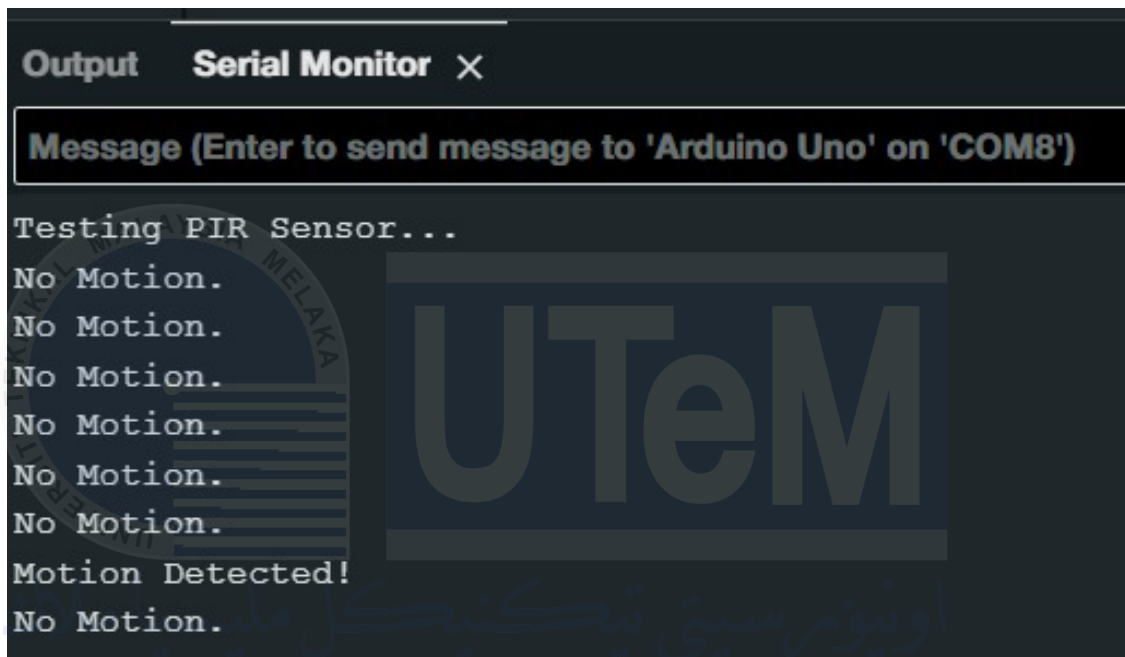


Figure 3.30: Messages shown in Arduino IDE Serial Monitor

3.9.3.2 MQ-135 Sensor Calibration

Carbon dioxide (CO₂) and other dangerous gases are measured in the environment using the MQ-135 gas sensor. Processing is required to transform the raw sensor output into a useful value, like the CO₂ concentration in parts per million (ppm). There were two steps involved in the MQ-135 calibration process.

First, the concentration of CO₂ was determined using a mathematical method based on the response curve of the sensor as shown in figure 3.31. The formula determines the ratio of the sensor resistance (rs) to the reference resistance (ro) and then uses constants from the

sensor's datasheet to convert this ratio to a CO₂ concentration. The snippet of code used in this computation is:

```
// Ratio of sensor resistance to reference resistance
float rs_ro_ratio = rs / ro;
// b and m are constants derived from the datasheet
float ppm = pow(10, (log10(rs_ro_ratio) - b) / m);

// rs = Resistance of sensor
// ro = Reference resistance of the sensor in clean air
// b & m = Constant specific to the sensor & derived from datasheets
```

Figure 3.31: Mathematical Coding for MQ-135 Sensor

As shown in Figure 3.32 an offset value of 64 was deducted from the gas level before mapping it to the intended CO₂ concentration range in order to further scale and modify the raw sensor results. The modified gas level was transformed into a more comprehensible range of 400 to 5000 ppm using the map() method.

```
// Adjust the raw gas level by subtracting the offset
int co2 = gasLevel - 64;
// Map the adjusted value to CO2 concentration range (400-5000 ppm)
int actual_co2 = map(co2, 0, 1024, 400, 5000);
```

Figure 3.32: Offset value in mapping

3.9.3.3 NTC Thermistor Sensor Calibration

For the NTC thermistor, temperature readings were calculated based on the sensor's resistance. The relationship between temperature and resistance for an NTC thermistor was modeled using the Steinhart-Hart equation. The resistance of the thermistor was first calculated using the following formula shown in Figure 3.33.

```
// Calculate resistance from ADC reading
float resistance = (1023.0 / analogValue - 1) * seriesResistor;
```

Figure 3.33: Resistance Calculated Based on Formula

Figure 3.34 illustrates how the Steinhart-Hart equation was used to calculate the temperature. The resistance was converted to temperature in degrees Celsius using this formula.

```
double tempK = 1.0 / ((1.0 / T0) + (1.0 / Beta) * log(resistance / R0));  
T0 = Reference Temperature (usually 25°C or 298.15 K).  
Beta = constant specific to the thermistor,  
R0 is the resistance of the thermistor at the reference temperature T0.
```

Figure 3.34: Steinhart-Hart Equation

This equation calculates the temperature in Kelvin (tempK), which is then converted to Celsius by subtracting 273.15. Additionally, a calibration offset of - 6.70°C is applied to adjust the sensor readings as shown in Figure 3.35 below.

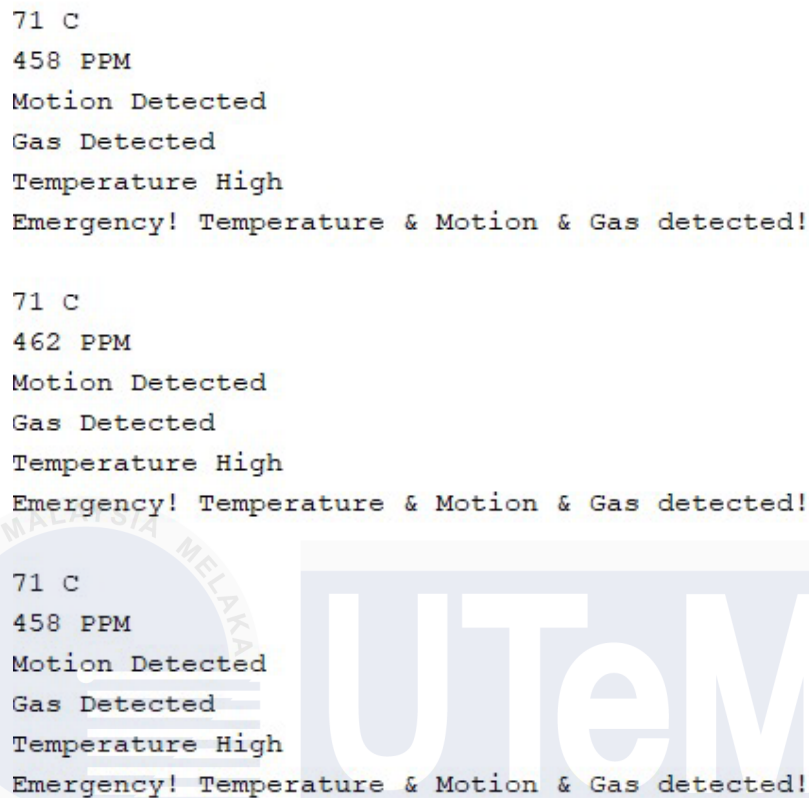
```
return tempK - 273.15 - 6.70;
```

Figure 3.35: Calibration Offset is applied in the coding

3.9.4 Real-Time Data Testing

Real-time data testing will be an important step in the validation process of the system, demonstrating its ability to continuously monitor and transmit live data coming from sensors to user interfaces or storage platforms. This guarantees smooth integration of the components and the verification of the performance of the system in real life in detecting critical thresholds of temperature and gas levels. The Arduino IDE Serial Monitor and ThingSpeak IoT platform were the tools of choice in the observation, debugging, and analysis of the system's functionality. Real-time testing as indicated in figure 3.36 showed the system to be reliable, responsive in delivering accurate data and triggering alerts

as expected.



```
71 C
458 PPM
Motion Detected
Gas Detected
Temperature High
Emergency! Temperature & Motion & Gas detected!

71 C
462 PPM
Motion Detected
Gas Detected
Temperature High
Emergency! Temperature & Motion & Gas detected!

71 C
458 PPM
Motion Detected
Gas Detected
Temperature High
Emergency! Temperature & Motion & Gas detected!
```

Figure 3.36: Real-Time Data Testing in Serial Monitor

Real-time data testing was conducted to ensure that the system was working in performance, capturing, processing, and transmitting sensor data accurately. Then, real-time sensor output observation was performed by using the Arduino Integrated Development Environment Serial Monitor as a debugging device to quickly understand how the system is functioning and thus can be able to detect any errors or inconsistencies. Besides, data visualization at a distance was done with ThingSpeak IoT to show that the ESP01 WiFi and GSM were working fine with respect to the different communication modules developed in this system.

Different conditions were applied to validate the performance of the system on detecting and acting against critical thresholds: a temperature over 45°C and gas concentrations over 800 ppm. Correct activation of the alerts and notifications beyond the threshold values was verified. Real-time monitoring with integrated IoT-based data

visualization displayed the performance of the system in continuously and reliably providing updates toward better safety and situational awareness.

3.10 Power And Energy Requirements for Anti-Child Locking System

This section will outline the recommended power and energy needs for all components that will be used, whether they are operating during the day or at night. Furthermore, figuring out the energy and power consumption will help establish how much power is available to keep the system running and strong enough to withstand power and energy demands.

- A. To calculate power for each component in Table 3.4, Formula 3.1 (Richard Ozenbaugh, 2004) will be used which,

$$P (\text{power}) = V(\text{voltage}) \times I(\text{Current}) \quad [3.1]$$

Table 3.4: Components and Power Consumptions

Arduino UNO R3	5V x 100mA = Approximately 0.5W
PIR Sensor	5V x 13mA = Approximately 0.065W
NTC Thermistor Sensor	5V x 10mA = Approximately 0.05W
MQ-135 Gas Detector Sensor	5V x 150mA = Approximately 0.75W
SIM-900A GSM Module (During Transmission)	5V x 450mA = Approximately 2.25W
LED Alarm Light Indicator	5V x 250mA = Approximately 1.25W

- B. Power Consumption during Standby Mode is calculated when only Arduino Uno & sensors are activated as shown in Formula 3.2.

$$P_{\text{Standby}} = P_{\text{Arduino}} + P_{\text{PIR}} + P_{\text{GasSensor}} + P_{\text{NTCSensor}} \quad [3.2]$$

$$P_{\text{Standby}} = 0.5W + 0.065W + 0.75W + 0.5W$$

$$P_{\text{Standby}} \approx 1.365W$$

C. Power Consumption during Active Mode is calculated when SIM-900 A GSM

Module & Alarm Light Indicator is activated as shown in Formula 3.3.

$$P_{\text{Active}} = P_{\text{Standby}} + P_{\text{GSM}} + P_{\text{AlarmLightIndicator}} \quad [3.3]$$

$$P_{\text{Active}} = 1.365W + 2.25W + 1.25W$$

$$P_{\text{Active}} \approx 4.865W$$

D. To calculate energy requirements for 9-Hour's period, Formula 3.4 (Beaty, 2001) will be used.

I. Standby Mode Energy within 9 Hours:

$$E_{\text{Standby}} = P_{\text{Standby}} \times \text{Hours} \quad [3.4]$$

$$E_{\text{Standby}} = 1.365W \times 9h$$

$$E_{\text{Standby}} \approx 12.285 \text{ Wh}$$

II. Active Mode Energy (Assumed 1 Hour for Alarm or Messages or Calls)

$$E_{\text{Active}} = P_{\text{Active}} \times \text{Hours} \quad [3.5]$$

$$E_{\text{Active}} = 4.865W \times 1h$$

$$E_{\text{Active}} \approx 4.865 \text{ Wh}$$

E. Total Energy Requirement (Daily)

$$E_{Total} = E_{Standby} + E_{Active} \quad [3.6]$$

$$E_{Total} = 12.285 \text{ Wh} + 4.865 \text{ Wh}$$

$$E_{Total} \approx 17.15 \text{ Wh}$$

F. Energy Provided by The Solar Panel

Assuming 5 Hours of effective sunlight hours per day,

$$E_{Solar} = P_{Solar} \times \text{SunlightHours} \quad [3.7]$$

$$E_{Solar} = 8\text{W} \times 5\text{h}$$

$$E_{Solar} \approx 40 \text{ Wh/Day}$$

G. Battery Bank Capacity formula as shown in Formula 3.8

As mentioned, battery capacity will be 6V, 4.5Ah

$$E_{Battery} = V_{Battery} \times Ah_{Battery} \quad [3.8]$$

$$E_{Battery} = 6\text{V} \times 4.5\text{Ah}$$

$$E_{Battery} \approx 27 \text{ Wh}$$

H. Energy Sufficiency & Efficiency

To calculate energy sufficiency during by using battery only, Formula 3.9 will be used,

$$E_{Remaining} = E_{Battery} - E_{Total} \quad [3.9]$$

1. Daily

$$E_{Remaining} = 27 \text{ Wh} - 17.15 \text{ Wh}$$

$$E_{Remaining} = 9.85 \text{ Wh}$$

2. Surplus Energy Efficiency During Daytime

To calculate energy sufficiency by using solar power only, Formula 3.10 will be used,

$$E_{Surplus} = E_{Solar} - E_{DayTotal} \quad [3.10]$$

$$E_{Surplus} = 40 \text{ Wh} - 17.15 \text{ Wh}$$

$$E_{Surplus} \approx 22.85 \text{ Wh}$$

— This surplus energy from the daytime will be used to recharge the battery bank.

I. Total Battery Capacity After Day Recharging

$$E_{Battery} = E_{DayRemaining} + E_{Surplus} \quad [3.11]$$

$$E_{Battery} = 9.85 \text{ Wh (Day)} + 22.85 \text{ Wh (Recharge)}$$

$$E_{Battery} \approx 32.7 \text{ Wh}$$

Anti-Child Locking System with Standby & Active Mode only requires 17.15 Wh per day. During daytime, the energy generated by solar & Battery bank both respectively 40Wh & 27 Wh. However, the sustainability is proved that this system will remain operational continuously.

3.11 Summary

This Chapter 3 unfolds a step-by-step procedure of development and implementation for the Anti-Child Lock System in vehicles. The chapter begins with the underlying importance of a structured approach to reliability, validity, and consistency in research or project outcomes. It emphasizes a research flowchart which pictorially details how the project should be executed.

The design of the system contains main elements, which are the Arduino Uno R3 microcontroller, varied sensors such as PIR, MQ-135, and NTC thermistor, a GSM module, and solar-powered energy. These sensors will monitor critical parameters related to motion, gas levels, and temperature inside the vehicle. This data is to be processed by the microcontroller for sending SMS, making calls, or even visual signals in case any threshold value is crossed to ensure safety for the occupants.

Hardware development focused on the selection, assembly, and testing of components such as solar panels, batteries, and sensors. Software development used the Arduino IDE for programming sensor data acquisition, decision-making, and communication with IoT platforms like ThingSpeak. Extensive testing and calibration of individual components were performed to ensure accuracy and reliability.

It goes on to discuss the power and energy requirements of the system, showing its sustainability with solar energy and battery storage. Real testing was performed that proved how effective the system could be in efficiently monitoring conditions and triggering timely alerts.

This chapter describes in detail a comprehensive methodology for designing a safe, efficient, and sustainable system for preventing child lock-related incidents inside vehicles.

CHAPTER 4

RESULT AND DISCUSSION

4.1 Introduction

This chapter presents the results obtained from the performance of the system during the testing phase. The results obtained indicate that the system can monitor environmental parameters such as ambient temperature, CO₂ gas concentration, and motion detection in real time. Full insight into the responsiveness, accuracy, and reliability of the system under various conditions is possible through data visualization using platforms such as Arduino IDE Serial Monitor and ThingSpeak. System response time, thresholds of the system, correlation between parameters-all these are critical key metrics for bringing forth strengths and shortcomings of the system. This chapter comparatively researches into trends and patterns of two days data for insights on system functionality, thereby putting a strong bearing on its capabilities to provide an alert on specified conditions. It also discusses implications of the results with a view to ascertaining the suitability of the system for real-life applications.

4.2 Display of Result

This analysis's usage of various platforms to display and track sensor data for remote accessibility and real-time feedback is demonstrated in the part that follows. Additionally, real-time visualization, data-driven insights, and system debugging are permitted on the online platforms.

4.2.1 Arduino IDE Serial Monitoring

The Arduino Serial Monitor as shown in Figure 4.1 was utilized as a primary debugging tool and for real-time sensor output visualization. During operation, sensor data was displayed in a structured format and updated every second. This immediate feedback helped monitor the accuracy and reliability of the sensors. The Serial Monitor also played a crucial role in troubleshooting, ensuring correct communication between components, and identifying any issues during development.

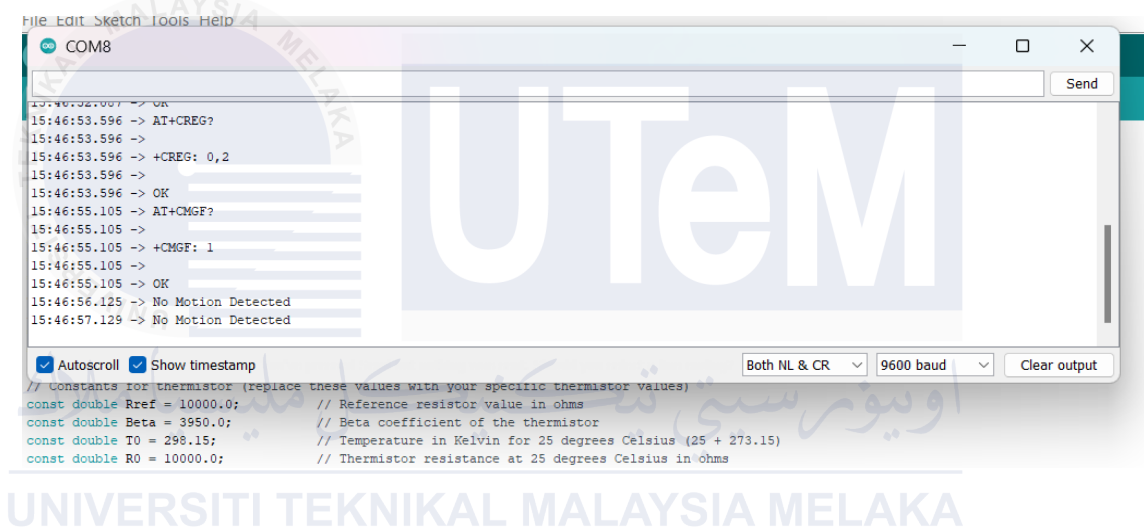


Figure 4.1: Arduino IDE Serial Monitor Interface

4.2.2 Dashboard ThingSpeak

ThingSpeak was employed as an IoT platform for remote data monitoring and visualization. The ESP01 WiFi module transmitted the sensor data to ThingSpeak, where it was dynamically displayed on interactive line charts. The platform enabled users to track trends in parameters such as temperature, gas concentration, or other critical metrics over time. Alerts were configured to notify users when values exceeded predefined thresholds, ensuring prompt action in the event of critical situations. The dashboard provided a user-friendly interface for real-time monitoring on any internet-enabled device, making the system

accessible and convenient.

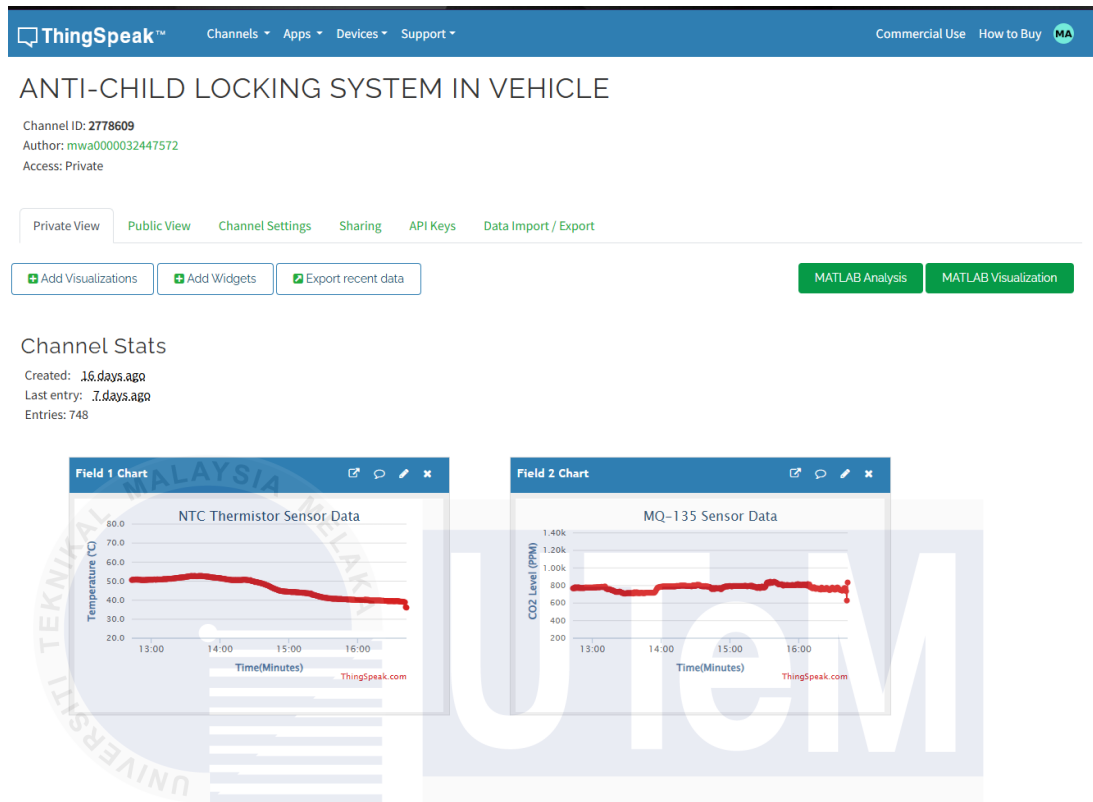


Figure 4.2: Display of ThingSpeak Dashboard

4.3 Data Collection and Comparison

Through two days of intense testing, the data collection as shown in Appendices C attempts to assess the system's performance, concentrating on important factors like response times, sensor accuracy, and system outputs. This examination highlights the system's capabilities in real-time detection, data transmission, and emergency alarm activation under various scenarios, offering insightful information about its dependability and effectiveness. The system's strengths and possible areas for improvement are determined by comparing the data gathered, guaranteeing that it is prepared for real-world deployment.

The discussion interprets the significance of the results, addressing how well the system performed under various conditions and its ability to respond to predefined

thresholds. This chapter also explores the operational behavior of the actuators, the responsiveness of the sensors, and the accuracy of the communication modules. The findings are critically analyzed to determine whether the system meets the requirements for ensuring vehicle safety and occupant monitoring, with emphasis on real-time alerts and efficient hazard identification.

4.3.1 Ambient Temperature Data (°C) Day-1 VS Day-2

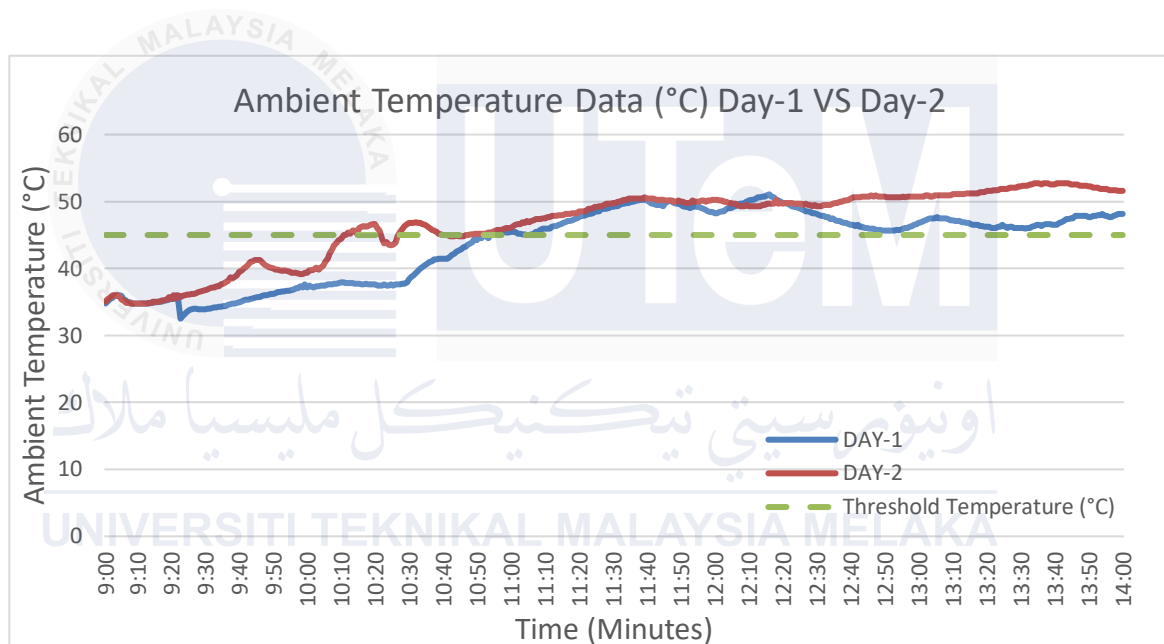


Figure 4.3: Ambient Temperature Data (°C) Day-1 vs Day-2

Figure 4.3 shows temperature readings over two days against a threshold temperature of 45°C represented by the horizontal green line. On Day-1 represented by the blue line, the temperature stays below the threshold. The trend of data for Day-1 reflects a gradual increase, with the temperature crossing the threshold at 10:53 a.m. at 44.53°C. After crossing, the temperature remains generally above the threshold, but it does go under it occasionally. By contrast, Day-2, as represented by the orange line, shows more gradual upward development. The temperature crosses the threshold earlier, at 10:12 a.m., reaching

45.36°C. For the rest of the day, the temperature remains above 45°C, though with frequent small dips. Compared to Day-1, Day-2 shows slightly higher overall temperatures after crossing the threshold.

In summary, both Day-1 and Day-2 recorded temperatures above the threshold of 45°C. However, Day 2 reached the threshold earlier and maintained a higher average temperature above it throughout the day.

4.3.2 CO₂ Gas Concentration Level Data (PPM) Day-1 VS Day-2

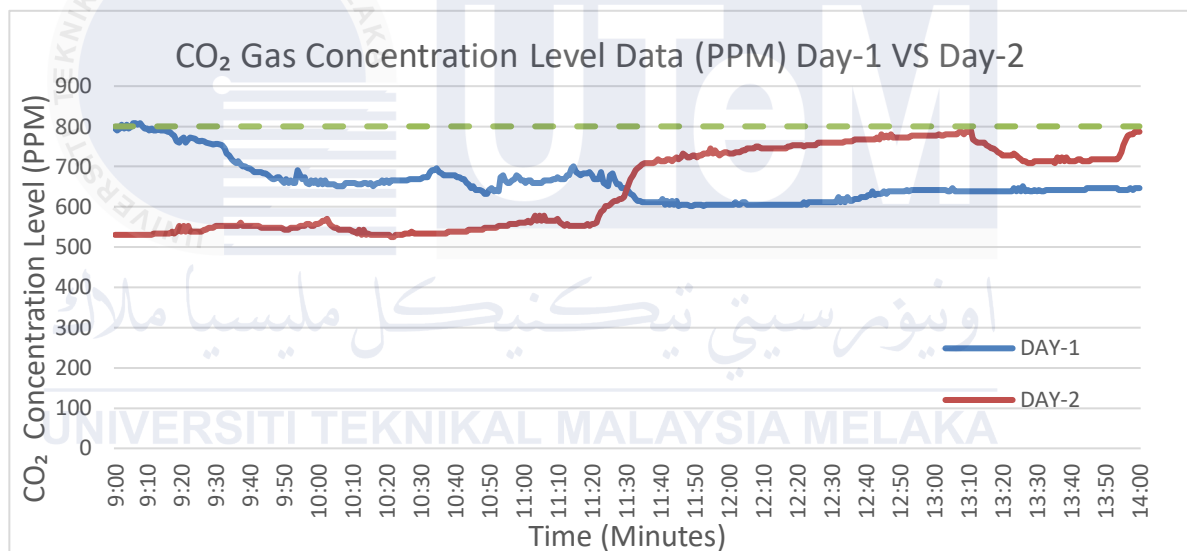


Figure 4.4: CO₂ Gas Concentration Level Data (°C) Day-1 vs Day-2

In Figure 4.4 shows that CO₂ concentration in PPM recorded over two days. Horizontal green line plots the threshold of CO₂ concentration at 800 PPM. For the blue line, on Day-1, it stays high and flickers to near 800 PPM. After gradually coming down, CO₂ level settles at the nearby value of 600 PPM. This decline reflects on the temperature and air quality over time, possibly due to increased ventilation or reduced contributing factors such as human activity. By contrast, Day-2, represented by the orange line, starts off at much lower CO₂ levels of about 550 PPM and holds steady for a few hours in the morning.

However, starting at 11:30 a.m., the CO₂ starts rising to eventually surpass the Day-1 levels, peaking close to the 800 PPM threshold. After this peak, the CO₂ concentration slowly decreases towards the end of the observation period. The differences in trends in the two days point to variance in environmental conditions, or ventilation efficiency.

In summary, Day-1 starts at a higher level of CO₂, which decreases gradually throughout the day, whereas Day-2 starts off at a lower level but sees a significant increase before levelling out. Neither day exceeds the 800 PPM threshold consistently, showing that despite fluctuations recorded, the environment remains within acceptable limits of air quality. The difference between the two days could be because of ventilation, or external environmental factors affecting the level of concentration of CO₂ (Barch et al., 2019).

4.3.3 Ambient Temperature VS Outdoor Temperature (°C) Day-1 & Day-2

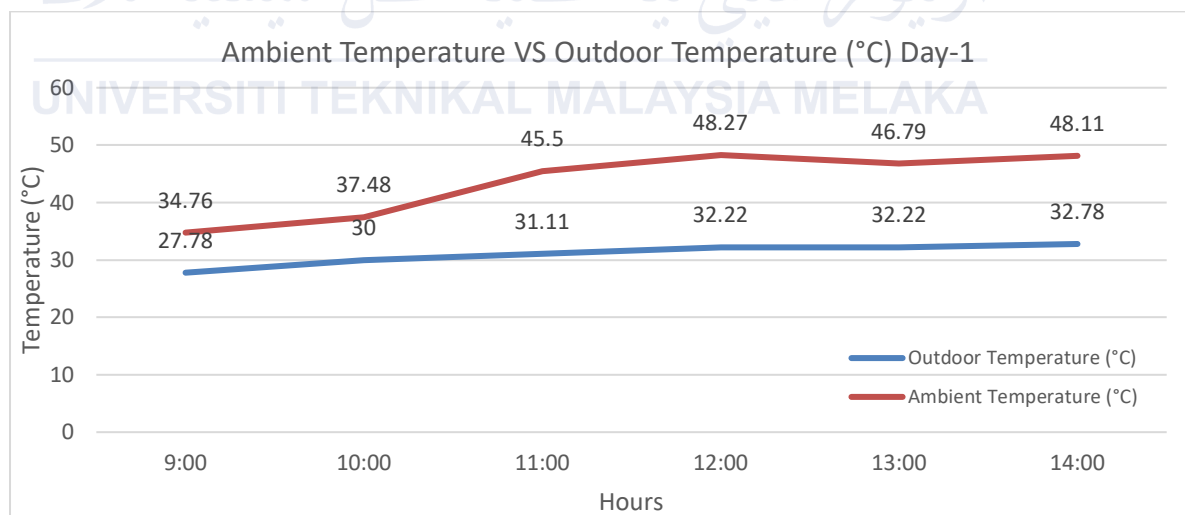


Figure 4.5: Ambient Temperature VS Outdoor Temperature (°C) Day-1

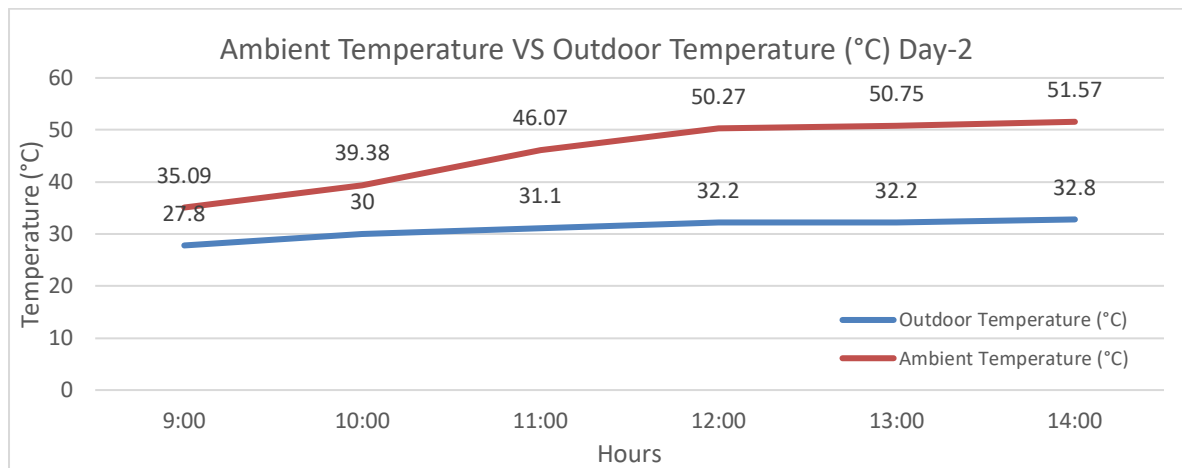


Figure 4.6: Ambient Temperature VS Outdoor Temperature (°C) Day-2

In Figure 4.5 and Figure 4.6 presents a comparison between ambient and outdoor temperatures recorded between 9:00 and 14:00 for Day-1 and Day-2. Starting with Day-1, the ambient temperature rises more significantly than the outdoor temperature throughout the observed period. Starting at 34.76°C at 9:00, the ambient temperature steadily increases and reaches its peak of 48.27°C at 12:00. Following this peak, there is a slight dip to 46.79°C at 13:00, before rising again to 48.11°C at 14:00. On the other hand, the outdoor temperature shows a more gradual increase, starting at 27.78°C at 9:00 and rising consistently throughout the day, reaching 32.78°C at 14:00. The data indicates that while both temperatures increase over time, the ambient temperature experiences larger fluctuations and rises more significantly than the outdoor temperature.

The graph for Day-2 also compares ambient and outdoor temperatures over the same time period. Similar to Day-1, the ambient temperature rises more sharply than the outdoor temperature. Starting at 35.09°C at 9:00, the ambient temperature increases steadily to its peak of 50.75°C at 12:00. After a slight decline to 50.27°C at 13:00, it climbs again to reach 51.57°C at 14:00. The outdoor temperature exhibits a gradual increase from 27.8°C at 9:00 to 32.8°C at 14:00. The trend is consistent throughout the day, with minimal fluctuations

compared to the ambient temperature. This further highlights the more dynamic behavior of the ambient temperature.

Across both days, the ambient temperature shows a more pronounced increase, and greater fluctuations compared to the outdoor temperature. On Day-1, the ambient temperature peaks at 48.27°C, whereas on Day-2, it reaches a higher peak of 50.75°C. The outdoor temperature, in contrast, maintains a steady rise with less variation, ending at 32.78°C and 32.8°C on Day-1 and Day-2, respectively. These observations suggest that ambient conditions are more sensitive to fluctuations in environmental factors compared to outdoor temperatures (Wei et al., 2018)

4.3.4 Comparison of Ambient Temperature Data (°C) & CO₂ Gas Concentration Level Data (PPM) Over Time (Minutes) Day-1 & Day-2

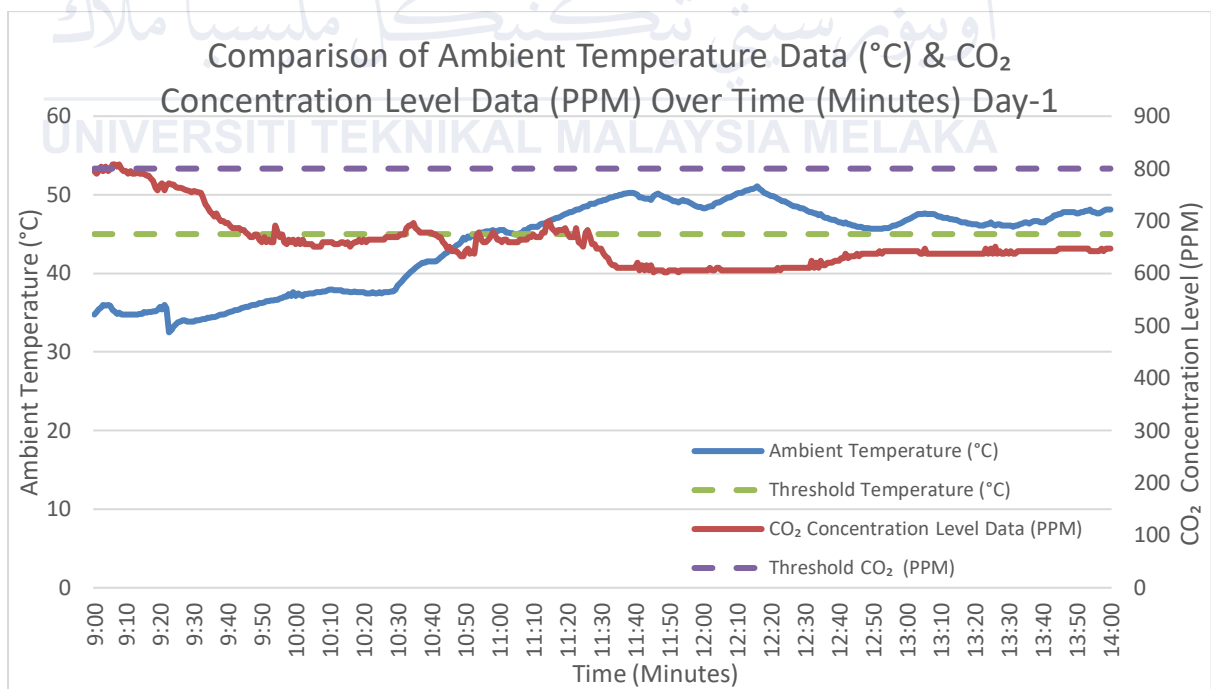


Figure 4.7: Comparison of Ambient Temperature Data (°C) & CO₂ Gas Concentration Level Data (PPM) Over Time (Minutes) Day-1

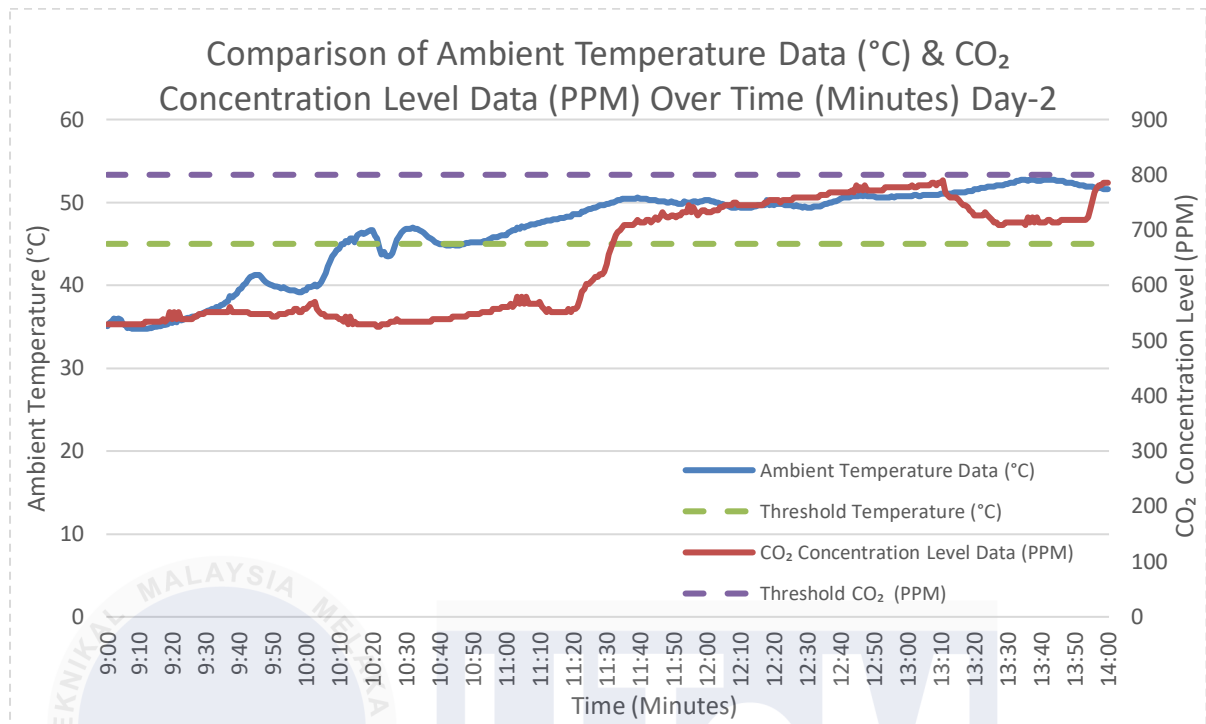


Figure 4.8: Comparison of Ambient Temperature Data (°C) & CO₂ Gas Concentration Level Data (PPM) Over Time (Minutes) Day-2

Analysis of graphs comparing the ambient temperature on Day 1 & Day 2 started off at about 40°C on Day 1 as shown in Figure 4.7, generally remained around that level with slight variations, and had a small rise toward the end. In contrast, CO₂ concentration started at about 700 PPM, drastically decreased in the beginning, and remained steady at approximately 600 PPM. This behavior suggests a lack of strong correlation between the two parameters because, while the temperature was showing an upward trend, CO₂ concentration was showing a downward trend. The disparity suggests other factors such as air circulation, gas diffusion, or sensor sensitivity may be influencing the observed patterns.

Analysis on Day 2 as illustrated in Figure 4.8, an entirely different pattern from Day 1 was observed: The ambient temperature on Day 2 had a more dramatic incline than the one on Day 1 from about 40°C to a high of close to 50°C, whereas the level of CO₂ during the observation went from about 600 PPM to 700 PPM; thus, for this day, CO₂ exhibited its positive trend and had a far more close relationship between the two variations. This might

be because of some changes in environmental dynamics, such as higher heat-induced emissions from vehicle materials or reduced ventilation over time.

Comparison of the two days shows different relations between temperature and CO₂. On Day 1, the two parameters are trending in opposite directions, which may indicate little interaction or influence between them. On Day 2, a positive relation is observed: the higher the temperature, the higher the amount of CO₂. The variability between the two days is indicative of the complexity of indoor air quality dynamics, which could be influenced by external factors such as humidity, material off-gassing, and the duration of exposure to heat.

4.4 Response Time Comparison Between Arduino IDE and ThingSpeak

The reaction times of the ThingSpeak platform and the Serial Monitor in the Arduino IDE are contrasted over ten data entries in Figure 4.9 below and shown in Appendice D. The findings unequivocally demonstrate how the two platforms handle and transmit sensor data differently.

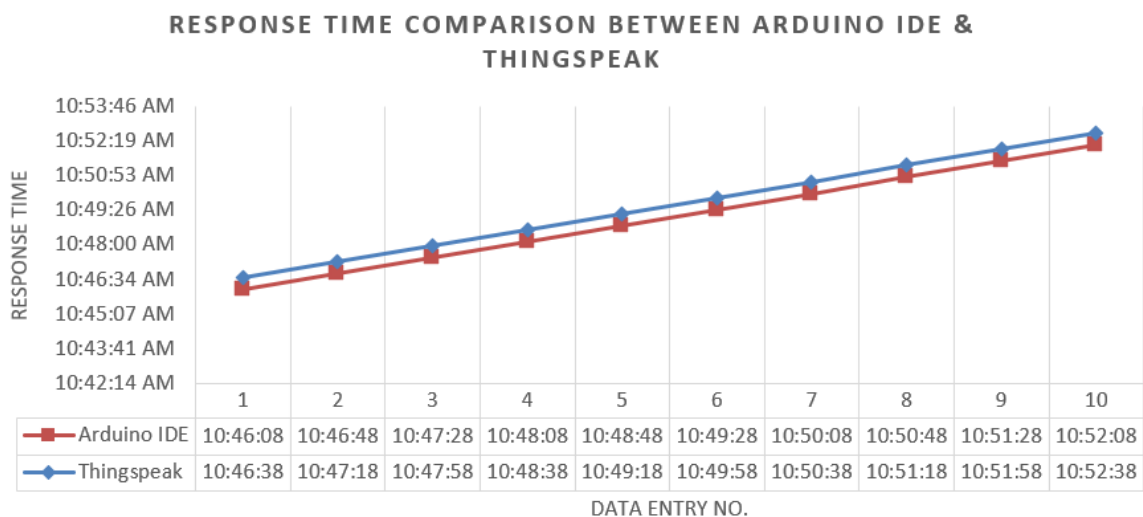


Figure 4.9: Response Time Comparison Between Arduino IDE and ThingSpeak

Across all data entries, the Arduino IDE serial monitor continuously showed quicker response times. For instance, the Arduino IDE reacted at 10:46:08 AM for the first data enter, whereas ThingSpeak responded at 10:46:38 AM, indicating a latency of almost 30 seconds. All of the entries that followed followed this pattern. The Arduino IDE's direct, local connection to the microcontroller, which eliminates the need for server processing or internet-based data transmission, accounts for its better speed. The Arduino IDE is ideal for applications that need instant feedback because of its direct approach, which minimises latency.

On the other hand, because ThingSpeak depends on internet connectivity for data processing and transmission, it showed a little longer response time. In comparison to the Arduino IDE, ThingSpeak displayed a delay of roughly 30 seconds for every data enter. This delay results from the network latency, server processing time, and data upload intervals that are a part of cloud-based systems. ThingSpeak is dependable for applications where real-time immediacy is not a crucial need since it maintains constant performance across all data entries notwithstanding the delay.

The comparison highlights both platforms' advantages and disadvantages. For on-site monitoring and prompt threat detection, the Arduino IDE excels at giving real-time input with low latency. On the other hand, ThingSpeak has the benefit of remote data visualisation and historical trend analysis, which makes it perfect for remote monitoring and long-term system evaluation. However, ThingSpeak's use is limited in scenarios that call for immediate responses due to its inherent delay.

The analysis concludes by highlighting how these two platforms play complementary roles. The Anti-Child Locking System strikes a balance by fusing the remote monitoring features of ThingSpeak with the real-time responsiveness of the Arduino IDE.

This integration meets the various needs of the system's operation by guaranteeing both instant hazard identification and thorough remote data logging.

4.5 System Performance Under Different Conditions

In This section is done to assess the performance of the system for several operational scenarios involving the detection of motion, temperature, and gas thresholds. Emphasized will be how the system behaves under certain conditions, pointing out the ability of accurate detection and response. The results are categorized into three distinct scenarios that show how functional and reliable the system would be in addressing critical safety concerns.

Table 4.1 summarizes the results of testing the system under all possible scenarios. The input conditions (motion, temperature, and gas concentration) are shown alongside the corresponding system response, including GSM notifications and LED alarm light activation.

4.5.1 Result of Summary Table

Table 4.1 summarizes the results of testing the system under all possible scenarios. The input conditions (motion, temperature, and gas concentration) are shown alongside the corresponding system response, including GSM notifications and LED alarm light activation.

Table 4.1: System Performance Under Different Conditions

Condition	Input Conditions	System Response	Observed Outcome
A	PIR = 1; Temperature $\leq 45^{\circ}\text{C}$; Gas ≤ 800 ppm	GSM sends a message .	Message sent successfully upon motion detection; no other actions triggered.
B	PIR = 1; (Temperature $> 45^{\circ}\text{C}$ OR Gas > 800 ppm)	GSM sends a message .	Message delivered to notify elevated temperature or gas levels alongside motion detection.
C	PIR = 1; Temperature $> 45^{\circ}\text{C}$ AND Gas > 800 ppm	GSM triggers a missed call and activates the LED alarm light for 20 seconds.	Both missed call and LED alarm light activated simultaneously for 20 seconds, ensuring high-priority notification of critical conditions.

The Functionality and reliability of the system were tested with three different conditions. The first case is when PIR sensor detected human motion, temperature $\leq 45^{\circ}\text{C}$, and gas concentration is < 800 ppm. The system gave the right action as the GSM sent a message “Hello, this is ANTI-CHILD LOCKING SYSTEM! Currently, there’s someone in Vehicle!” without any unnecessary alarm light turning on or any missed calls. It was concluded that the system handled the standard conditions correctly. Figure 4.10 indicates the messages were sent to the registered number.

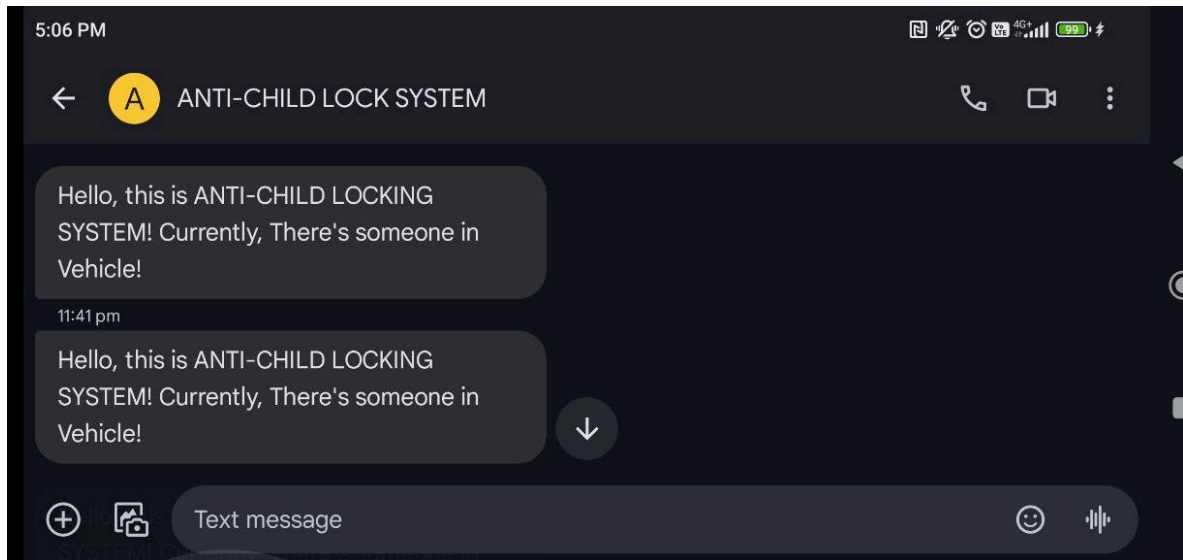


Figure 4.10: The message sent to the registered phone number

In the second case, with the PIR sensor turned On and either temperature above 45°C or carbon dioxide gas concentration over 800 ppm, the system gave quite good results with sending notifications through GSM messaging. The system sent a message “Hello, this is ANTI-CHILD LOCKING SYSTEM! Currently, there’s someone in Vehicle! (TEMP HIGH)” OR the system sent a message “Hello, this is ANTI-CHILD LOCKING SYSTEM! Currently, there’s someone in Vehicle! (CO2 HIGH)” depending on which sensor triggered. It was shown that it is possible to distinguish between light and critical notifications using the system to ensure only the latter are sent. Figure 4.11 indicates the messages were sent to the registered number.

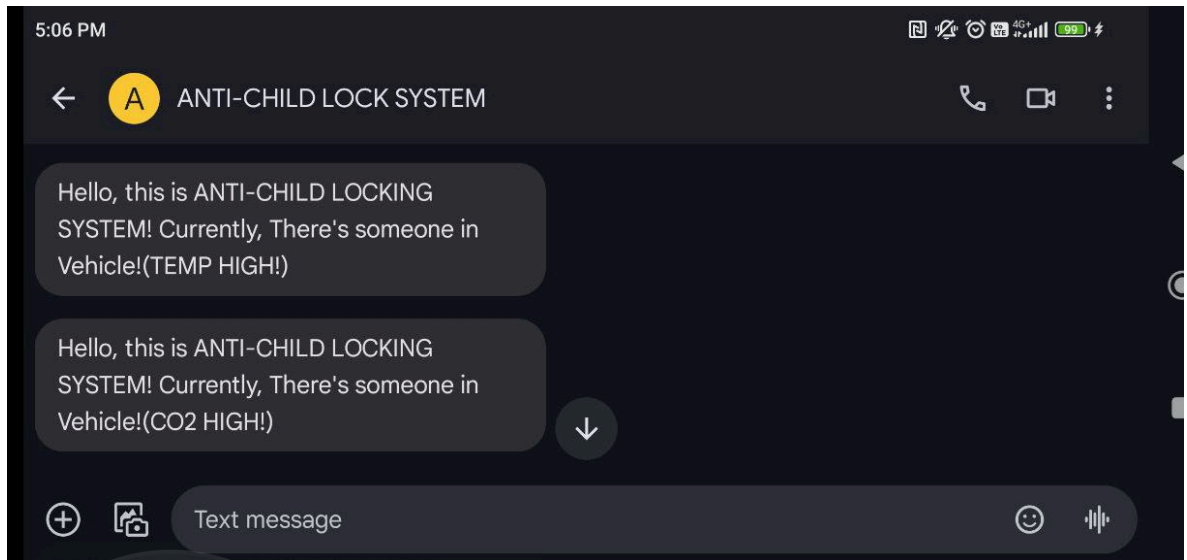
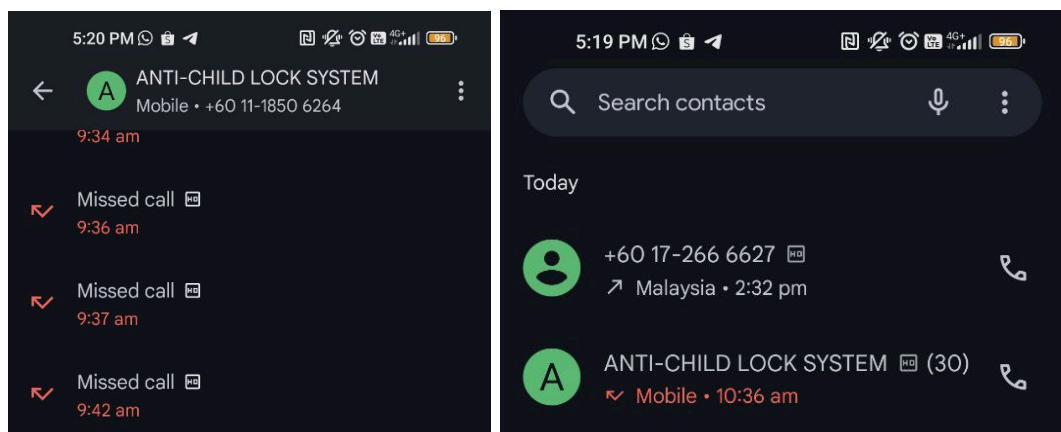


Figure 4.11: The messages sent to the registered phone number

In the third case, which involved triggering through the PIR sensor, exceeding the temperature of more than 45°C , and when the concentration of gas exceeded above 800 ppm, the system properly detected that situation as critical. It triggers two actuators-the missed call alert as shown in Figure 4.11 and the LED alarm light indicator as shown in Figure 4.12 firing both for a time span of 20 seconds each. Through testing, these actuators also worked concurrently, without any failures, with this duration being long enough to address the impending hazard.



(a)

(b)

Figure 4.12: (a) Anti-Child Locking System call logs (b) The GSM missed calls to the registered phone



(a)

(b)

Figure 4.13: (a) The LED Alarm Light Indicator is turned ON (b) Closer view of LED Alarm Light Indicator activation

4.6 System Insights and Implications

The examination of environmental and motion data is of critical importance in the determination of system performance and behaviour under real-time conditions. This section is directed towards the assessment of the ambient temperature °C, CO₂ concentration levels PPM, and the record of motion detection data over two successive days. Data visualization is done on two graphs shown in Figure 4.14 & Figure 4.15, analyzing different time intervals of 10 minutes each and color-coded zones-yellow, pink, and blue-showing how the system responded to different environmental conditions and motion triggers. The chapter will seek to show from these data trends and patterns the efficacy of the system in integrating environmental monitoring with automated alert mechanisms. Additionally, a day-to-day comparison of the two will also give clues regarding the consistency, robustness, and feature improvement that the system expresses under dynamic conditions. The data shows different behaviours of the system and how it reacts to changes in the surroundings and motion detection at 10-minute intervals. The graph's color-coded sections yellow, pink, and blue will be representing the distinct zones that correspond to each interval.

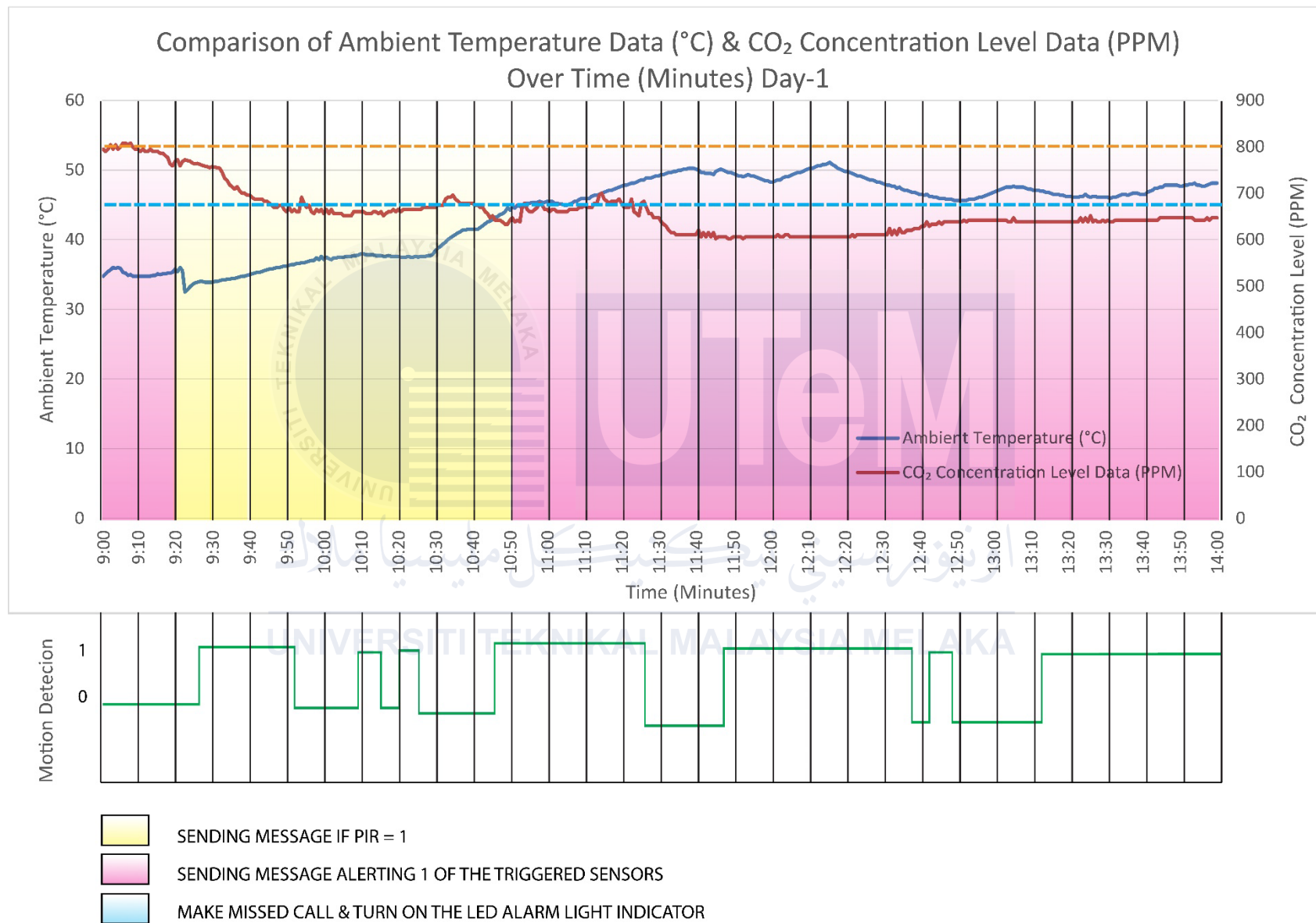


Figure 4.14: Comparison of Insight and Implications of Day-1

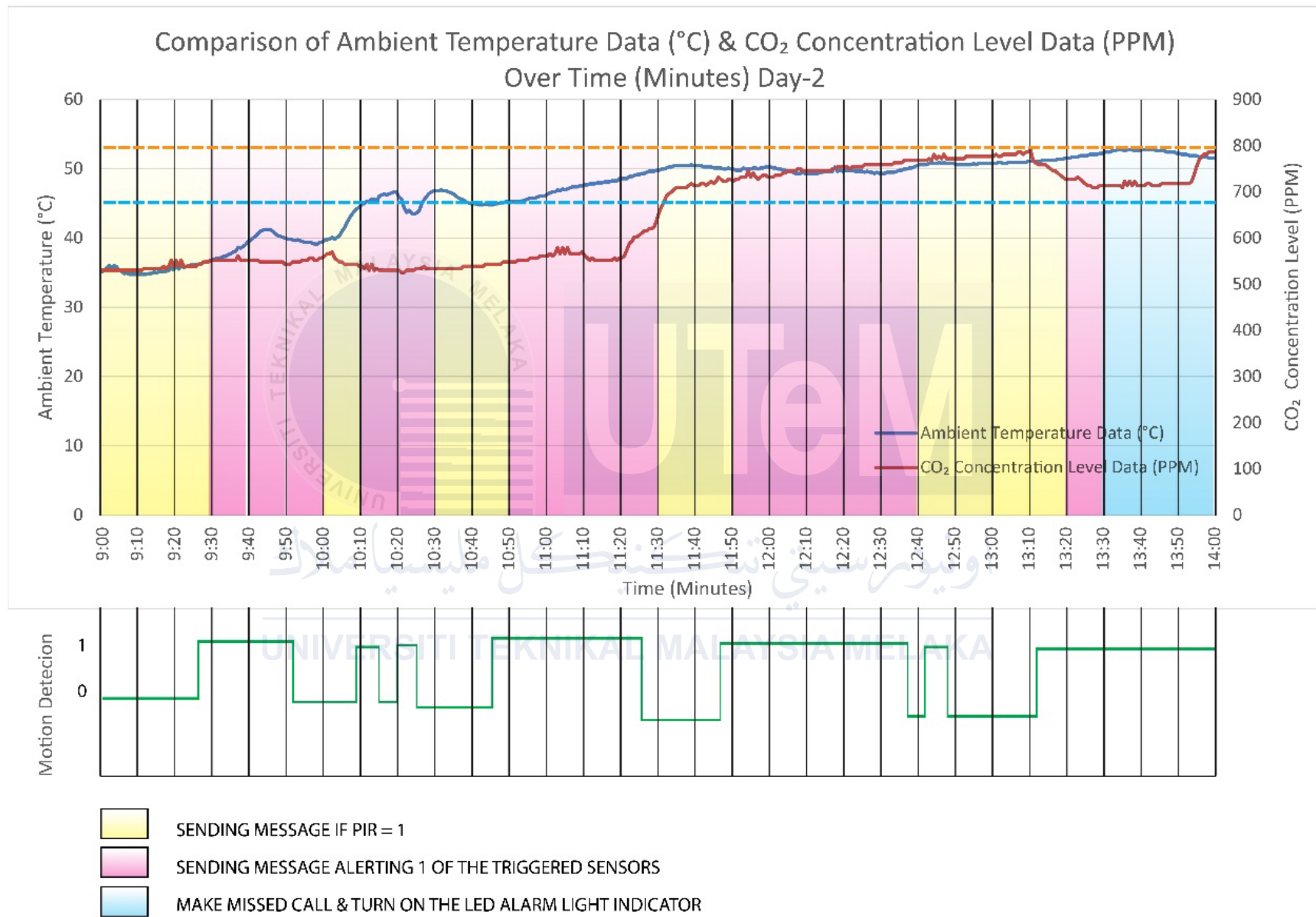


Figure 4.15: Comparison of Insight and Implications of Day-2

The system sends messages when the PIR sensor detects motion in yellow zones: $PIR = 1$ as shown in figure 4.10. These zones show the capability of the system to detect motion and immediately send an alert response based on detected activity. The functionality highlights the system's efficiency in monitoring and responding to motion in real time.

The pink areas as shown in figure 4.14 & figure 4.15 indicate time intervals where one or more sensors trigger alerts due to sensitivity with changes in environmental factors such as temperature, CO₂ levels, or movement. These tend to follow those described above as being highly active, indicating the system is sensitive to fluctuating conditions. Within these periods, proper messages have been given by the system using sensor data correctly as shown in figure 4.11, even when the detection of motion is spasmodic.

When all sensors are activated, the blue zone signals an emergency response. The system will immediately make a missed call to the registered device and turn on the LED alarm light indicator to warn the owner and any onlookers about the entrapment conditions inside the vehicle cabin. Figures 4.12 and 4.13 contain references to these simulations.

In a nutshell, this interaction of yellow, pink and blue zones acts out the capability of the system to integrate multiple data sources, thus giving timely alerts on varying environmental and activity-based inputs. These findings emphasize how the system effectively integrates real-time data to respond to environmental and activity-related changes. By utilizing color-coded intervals, the graph clearly delineates the system's operational logic, offering valuable insights into its functionality and responsiveness over time.

4.7 Summary

This chapter shall demonstrate how the Anti-Child Locking System monitors critical conditions within a vehicle for ambient temperature, CO₂ gas concentration, and motion detection. It was able to detect unsafe conditions, such as high temperatures above 45°C or CO₂ levels over 800 PPM, and trigger appropriate responses, including alerts and alarms within two days of testing. While operational, the system's performance has been segregated into three states: yellow zones for the detection of motion, pink zones for sensor-driven alerts due to environmental changes after detection some motions, and blue zones highlighting a very critical condition that urgently needs attention. For instance, upon detection of high temperature with CO₂, the alarm triggers and emergency notifications go off to call for child safety.

Day 1 versus Day 2 comparison represents the influence of the environment on the system's behavior, on Day 2, it shows higher averages for temperature and CO₂. For the fast real-time response within the vehicle, Arduino IDE serial monitoring has been utilized, and for remote monitoring with safety tracking over longer intervals, ThingSpeak platform.

Overall, the Anti-Child Locking System proves to be reliable and responsive to different dangers appearing inside the car and helps in child safety through timely alerts due to active ambient monitoring.

CHAPTER 5

CONCLUSION AND RECOMMENDATION

5.1 Conclusion

This project successfully designed and implemented an Anti-Child Locking System that provides improved vehicle safety in terms of the possible hazards related to the accidental entrapment of a child. The system involves several sensing technologies, including motion detection, temperature, and gas level, which guarantee thorough safety measures and achieve the goals indicated. The additional integration of a solar-powered rechargeable battery ensures supplementary sustainable and reliable energy for the system, continuously and independently operable even in emergency situations.

This system was tested extensively for days under different conditions, and indeed, the results proved the efficiency of the system in detecting critical thresholds and acting accordingly. The functionality of the system was monitored using the Arduino IDE and ThingSpeak platforms for real-time and remote monitoring, respectively. The analysis showed that Arduino IDE provides very minimal latency, which is appropriate for immediate hazard detection, while ThingSpeak allows for remote data visualization and trend analysis for long-term system evaluation from time to time. Moreover, the project findings also highlight how the integration of local actuators, such as a GSM module and LED light alarm indicator, is necessary to provide immediate alerts in critical situations, as mentioned in the third objectives. Some of these features guarantee the timely turn-on of safety measures so that delays which may mean lives are not incurred.

In the end, the Anti-Child Locking System meets not only the objectives of the

project but also paves the way for a new frontier in vehicle safety technology. This project can be further optimized, extended by testing, and taken to the industrial stakeholders for potential market product development that could save lives from child entrapment incidents. This lays the foundation for further development in safety systems, with innovation, sustainability, and the sanctity of human life being the cornerstone of such development.

5.2 Recommendations

Several recommendations are put forward to enhance the Anti-Child Locking System in vehicle. First, increasing the sensitivity and precision of sensors will reduce false positives and accurately detect hazards in various environmental conditions. A camera-based monitoring system with AI recognition capabilities could visually confirm the presence of a human being, thus making the system more reliable.

A big improvement could be designing an in-house PCB for the system. The main advantages of having a PCB are that it will minimize the hassle of wiring, which means more durability and optimization in power consumption. This will also pave the way to make the product small and lighter to place it in compact spaces like vehicle dashboards or rear-view mirrors.

Other significant improvements include setting the system to work for motionless babies, solving those cases where infants stay still and thus can't be recognized by the normal motion sensors. Inclusion of either thermal imaging sensors or sophisticated algorithms to detect minute breathing will ensure such incidences are picked out on time, ensuring safety for the most vulnerable passengers.

Secondly, the alert mechanism will be extended to mobile applications or cloud-

based platforms for convenience by allowing location tracking and live video feeds. It is also recommended to collaborate further with vehicle manufacturers, allowing in-vehicle integration of the system for wide adoption ease and to make its use a standard safety feature.

Finally, durability testing in extreme environmental conditions of high temperature and humidity should be performed to ensure the robustness of the system in various real-life scenarios. With these recommendations, the Anti-Child Locking System can become a comprehensive, user-friendly, highly effective vehicle safety solution.



REFERENCES


- Abdulrahman Abdullah, K., Hamid Ismail Mourad, A., & Uba Muhammad, A. (2020). 2020 *Advances in Science and Engineering Technology International Conferences (ASET)*.
 Abubakar, M., Salman Siddiqui, M., Owaisoddin, M., & professor-Ms Sapna Gangrade, A. (2023). *Implementation of Child Safety Alert System in Automobiles* (Vol. 11).
<https://seer-ufu-br.online>
- Aithal, S., Chakraborty, S., & Aithal, P. S. (2024). Google Scholar Citation: IJAEML. *International Journal of Applied Engineering and Management Letters (IJAEML) A Refereed International Journal of Srinivas University, ISSN(1), 2581–7000*.
<https://doi.org/10.5281/zenodo.10562843>
- Aleksic, S. O., Mitrovic, N. S., Nikolic, Z., Lukovic, M. D., Obradovic, N. N., & Lukovic, S. G. (2019). Three-Axis' Heat Loss Anemometer Comprising Thick-Film Segmented Thermistors. *IEEE Sensors Journal*, 19(22), 10228–10235.
<https://doi.org/10.1109/JSEN.2019.2929356>
- Almadhhachi, M., Seres, I., & Farkas, I. (2022). Comparison of the Efficiency of Polycrystalline and Thin-Film Photovoltaic Outdoors. *European Journal of Energy Research*, 2(2), 9–12. <https://doi.org/10.24018/ejenergy.2022.2.2.43>
- AL-SULTAN, M. A. M., & ALTINOLUK, S. (2022). ON THE PERFORMANCE LIMITS FOR MONO CRYSTALLINE SILICON SOLAR CELLS: A COMPARATIVE STUDY. *Mugla Journal of Science and Technology*, 8(2), 82–89.
<https://doi.org/10.22531/muglajsci.1101048>
- Anwar Ahmad. (2018). *Police rescue child trapped inside car | Transport – Gulf News*.
<https://gulfnews.com/uae/transport/police-rescue-child-trapped-inside-car-1.2276790>
- Asyrani, H., Sulaiman, B., Fareez Bin, M., Afif, M., Azlishah, M., Othman, B., Harris, M., Misran, B., Binti, A., & Said, M. (2013). *Wireless based Smart Parking System using Zigbee*.
- Barch, G., Alastair, M., Bsc, H., Barch, Z., & Phd, M. A. (2019). *Investigating the relationship between indoor environment and workplace productivity in naturally and mechanically-ventilated office environments*.
- Beaty, H. Wayne. (2001). *Handbook of electric power calculations*. McGraw-Hill.
- Ben Lutkevich. (2023). *What is a Microcontroller and How Does it Work?*
<https://www.techtarget.com/iotagenda/definition/microcontroller>
- Bondavenko V.E. (2019). *A MODERN TECHNOLOGY OF TEACHING AND TESTING MICROCONTROLLER SYSTEM DESIGNERS*.
- CC Goh, L.M. Kamarudin, S. Shukri, N.S. Abdullah, & A. Zakaria. (2016). *Monitoring of Carbon Dioxide (CO2) Accumulation in Vehicle Cabin*. IEEE.
- Cecelia. (2022). *Infrared Sensor: Types, Working Principle, and Applications | Easybom*.
<https://www.easybom.com/blog/a/infrared-sensor-types-working-principle-and-applications>
- Chi, Y. H., Hu, L. H., Gao, X., & Li, S. F. (2020). Research on infrared passive ranging algorithm based on unscented Kalman filter and modified spherical coordinates. *Journal of Physics: Conference Series*, 1629(1). <https://doi.org/10.1088/1742-6596/1629/1/012066>
- Chiu, E., Welman Simatupang, J., Hakiki, R., & Maratur Sidjabat, F. (2021). Prototype of Air Quality Sensor for Gas Pollutants Monitoring System in Industrial and Residential Estates. *Jurnal Ilmiah Teknik Elektro*, 17(1), 96–123.
<https://doi.org/10.25105/jetri.v17i1.9812>
- Cicchino, J. B., & Jermakian, J. S. (2015). Vehicle characteristics associated with LATCH use and correct use in real-world child restraint installations. *Journal of Safety Research*, 53, 77–85. <https://doi.org/10.1016/j.jsr.2015.03.009>
- Cotfas, D. T., & Cotfas, P. A. (2019). Comparative Study of Two Commercial Photovoltaic

- Panels under Natural Sunlight Conditions. *International Journal of Photoenergy*, 2019. <https://doi.org/10.1155/2019/8365175>
- Danny Jost. (2019). *What is an infrared sensor (IR)?* | Fierce Electronics. <https://www.fierceelectronics.com/sensors/what-ir-sensor>
- De Oliveira, V. I., Martins, H. M., Rosa, F. N., Dos Santos, J. P., De Moraes, D. M. G., & Junger, A. P. (2021). TEACHING USING THE ARDUINO PLATFORM APPLIED TO THE CONCEPT OF IoT AS SUPPORT TO MICROCONTROLLER CLASS. *South American Development Society Journal*, 7(20), 397. <https://doi.org/10.24325/issn.2446-5763.v7i20p397-408>
- Dietz, H., Abney, D., Eberhart, P., Santini, N., Davis, W., Wilson, E., & McKenzie, M. (2022). ESP32-CAM as a programmable camera research platform. *IS and T International Symposium on Electronic Imaging Science and Technology*, 34(7). <https://doi.org/10.2352/EI.2022.34.7.ISS-232>
- Drozd, O., & Scherbak, L. (2021). EN Solar panels work and control system modeling in LabVIEW and LTSpice XVII. Comparison of the perspectives of panels using. *Refrigeration Engineering and Technology*, 57(1), 37–44. <https://doi.org/10.15673/ret.v57i1.1977>
- Ernesto Serrato Maldonado, M., Alfonso Blanco Canon, R., & Barrera Prieto, F. (2020). Pedagogical tool for programming and reading a PIC microcontroller by means of an embedded Raspberry pi system and an easy-to-use graphical interface. *KnE Engineering*. <https://doi.org/10.18502/keg.v5i1.5924>
- ESP 8266 DATASHEET. (2015).
- Farah Nini Dusuki. (2023). Press-Statement-No.-42-2023_Child-Death-Left-in-Cars-Children-Commissioners-Urges-Immediate-Action-and-Awareness. *Child Death Left IN Cars*, 1.
- Fluieraru, C. P., Preducă, G., Andrei, H., Diaconu, E., Cotfas, P. A., & Cotfas, D. T. (2019). Determination of Technological Features of a Solar Photovoltaic Cell Made of Monocrystalline Silicon P+PNN+. *International Journal of Photoenergy*, 2019. <https://doi.org/10.1155/2019/7945683>
- Garg, H., & Agrawal, A. (2020). A comparative study on vehicles safety systems. *PDGC 2020 - 2020 6th International Conference on Parallel, Distributed and Grid Computing*, 172–176. <https://doi.org/10.1109/PDGC50313.2020.9315786>
- Gong, J., Li, C., & Wasielewski, M. R. (2019). Advances in solar energy conversion. *Chemical Society Reviews*, 48(7), 1862–1864. <https://doi.org/10.1039/C9CS90020A>
- Haram, M. H. S. M., Lee, J. W., Ramasamy, G., Ngu, E. E., Thiagarajah, S. P., & Lee, Y. H. (2021). Feasibility of utilising second life EV batteries: Applications, lifespan, economics, environmental impact, assessment, and challenges. In *Alexandria Engineering Journal* (Vol. 60, Issue 5, pp. 4517–4536). Elsevier B.V. <https://doi.org/10.1016/j.aej.2021.03.021>
- Hardian, A., Greshela, S., Yuliana, T., Budiman, S., Murniati, A., Kusumaningtyas, V. A., & Syarif, D. G. (2021). Cu-Mn Co-doped NiFe₂O₄ based thick ceramic film as negative temperature coefficient thermistors. *IOP Conference Series: Earth and Environmental Science*, 882(1). <https://doi.org/10.1088/1755-1315/882/1/012017>
- Hercog, D., Lerher, T., Truntič, M., & Težak, O. (2023). Design and Implementation of ESP32-Based IoT Devices. *Sensors*, 23(15). <https://doi.org/10.3390/s23156739>
- Ibrahim, A. B., Zulkifli, C. Z., Hanafi, H. F., & Zakaria, F. A. (2021). The Global System for Mobile Communications (GSM) for Wireless Home Security with Arduino and Web CAM. *European Journal of Electrical Engineering and Computer Science*, 5(1), 76–79. <https://doi.org/10.24018/ejece.2021.5.1.299>
- Jan Null. (2023). *FACT SHEET Pediatric Vehicular Heatstroke (PVH)*.
- Kastek, M., Madura, H., & Sosnowski, T. (2013). Passive infrared detector for security systems design, algorithm of people detection and field tests result. *International Journal of Safety and Security Engineering*, 3(1), 10–23. <https://doi.org/10.2495/SAFE-V3-N1-10-23>
- Kot, A., Nawrocka, A., IEEE Industry Applications Society, Institute of Electrical and

- Electronics Engineers, & Akademia Górniczo-Hutnicza im. S. Staszica w Krakowie. Wydział Inżynierii Mechanicznej i Robotyki. Department of Process Control. (2019). *Proceedings of the 2019 20th International Carpathian Control Conference (ICCC) : Kraków - Wieliczka, Hotel Turówka, Poland, May 26-29, 2019.*
- Kruizinga, M. D., Noordzij, J. G., van Houten, M. A., Wieringa, J., Tramper-Stranders, G. A., Hira, V., Bekhof, J., Vet, N. J., Driessen, G. J. A., & van Veen, M. (2023). Effect of lockdowns on the epidemiology of pediatric respiratory disease—A retrospective analysis of the 2021 summer epidemic. *Pediatric Pulmonology*, 58(4), 1229–1236. <https://doi.org/10.1002/ppul.26327>
- Kurnia, Y., & Li Sie, J. (2019). Prototype of Warehouse Automation System Using Arduino Mega 2560 Microcontroller Based on Internet of Things. *Bit-Tech*, 1(3). <http://jurnal.kdi.or.id/index.php/bt>
- Li, M., & Ge, X. (2021). Application of Electronic Technology in Automobile Safety System. *Journal of Physics: Conference Series*, 1948(1). <https://doi.org/10.1088/1742-6596/1948/1/012072>
- Lopez-Garcia, T. B., Sanchez, E. N., & Ruiz-Cruz, R. (2019). Real-time implementation of battery bank charge–discharge based on neural inverse optimal control. *IET Renewable Power Generation*, 13(16), 3124–3132. <https://doi.org/10.1049/iet-rpg.2019.0581>
- Lumbangaol, Sudirman., Siagian, R., Siahaan, F., & Sitinjak, E. (2022, August 18). *IOT-Based Pollution and Air Quality Monitoring Equipment with ESP-8266*. <https://doi.org/10.4108/eai.11-10-2021.2319568>
- Mahdin, H., Omar, A. H., Yaacob, S. S., Kasim, S., & Fudzee, M. F. M. (2016). Minimizing Heatstroke Incidents for Young Children Left inside Vehicle. *IOP Conference Series: Materials Science and Engineering*, 160(1). <https://doi.org/10.1088/1757-899X/160/1/012094>
- Marinho da Silva, A., Marinho da Silva, A., & Pinheiro Pires, Y. (2024). Prototype for automating the irrigation system using the arduino UNO R3 prototyping board for water control. *REVISTA INTERDISCIPLINAR E DO MEIO AMBIENTE (RIMA)*, 6(1), e235. <https://doi.org/10.52664/rima.v6.n1.2024.e235>
- Martinez-Acosta, A., Tafoya, R. R., Quinones, S. A., & Secor, E. B. (2021). Modular motion control software development to support a versatile, low-cost aerosol jet platform for printed electronics. *Additive Manufacturing*, 40. <https://doi.org/10.1016/j.addma.2021.101932>
- Mohamed, N., Voon, W. S., Hanis, H., & Othman, H. I. (2021). *MRR 03/2011 An Overview of Road Traffic Injuries Among Children in Malaysia and Its Implication on Road Traffic Injury Prevention Strategy.*
- Nicola, A., Vitan, C., Aron, C., Matei, D., & Grecea, I. (2021). Study of photovoltaic systems using modelling and simulation. *MATEC Web of Conferences*, 342, 03007. <https://doi.org/10.1051/mateconf/202134203007>
- Pawar, P., Langade, S., & Bandgar, M. (2008). A Paper on IOT Based Digital Notice Board using Arduino ATmega 328. *International Research Journal of Engineering and Technology*, 7509. www.irjet.net
- Perera, A. G. U. (2021). Editorial for the special issue on semiconductor infrared devices and applications. In *Micromachines* (Vol. 12, Issue 9). MDPI. <https://doi.org/10.3390/mi12091069>
- Pérez, I. G., Godoy, A. J. C., Godoy, M. C., & González, J. F. G. (2019). Survey about the utilization of open source arduino for control and measurement systems in advanced scenarios. Application to smart micro-grid and its digital replica. *ICINCO 2019 - Proceedings of the 16th International Conference on Informatics in Control, Automation and Robotics*, 2, 214–220. <https://doi.org/10.5220/0007830202140220>
- Picking, R., Glyndŵr University. ARCLab, Institute of Electrical and Electronics Engineers. United Kingdom and Republic of Ireland Section, & Institute of Electrical and Electronics Engineers. (2017). *2017 Internet Technologies and Applications (ITA) : proceedings of the Seventh International Conference : Tuesday 12th - Friday 15th*

September 2017, Wrexham Glyndŵr University, Wales, UK.

- Popa, D., Zeeshan Ali, S., Hopper, R., Dai, Y., & Udrea, F. (2019). *A smart CMOS mid-infrared sensor array*. <https://doi.org/10.1364/ao.XX.XXXXXX>
- Prof. Neha V. Sulakhe, Saurabh Pardeshi, Rahul Mochi, & Vashnavi Badale. (2022). Hybrid Generation with Inverter and Battery. *INTERANTIONAL JOURNAL OF SCIENTIFIC RESEARCH IN ENGINEERING AND MANAGEMENT*, 06(06). <https://doi.org/10.55041/ijsrem14490>
- Qasim, H. H., Jasim, A. M., & Hashim, K. A. (2023). Real-time monitoring system based on integration of internet of things and global system of mobile using Raspberry Pi. *Bulletin of Electrical Engineering and Informatics*, 12(3), 1418–1426. <https://doi.org/10.11591/eei.v12i3.4699>
- Reza, Md. S. (2022). Low-cost approach plan and development of GSM-based smart home automation system. *International Journal of Research In Science & Engineering*, 31, 1–8. <https://doi.org/10.55529/ijrise.31.1.8>
- Richard Ozenbaugh. (2004). *Chapter 21 Derivations for the Design Equations*.
- Rustam, I., Sahril, A. S., & Ja' Afar, H. (2023). Child Car Seat Alert System via Load and Temperature Sensing. *ICSET 2023 - 2023 IEEE 13th International Conference on System Engineering and Technology, Proceeding*, 96–99. <https://doi.org/10.1109/ICSET59111.2023.10295155>
- Saleh, M., Charkie, F., Al-Hamad, R., & Almisned, F. (2022). Designing a Smart Alarm System to Prevent Child Heatstroke in Vehicles. *2022 International Conference on Smart Systems and Power Management, IC2SPM 2022*, 58–63. <https://doi.org/10.1109/IC2SPM56638.2022.9988856>
- Selvakumar, M. (2023). Fabrication of Vehicle Safety using Power Window Mechanism. *International Journal for Research in Applied Science and Engineering Technology*, 11(5), 2795–2799. <https://doi.org/10.22214/ijraset.2023.51966>
- Seri, M., Mercuri, F., Ruani, G., Feng, Y., Li, M., Xu, Z. X., & Muccini, M. (2021). Toward Real Setting Applications of Organic and Perovskite Solar Cells: A Comparative Review. In *Energy Technology* (Vol. 9, Issue 5). John Wiley and Sons Inc. <https://doi.org/10.1002/ente.202000901>
- Shekoofa, O., Wang, J., Li, D., & Luo, Y. (2020). Investigation of microcrystalline silicon thin film fabricated by magnetron sputtering and copper-induced crystallization for photovoltaic applications. *Applied Sciences (Switzerland)*, 10(18). <https://doi.org/10.3390/APP10186320>
- Shyma Sasidharan, & Venkatesan Kanagarajan. (2015). *2015 International Conference on Computer Communication and Informatics : January 08-10, 2015, Coimbatore, India*.
- Slamin, Universitas Negeri Jember, Institute of Electrical and Electronics Engineers. Indonesia Section, Institute of Electrical and Electronics Engineers. Indonesia Section. Computer Society Chapter, & Institute of Electrical and Electronics Engineers. (2019). *Proceedings, 2019 International Conference on Computer Science, Information Technology, and Electrical Engineering (ICOMITEE 2019) : October 16th-17th 2019, Jember, Indonesia*.
- Sofijan, A. (2019). THE SOLAR RENEWABLE ENERGY SYSTEM STUDY WITH A CAPACITY OF 1300 W UTILITIZING POLYCRYSTALLINE PHOTOVOLTAIC. *Journal of Mechanical Science and Engineering*, 6(1), 5–011.
- Srinavya, E., Bhaswitha, M., Vineeth, S. S., & Priya, B. K. (2021, October 1). Implementation of Child Safety Alert System in Automobiles. *2021 2nd Global Conference for Advancement in Technology, GCAT 2021*. <https://doi.org/10.1109/GCAT52182.2021.9587764>
- Stela Muncut, E., & Ioana Culda, L. (2022). *AUTOMATION OF THE PROCESS FOR OBTAINING THE SAFETY PANEL USED ON A ROAD VEHICLE*.
- Sudhan, R. H., Kumar, M. G., Prakash, A. U., Devi, S. A. R., & P., S. (2015). ARDUINO ATMEGA-328 MICROCONTROLLER. *IJIREICE*, 3(4), 27–29. <https://doi.org/10.17148/ijireeice.2015.3406>

- Tamara Jude, & Angela Bunt. (2024). *Monocrystalline vs. Polycrystalline Solar Panels: 2024 Guide*. <https://www.marketwatch.com/guides/solar/monocrystalline-vs-polycrystalline-solar-panels/>
- Teixeira, J. L. V., & Pinto, F. R. (2020). Solar Panel: A Sustainable Development Alternative for Industries. *International Journal of Advanced Engineering Research and Science*, 7(12), 160–163. <https://doi.org/10.22161/ijaers.712.24>
- Ullah, K., Brézard-Oudot, A., Migan-Dubois, A., Diallo, D., Ullah Jan, K., Brézard Oudot, A., & Migan Dubois, A. (2021). *Experimental Evaluation of the True Remaining Capacity of Legacy Lead-Acid Batteries*. <https://hal.science/hal-03312365>
- Vaish, A. (2021, September 13). An electronic system with integrated alerting and cooling mechanisms to save the life of an unattended child in a vehicle. *ISSE 2021 - 7th IEEE International Symposium on Systems Engineering, Proceedings*. <https://doi.org/10.1109/ISSE51541.2021.9582492>
- Vanos, J., Guzman-Echavarria, G., Baldwin, J. W., Bongers, C., Ebi, K. L., & Jay, O. (2023). A physiological approach for assessing human survivability and liveability to heat in a changing climate. *Nature Communications*, 14(1). <https://doi.org/10.1038/s41467-023-43121-5>
- Via Andrea Appiani. (2024). *Arduino® UNO R3 Product Reference Manual SKU: A000066*.
- Villarreal-Rios, A. L., Bedoya-Calle, H., Caro-Lopera, F. J., Ortiz-Méndez, U., García-Méndez, M., & Pérez-Ramírez, F. O. (2019). Ultrathin tunable conducting oxide films for near-IR applications: an introduction to spectroscopy shape theory. *SN Applied Sciences*, 1(12). <https://doi.org/10.1007/s42452-019-1569-y>
- Wei, P., Ning, Z., Ye, S., Sun, L., Yang, F., Wong, K. C., Westerdahl, D., & Louie, P. K. K. (2018). Impact analysis of temperature and humidity conditions on electrochemical sensor response in ambient air quality monitoring. *Sensors (Switzerland)*, 18(2). <https://doi.org/10.3390/s18020059>
- Williams, N. P., Roumen, L., McCauley, G., & O'Shaughnessy, S. M. (2021). Performance evaluation of thermoelectric generators under cyclic heating. *Journal of Physics: Conference Series*, 2116(1). <https://doi.org/10.1088/1742-6596/2116/1/012087>
- Yang, I., & Yamamoto, L. (2021). Redesigning the Door Reduces the Potential for Finger Injuries in Children. *American Journal of Pediatrics*, 7(1), 34. <https://doi.org/10.11648/j.ajp.20210701.18>
- Yeom, S. (2021). Moving people tracking and false track removing with infrared thermal imaging by a multicopter. *Drones*, 5(3). <https://doi.org/10.3390/drones5030065>
- York State Department of Health, N. (2002). *Get the facts about LATCH*  *Securing Child Safety Seats*. www.safeny.com
- Yuan, K., Pacheco, M., Jurado-Sánchez, B., & Escarpa, A. (2021). Design and Control of the Micromotor Swarm Toward Smart Applications. *Advanced Intelligent Systems*, 3(6). <https://doi.org/10.1002/aisy.202100002>

APPENDICES

Appendices A: Gantt Chart Project 1

Activities Project	Bachelor's Degree Project 1 (BDP 1)														
	Week (Semester 6)														
	W1	W2	W3	W4	W5	W6	W7	W8	W9	W10	W11	W12	W13	W14	W15
Discussion About BDP Title Project	Plan	Actual													
Finding Issues or Problem Statements		Actual	Actual												
Identifying Objectives, aim & Scope projects		Actual	Actual	Actual	Actual										
Literature Review Findings			Actual	Actual	Actual	Actual	Actual	Actual	Actual	Actual					
Review Journals & Articles Findings			Actual	Actual	Actual	Actual	Actual	Actual	Actual	Actual					
Methodology of Research Project						Actual	Actual	Actual	Actual						
Discussion & Correction of Draft Report BDP 1									Actual	Actual	Actual	Actual			
Preliminary Result & Summary Writing										Actual	Actual	Actual			
Submission of Draft Report Writing													Actual	Actual	
Presentation of PSM 1															Actual
Finalized Report Submission															Actual

Plan



Actual



Appendices B: Gantt Chart Project 2

Activities Project	Bachelor's Degree Project 2 (BDP 2)														
	Week (Semester 6)														
	W1	W2	W3	W4	W5	W6	W7	W8	W9	W10	W11	W12	W13	W14	W15
Finalize Components List	Plan	Actual													
Purchasing Components	Plan	Actual	Plan												
Finalize Coding		Plan	Actual	Plan											
Testing & Debugging Code			Plan	Actual	Plan	Actual	Plan	Actual	Plan	Actual					
Design & Fabricate Casing		Plan	Actual	Plan	Actual	Plan									
Wiring & Assembly				Plan	Actual	Plan	Actual	Plan	Actual						
Integrate & Testing Full System									Plan	Actual	Plan	Actual			
System Optimization										Plan	Actual	Plan	Actual		
Sensor Integration Test													Plan	Actual	
Documentation & Final Review Adjustment													Plan	Actual	Plan
Project Submission & Presentation															Plan
															Actual

Plan



Actual



Appendices C: Table of Analysis Data for 2 Days

DAY-1				DAY-2			
NTC Thermistor Sensor Data (°C)	MQ-135 Sensor Data (PPM)	TIMESTA MPS (MINUTES)	TIMESTA MPS (MINUTES)	NTC Thermistor Sensor Data (°C)	MQ-135 Sensor Data (PPM)	Threshold CO ₂ (PPM)	Threshold Temperature (°C)
34.76	795	9:00	9:00	35.09	530	800	45
35.09	790	9:01		35.43	530	800	45
35.43	795	9:02		35.65	530	800	45
35.65	804	9:02		35.99	530	800	45
35.99	795	9:03		35.87	530	800	45
35.87	804	9:04		35.99	530	800	45
35.99	795	9:04		35.87	530	800	45
35.87	799	9:05		35.31	530	800	45
35.31	808	9:06		35.2	530	800	45
35.2	808	9:06		34.87	530	800	45
34.87	804	9:07		34.98	530	800	45
34.98	808	9:08		34.76	530	800	45
34.76	799	9:08		34.76	530	800	45
34.76	795	9:09		34.76	530	800	45
34.76	795	9:10	9:10	34.76	530	800	45
34.76	790	9:10		34.76	530	800	45
34.76	795	9:11		34.76	530	800	45
34.76	790	9:12		34.76	534	800	45
34.76	790	9:12		34.76	534	800	45
34.76	795	9:13		34.87	534	800	45
34.87	790	9:14		34.87	534	800	45
34.87	790	9:14		35.09	534	800	45
35.09	790	9:15		34.98	534	800	45
34.98	786	9:16		35.09	534	800	45
35.09	786	9:16		35.09	534	800	45
35.09	781	9:17		35.2	539	800	45
35.2	777	9:18		35.2	534	800	45
35.2	763	9:18		35.31	539	800	45
35.31	759	9:19		35.76	552	800	45
35.76	768	9:20	9:20	35.43	539	800	45
35.43	772	9:20		35.99	552	800	45
35.99	759	9:21		35.54	539	800	45
35.54	768	9:22		35.99	552	800	45
32.5	772	9:22		35.76	539	800	45
32.81	770	9:23		35.87	539	800	45
33.24	769	9:24		35.99	539	800	45
33.56	765	9:24		36.1	539	800	45

33.78	763	9:25		36.1	539	800	45
33.89	764	9:26		36.21	539	800	45
33.99	762	9:26		36.21	543	800	45
33.99	760	9:27		36.33	543	800	45
33.89	758	9:28		36.44	548	800	45
33.89	757	9:28		36.56	548	800	45
33.89	755	9:29		36.67	548	800	45
33.89	757	9:30	9:30	36.78	552	800	45
33.99	756	9:30		36.9	552	800	45
33.99	755	9:31		37.02	552	800	45
34.1	754	9:32		37.13	552	800	45
34.21	745	9:32		37.13	552	800	45
34.21	732	9:33		37.36	552	800	45
34.32	727	9:34		37.36	552	800	45
34.32	718	9:34		37.6	552	800	45
34.43	714	9:35		37.71	552	800	45
34.43	709	9:36		37.95	552	800	45
34.54	714	9:36		38.07	552	800	45
34.65	705	9:37		38.66	561	800	45
34.76	700	9:38		38.54	552	800	45
34.76	700	9:38		38.78	552	800	45
34.87	696	9:39		39.02	552	800	45
34.98	696	9:40	9:40	39.5	552	800	45
35.09	691	9:40		39.63	552	800	45
35.2	687	9:41		39.99	552	800	45
35.31	687	9:42		40.24	552	800	45
35.31	687	9:42		40.61	552	800	45
35.43	687	9:43		40.99	548	800	45
35.54	683	9:44		41.12	548	800	45
35.65	683	9:44		41.24	548	800	45
35.76	678	9:45		41.24	548	800	45
35.76	674	9:46		41.24	548	800	45
35.87	669	9:46		40.99	548	800	45
35.99	669	9:47		40.61	548	800	45
35.99	674	9:48		40.36	548	800	45
36.1	674	9:48		40.24	548	800	45
36.21	665	9:49		40.12	548	800	45
36.21	660	9:50	9:50	39.99	543	800	45
36.33	669	9:50		39.87	543	800	45
36.44	660	9:51		39.87	543	800	45
36.44	665	9:52		39.75	548	800	45
36.56	660	9:52		39.63	548	800	45
36.56	660	9:53		39.75	548	800	45
36.67	691	9:54		39.63	548	800	45
36.67	678	9:54		39.5	552	800	45
36.78	669	9:55		39.38	552	800	45

36.9	674	9:56		39.38	552	800	45
37.02	660	9:56		39.38	557	800	45
37.02	656	9:57		39.26	557	800	45
37.36	665	9:58		39.14	552	800	45
37.13	660	9:58		39.14	552	800	45
37.6	665	9:59		39.38	557	800	45
37.13	656	10:00	10:00	39.38	557	800	45
37.48	665	10:00		39.75	561	800	45
37.25	656	10:01		39.75	566	800	45
37.13	665	10:02		39.87	566	800	45
37.36	656	10:02		40.12	570	800	45
37.36	656	10:03		39.87	557	800	45
37.48	656	10:04		40.12	552	800	45
37.48	656	10:04		40.36	548	800	45
37.48	651	10:05		40.99	548	800	45
37.6	651	10:06		41.5	543	800	45
37.6	651	10:06		42.27	543	800	45
37.6	651	10:07		42.92	543	800	45
37.71	660	10:08		43.45	543	800	45
37.71	660	10:08		43.85	543	800	45
37.83	660	10:09		44.26	543	800	45
37.95	660	10:10	10:10	44.4	539	800	45
37.95	660	10:10		44.95	539	800	45
37.83	656	10:11		44.95	534	800	45
37.83	656	10:12		45.36	543	800	45
37.83	656	10:12		45.22	530	800	45
37.83	660	10:13		45.64	543	800	45
37.71	660	10:14		45.64	530	800	45
37.71	656	10:14		45.22	534	800	45
37.71	660	10:15		46.07	530	800	45
37.6	651	10:16		46.21	530	800	45
37.6	656	10:16		46.36	530	800	45
37.71	660	10:17		46.21	530	800	45
37.6	660	10:18		46.36	530	800	45
37.6	665	10:18		46.5	530	800	45
37.6	660	10:19		46.64	530	800	45
37.6	665	10:20	10:20	46.64	530	800	45
37.48	660	10:20		45.93	530	800	45
37.48	665	10:21		45.64	525	800	45
37.48	665	10:22		44.4	525	800	45
37.6	665	10:23		43.72	530	800	45
37.48	665	10:23		43.99	530	800	45
37.48	665	10:24		43.59	530	800	45
37.6	665	10:25		43.45	530	800	45
37.48	665	10:25		43.59	534	800	45
37.6	665	10:26		43.85	534	800	45

37.6	669	10:27		44.81	534	800	45
37.6	669	10:27		45.5	539	800	45
37.71	669	10:28		45.93	534	800	45
37.71	669	10:29		46.36	534	800	45
37.95	669	10:29		46.64	534	800	45
38.42	669	10:30	10:30	46.79	534	800	45
38.78	674	10:31		46.79	534	800	45
39.02	674	10:31		46.79	534	800	45
39.38	674	10:32		46.93	534	800	45
39.63	687	10:33		46.79	534	800	45
39.99	691	10:33		46.79	534	800	45
40.24	691	10:34		46.64	534	800	45
40.49	696	10:35		46.5	534	800	45
40.74	687	10:35		46.36	534	800	45
40.99	683	10:36		46.07	534	800	45
41.12	678	10:37		45.79	534	800	45
41.37	678	10:37		45.64	534	800	45
41.37	678	10:38		45.5	539	800	45
41.5	678	10:39		45.22	539	800	45
41.5	678	10:39		45.09	539	800	45
41.5	678	10:40	10:40	44.95	539	800	45
41.5	674	10:41		44.95	539	800	45
41.5	674	10:41		44.95	539	800	45
41.75	669	10:42		44.81	539	800	45
42.01	669	10:43		44.81	539	800	45
42.27	660	10:43		44.81	539	800	45
42.53	656	10:44		44.95	543	800	45
42.66	647	10:45		44.81	543	800	45
42.92	651	10:45		44.81	543	800	45
43.19	642	10:46		44.81	543	800	45
43.32	642	10:47		44.95	543	800	45
43.59	642	10:47		44.95	543	800	45
43.72	638	10:48		45.09	543	800	45
43.99	633	10:49		45.09	548	800	45
44.53	633	10:49		45.22	548	800	45
44.26	642	10:50	10:50	45.22	548	800	45
44.67	647	10:51		45.22	548	800	45
44.53	638	10:51		45.22	548	800	45
44.95	642	10:52		45.22	548	800	45
44.81	638	10:53		45.22	552	800	45
44.53	674	10:53		45.36	552	800	45
45.22	678	10:54		45.36	552	800	45
45.22	665	10:55		45.5	552	800	45
45.22	660	10:55		45.64	552	800	45
45.36	660	10:56		45.79	557	800	45
45.36	665	10:57		45.79	557	800	45

45.36	669	10:57		45.79	557	800	45
45.5	678	10:58		45.93	557	800	45
45.36	674	10:59		46.07	561	800	45
45.36	665	10:59		46.07	561	800	45
45.5	665	11:00	11:00	46.07	561	800	45
45.5	660	11:01		46.36	561	800	45
45.5	665	11:01		46.5	566	800	45
45.22	665	11:02		46.64	561	800	45
45.22	660	11:03		46.64	566	800	45
45.09	660	11:03		46.93	579	800	45
45.09	660	11:04		46.79	566	800	45
44.95	660	11:05		47.08	579	800	45
44.95	660	11:05		46.93	566	800	45
45.09	665	11:06		47.08	579	800	45
45.22	665	11:07		47.23	566	800	45
45.5	665	11:07		47.37	566	800	45
45.5	665	11:08		47.37	566	800	45
45.79	669	11:09		47.37	566	800	45
45.93	669	11:09		47.52	566	800	45
45.93	674	11:10	11:10	47.52	570	800	45
45.93	669	11:11		47.67	561	800	45
45.93	669	11:11		47.67	557	800	45
46.21	669	11:12		47.82	552	800	45
46.36	678	11:13		47.82	557	800	45
46.36	678	11:13		47.82	552	800	45
46.5	696	11:14		47.97	552	800	45
46.64	700	11:15		47.97	552	800	45
46.79	687	11:15		47.97	552	800	45
46.93	683	11:16		48.11	552	800	45
47.08	678	11:17		48.11	552	800	45
47.08	683	11:17		48.11	552	800	45
47.23	683	11:18		48.27	552	800	45
47.37	683	11:19		48.27	557	800	45
47.52	687	11:19		48.27	552	800	45
47.67	678	11:20	11:20	48.57	557	800	45
47.82	669	11:21		48.57	557	800	45
47.82	669	11:21		48.57	561	800	45
47.97	669	11:22		48.57	575	800	45
48.11	687	11:23		48.87	588	800	45
48.11	660	11:23		48.87	593	800	45
48.27	656	11:24		49.03	602	800	45
48.42	651	11:25		49.18	602	800	45
48.57	678	11:25		49.18	606	800	45
48.57	683	11:26		49.33	611	800	45
48.87	669	11:27		49.33	615	800	45
48.87	656	11:27		49.49	615	800	45

48.87	656	11:28		49.64	620	800	45
49.03	647	11:29		49.64	620	800	45
49.18	647	11:29		49.64	624	800	45
49.18	647	11:30	11:30	49.8	638	800	45
49.33	638	11:31		49.8	656	800	45
49.33	633	11:31		49.96	669	800	45
49.49	629	11:32		49.96	678	800	45
49.64	620	11:33		50.12	691	800	45
49.64	615	11:33		50.27	696	800	45
49.8	615	11:34		50.27	700	800	45
49.8	611	11:35		50.43	705	800	45
49.96	611	11:35		50.43	709	800	45
49.96	611	11:36		50.43	709	800	45
50.12	611	11:37		50.43	709	800	45
50.12	611	11:37		50.43	709	800	45
50.27	611	11:38		50.43	709	800	45
50.27	611	11:39		50.43	714	800	45
50.27	611	11:39		50.59	718	800	45
50.12	611	11:40	11:40	50.43	714	800	45
49.96	620	11:41		50.43	714	800	45
49.64	606	11:41		50.43	714	800	45
49.64	615	11:42		50.43	718	800	45
49.49	606	11:43		50.27	718	800	45
49.49	615	11:43		50.27	714	800	45
49.49	606	11:44		50.27	718	800	45
49.33	615	11:45		50.27	723	800	45
49.8	602	11:45		50.12	718	800	45
49.96	606	11:46		50.12	723	800	45
50.12	606	11:47		50.12	732	800	45
49.96	606	11:47		50.12	727	800	45
49.8	606	11:48		49.96	723	800	45
49.64	602	11:49		49.96	723	800	45
49.64	602	11:49		50.12	727	800	45
49.49	606	11:50	11:50	49.96	727	800	45
49.33	606	11:51		49.96	723	800	45
49.18	606	11:51		49.8	727	800	45
49.18	606	11:52		49.8	727	800	45
49.03	602	11:53		49.8	732	800	45
49.18	606	11:53		50.12	732	800	45
49.33	606	11:54		49.96	732	800	45
49.18	606	11:55		49.96	745	800	45
49.18	606	11:55		49.96	732	800	45
49.03	606	11:56		50.12	741	800	45
48.87	606	11:57		50.12	732	800	45
48.72	606	11:57		49.96	727	800	45
48.57	606	11:58		50.12	732	800	45

48.42	606	11:59		50.12	736	800	45
48.42	606	11:59		50.27	736	800	45
48.27	606	12:00	12:00	50.27	732	800	45
48.27	606	12:01		50.27	732	800	45
48.42	606	12:01		50.12	732	800	45
48.57	611	12:02		50.12	736	800	45
48.57	606	12:03		49.96	736	800	45
48.87	606	12:03		49.96	736	800	45
49.03	611	12:04		49.8	741	800	45
49.03	611	12:05		49.8	741	800	45
49.18	606	12:05		49.64	745	800	45
49.33	606	12:06		49.64	745	800	45
49.49	606	12:07		49.49	745	800	45
49.64	606	12:07		49.33	745	800	45
49.64	606	12:08		49.33	750	800	45
49.8	606	12:09		49.33	750	800	45
49.96	606	12:09		49.49	745	800	45
50.12	606	12:10	12:10	49.33	745	800	45
50.27	606	12:11		49.33	745	800	45
50.27	606	12:11		49.33	745	800	45
50.43	606	12:12		49.33	745	800	45
50.59	606	12:13		49.33	745	800	45
50.59	606	12:13		49.33	745	800	45
50.75	606	12:14		49.49	745	800	45
50.75	606	12:15		49.49	745	800	45
50.91	606	12:15		49.64	745	800	45
51.08	606	12:16		49.64	745	800	45
50.75	606	12:17		49.64	745	800	45
50.59	606	12:17		49.64	750	800	45
50.27	606	12:18		50.27	750	800	45
50.12	606	12:19		49.64	754	800	45
49.96	606	12:19		49.8	754	800	45
49.8	606	12:20	12:20	49.64	754	800	45
49.8	606	12:21		49.8	754	800	45
49.64	606	12:21		49.8	754	800	45
49.49	611	12:22		49.8	750	800	45
49.33	606	12:23		49.8	754	800	45
49.18	611	12:23		49.64	754	800	45
49.18	611	12:24		49.64	754	800	45
49.03	611	12:25		49.64	754	800	45
48.87	611	12:25		49.64	754	800	45
48.72	611	12:26		49.49	759	800	45
48.57	611	12:27		49.64	759	800	45
48.57	611	12:27		49.49	759	800	45
48.42	611	12:28		49.49	759	800	45
48.27	611	12:29		49.33	759	800	45

48.27	611	12:29		49.49	759	800	45
48.11	611	12:30	12:30	49.33	759	800	45
47.97	611	12:31		49.33	759	800	45
47.82	611	12:31		49.33	759	800	45
47.82	624	12:32		49.49	759	800	45
47.67	611	12:33		49.49	759	800	45
47.67	620	12:33		49.49	759	800	45
47.37	611	12:34		49.49	763	800	45
47.52	624	12:35		49.64	763	800	45
47.23	615	12:35		49.8	763	800	45
47.08	615	12:36		49.8	763	800	45
47.08	620	12:37		49.96	768	800	45
46.93	620	12:37		49.96	768	800	45
46.79	620	12:38		50.12	768	800	45
46.79	624	12:39		50.12	768	800	45
46.64	624	12:39		50.27	768	800	45
46.5	624	12:40	12:40	50.43	768	800	45
46.5	629	12:41		50.59	768	800	45
46.36	629	12:41		50.59	768	800	45
46.5	638	12:42		50.59	768	800	45
46.21	629	12:43		50.59	768	800	45
46.21	633	12:43		50.75	772	800	45
46.07	633	12:44		50.75	768	800	45
46.07	633	12:45		50.75	781	800	45
45.93	638	12:45		50.75	772	800	45
45.93	633	12:46		50.91	777	800	45
45.93	638	12:47		50.75	772	800	45
45.79	638	12:47		50.91	781	800	45
45.79	638	12:48		50.75	772	800	45
45.79	638	12:49		50.75	772	800	45
45.64	638	12:49		50.75	772	800	45
45.64	638	12:50	12:50	50.75	772	800	45
45.64	638	12:51		50.59	772	800	45
45.64	638	12:51		50.59	772	800	45
45.64	642	12:52		50.59	772	800	45
45.64	638	12:53		50.59	772	800	45
45.79	642	12:53		50.59	777	800	45
45.79	642	12:54		50.59	777	800	45
45.79	642	12:55		50.59	777	800	45
45.93	642	12:55		50.75	777	800	45
46.07	642	12:56		50.59	777	800	45
46.07	642	12:57		50.75	777	800	45
46.21	642	12:57		50.75	777	800	45
46.36	642	12:58		50.75	777	800	45
46.5	642	12:59		50.75	777	800	45
46.64	642	12:59		50.75	777	800	45

46.79	642	13:00	13:00	50.75	777	800	45
46.93	642	13:01		50.75	777	800	45
47.08	642	13:01		50.75	781	800	45
47.23	642	13:02		50.91	777	800	45
47.37	642	13:03		50.91	777	800	45
47.52	642	13:03		50.75	781	800	45
47.52	638	13:04		50.75	781	800	45
47.52	638	13:05		50.91	781	800	45
47.67	647	13:05		50.91	781	800	45
47.52	638	13:06		50.91	781	800	45
47.52	638	13:07		50.91	781	800	45
47.52	638	13:07		50.91	786	800	45
47.52	638	13:08		50.91	786	800	45
47.37	638	13:09		50.91	781	800	45
47.23	638	13:09		50.91	786	800	45
47.23	638	13:10	13:10	51.08	786	800	45
47.08	638	13:11		51.08	790	800	45
47.08	638	13:11		51.08	768	800	45
47.08	638	13:12		51.08	763	800	45
46.93	638	13:13		51.08	759	800	45
46.93	638	13:13		51.08	759	800	45
46.79	638	13:14		51.24	759	800	45
46.79	638	13:15		51.24	759	800	45
46.64	638	13:15		51.24	754	800	45
46.5	638	13:16		51.24	750	800	45
46.5	638	13:17		51.24	745	800	45
46.5	638	13:17		51.24	745	800	45
46.36	638	13:18		51.4	741	800	45
46.36	638	13:19		51.4	736	800	45
46.21	638	13:19		51.4	732	800	45
46.21	638	13:20	13:20	51.57	727	800	45
46.21	638	13:21		51.57	727	800	45
46.07	638	13:21		51.57	727	800	45
46.07	638	13:22		51.73	727	800	45
46.07	638	13:23		51.73	727	800	45
46.21	647	13:23		51.73	732	800	45
46.21	638	13:24		51.9	727	800	45
46.5	647	13:25		51.9	723	800	45
46.21	638	13:25		51.9	718	800	45
46.07	651	13:26		51.9	714	800	45
46.21	638	13:27		52.06	714	800	45
46.21	642	13:27		52.06	709	800	45
46.07	638	13:28		52.06	709	800	45
46.07	638	13:29		52.06	709	800	45
46.07	642	13:29		52.23	714	800	45
46.07	638	13:30	13:30	52.23	714	800	45

46.07	642	13:31		52.4	714	800	45
45.93	638	13:31		52.4	714	800	45
46.07	638	13:32		52.4	714	800	45
46.07	642	13:33		52.57	714	800	45
46.21	642	13:33		52.57	714	800	45
46.36	642	13:34		52.73	714	800	45
46.5	642	13:35		52.73	714	800	45
46.5	642	13:35		52.73	709	800	45
46.36	642	13:36		52.57	723	800	45
46.5	642	13:37		52.73	714	800	45
46.64	642	13:37		52.73	723	800	45
46.64	642	13:38		52.73	714	800	45
46.64	642	13:39		52.57	723	800	45
46.5	642	13:39		52.57	714	800	45
46.5	642	13:40	13:40	52.57	714	800	45
46.5	642	13:41		52.73	714	800	45
46.79	642	13:41		52.73	714	800	45
46.93	642	13:42		52.73	718	800	45
47.08	642	13:43		52.73	718	800	45
47.37	642	13:43		52.73	714	800	45
47.37	642	13:44		52.73	714	800	45
47.52	647	13:45		52.57	714	800	45
47.52	647	13:45		52.57	714	800	45
47.82	647	13:46		52.57	718	800	45
47.82	647	13:47		52.57	718	800	45
47.82	647	13:47		52.4	718	800	45
47.82	647	13:48		52.4	718	800	45
47.82	647	13:49		52.4	718	800	45
47.82	647	13:49		52.4	718	800	45
47.67	647	13:50	13:50	52.23	718	800	45
47.67	647	13:51		52.23	718	800	45
47.82	647	13:51		52.06	718	800	45
47.82	647	13:52		52.06	718	800	45
47.97	647	13:53		52.06	718	800	45
47.97	647	13:53		51.9	718	800	45
48.11	642	13:54		51.9	723	800	45
47.82	642	13:55		51.9	736	800	45
47.82	642	13:55		51.9	754	800	45
47.67	642	13:56		51.73	768	800	45
47.67	642	13:57		51.73	777	800	45
47.82	647	13:57		51.73	781	800	45
47.97	642	13:58		51.73	781	800	45
48.11	647	13:59		51.57	786	800	45
48.11	647	13:59		51.57	786	800	45
48.11	647	14:00	14:00	51.57	786	800	45

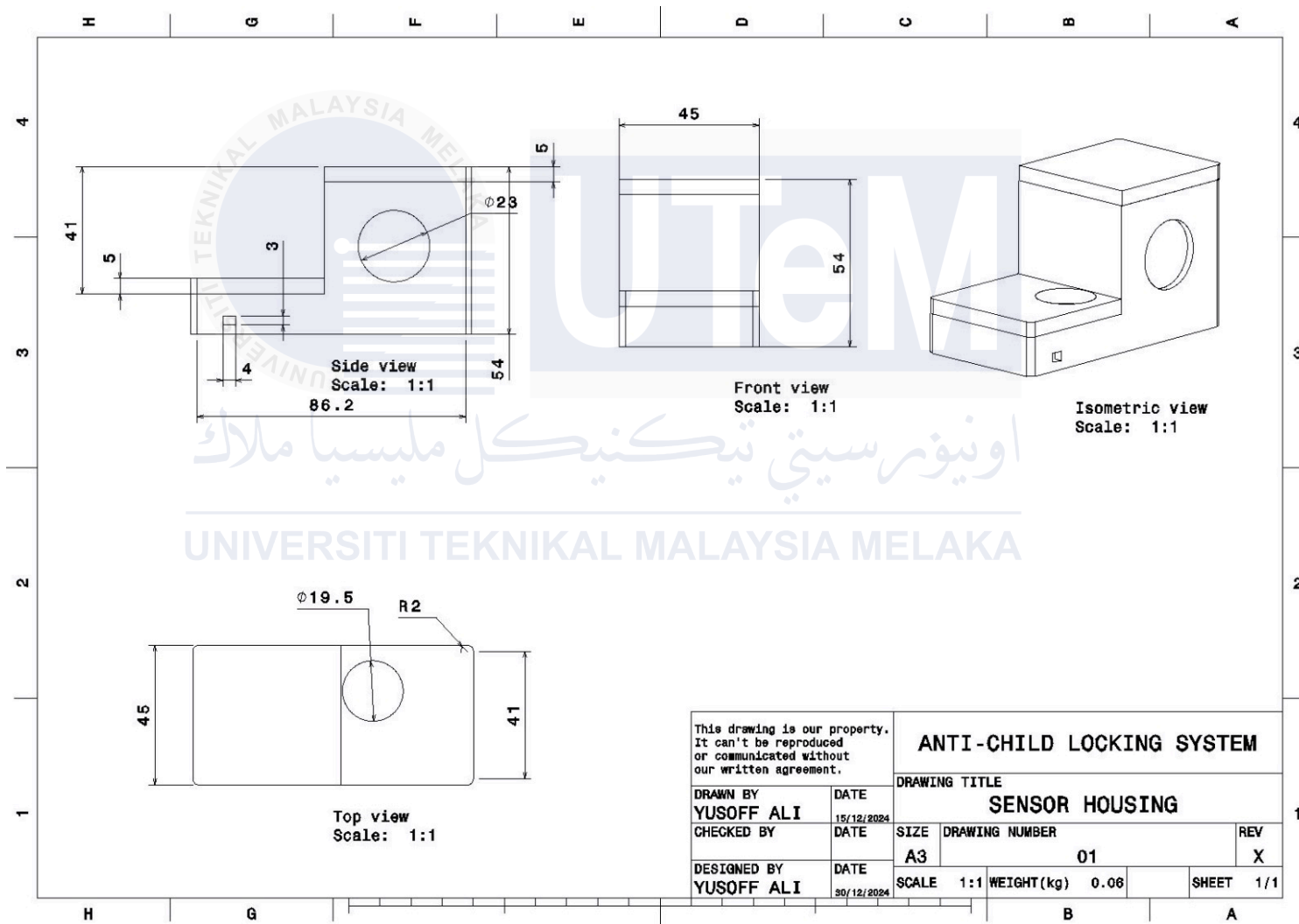
Appendices D: Table of Time Response Data between Arduino IDE and ThingSpeak

Arduino IDE VS ThingSpeak Response Timetable

Arduino IDE	Thingspeak	Data Entry No.
10:46:08 AM	10:46:38 AM	1
10:46:48 AM	10:47:18 AM	2
10:47:28 AM	10:47:58 AM	3
10:48:08 AM	10:48:38 AM	4
10:48:48 AM	10:49:18 AM	5
10:49:28 AM	10:49:58 AM	6
10:50:08 AM	10:50:38 AM	7
10:50:48 AM	10:51:18 AM	8
10:51:28 AM	10:51:58 AM	9
10:52:08 AM	10:52:38 AM	10



Appendices E: 3D Print Casing for Sensor Design Drafting



Appendices G: AI Index Turnitin Report





25% detected as AI

The percentage indicates the combined amount of likely AI-generated text as well as likely AI-generated text that was also likely AI-paraphrased.

Caution: Review required.

It is essential to understand the limitations of AI detection before making decisions about a student's work. We encourage you to learn more about Turnitin's AI detection capabilities before using the tool.

Detection Groups

-  **1 AI-generated only 22%**
Likely AI-generated text from a large-language model.
-  **2 AI-generated text that was AI-paraphrased 3%**
Likely AI-generated text that was likely revised using an AI-paraphrase tool or word spinner.

Disclaimer

Our AI writing assessment is designed to help educators identify text that might be prepared by a generative AI tool. Our AI writing assessment may not always be accurate (it may misidentify writing that is likely AI generated and AI paraphrased or likely AI generated and AI paraphrased writing as only AI generated) so it should not be used as the sole basis for adverse actions against a student. It takes further scrutiny and human judgment in conjunction with an organization's application of its specific academic policies to determine whether any academic misconduct has occurred.

Frequently Asked Questions

How should I interpret Turnitin's AI writing percentage and false positives?

The percentage shown in the AI writing report is the amount of qualifying text within the submission that Turnitin's AI writing detection model determines was either likely AI-generated text from a large-language model or likely AI-generated text that was likely revised using an AI-paraphrase tool or word spinner.

False positives (incorrectly flagging human-written text as AI-generated) are a possibility in AI models.

AI detection scores under 20%, which we do not surface in new reports, have a higher likelihood of false positives. To reduce the likelihood of misinterpretation, no score or highlights are attributed and are indicated with an asterisk in the report (*%).

The AI writing percentage should not be the sole basis to determine whether misconduct has occurred. The reviewer/instructor should use the percentage as a means to start a formative conversation with their student and/or use it to examine the submitted assignment in accordance with their school's policies.

What does 'qualifying text' mean?

Our model only processes qualifying text in the form of long-form writing. Long-form writing means individual sentences contained in paragraphs that make up a longer piece of written work, such as an essay, a dissertation, or an article, etc. Qualifying text that has been determined to be likely AI-generated will be highlighted in cyan in the submission, and likely AI-generated and then likely AI-paraphrased will be highlighted purple.

Non-qualifying text, such as bullet points, annotated bibliographies, etc., will not be processed and can create disparity between the submission highlights and the percentage shown.

